

ductility demand has, in general, only a small effect on displacement demand applies equally to the standard Takeda oscillator and to Takeda oscillators that exhibit pinching. The Takeda5 oscillators with initially reduced strength, given by $RSR = 0.6$, tended to have a response amplified to a much greater extent than is observed for the TakPinch model, reflecting the more dramatic form of strength degradation that was implemented in the Takeda5 model.

6.4.3.3 Response of Takeda10 Model

The Takeda10 model is a Takeda model having post-yield stiffness equal to -10% of the yield-point secant stiffness. As has been found previously by others, models with negative post-yield stiffness are prone to collapse, where collapse is defined as the point at which the displacement is large enough that the force resisted by the oscillator decreases to zero. Comparisons of peak displacement response are of limited value when collapse occurs. Instead, the likelihood of collapse is used to assess the impact of prior damage on response for the Takeda10 models.

Figures 6-51 to 6-53 plot the ratio, d'_d/d_d , of damaged and undamaged peak displacement response for the

Takeda10 oscillators having $DDD = 2$. Collapse of the damaged oscillators (whether the corresponding undamaged oscillator collapsed or not) is indicated by a ratio equal to six, and collapse of the undamaged oscillators is indicated by a ratio equal to zero. Approximately 10% of the oscillators having $DDD = 2$ collapsed with no prior damage. This indicates that structures characterized by negative post-yield stiffnesses must remain nearly elastic if collapse is to be avoided. Prior ductility demand may cause displacement response to either increase or decrease for those oscillators that do not collapse.

Figure 6-54 plots the displacement time-history of a one-second oscillator having $DDD = 8$ and PDD ranging from 0 (undamaged) to 8, subjected to the NS component of the 1940 El Centro record. It can be observed that prior ductility demand helps to avoid collapse in some cases, and may cause collapse in others.

6.4.4 Response Statistics

Summary response statistics were prepared to identify general trends in the data.

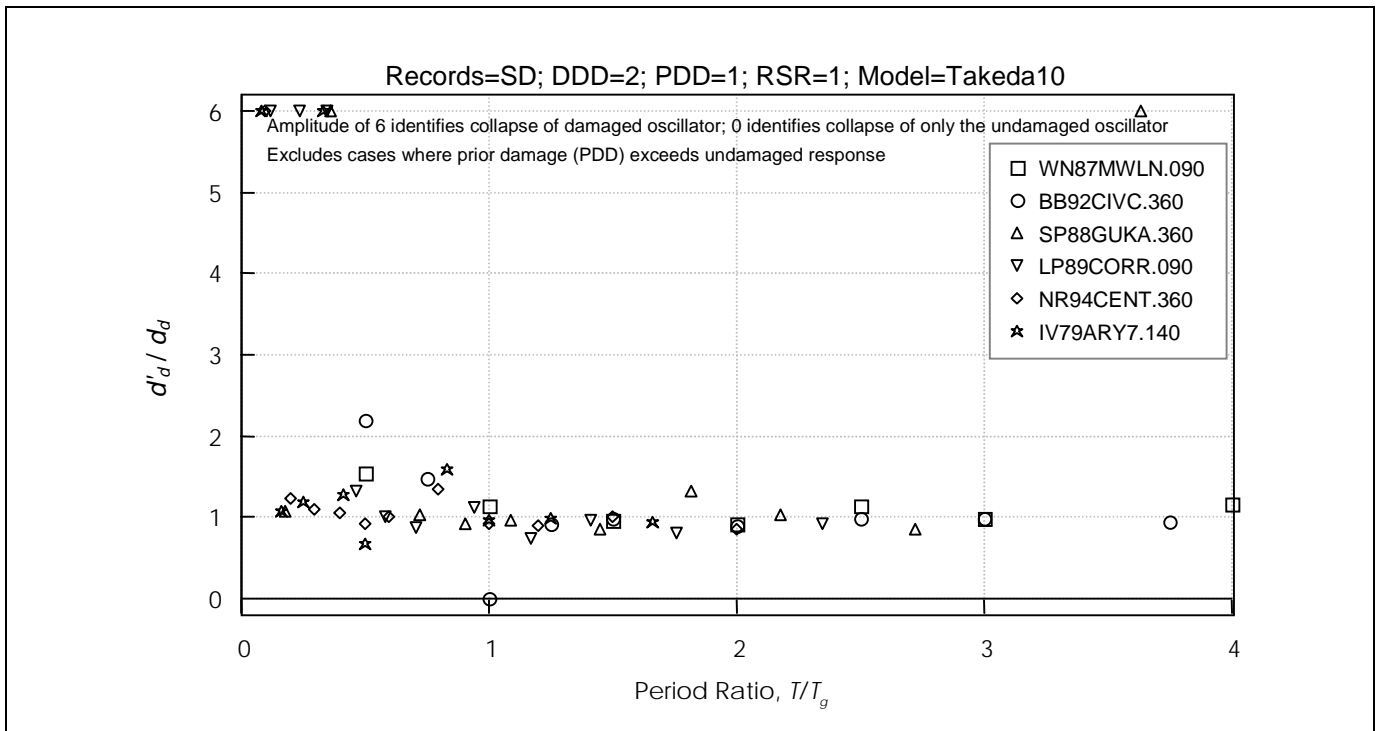


Figure 6-51 Effect of Cracking on Displacement Response of Takeda10 Model for Short Duration Records ($DDD = 8$ and $PDD = 1$)
 $DDD =$ Design Displacement Ductility; $PDD =$ Prior Ductility Demand; $RSR =$ Reduced Strength Ratio

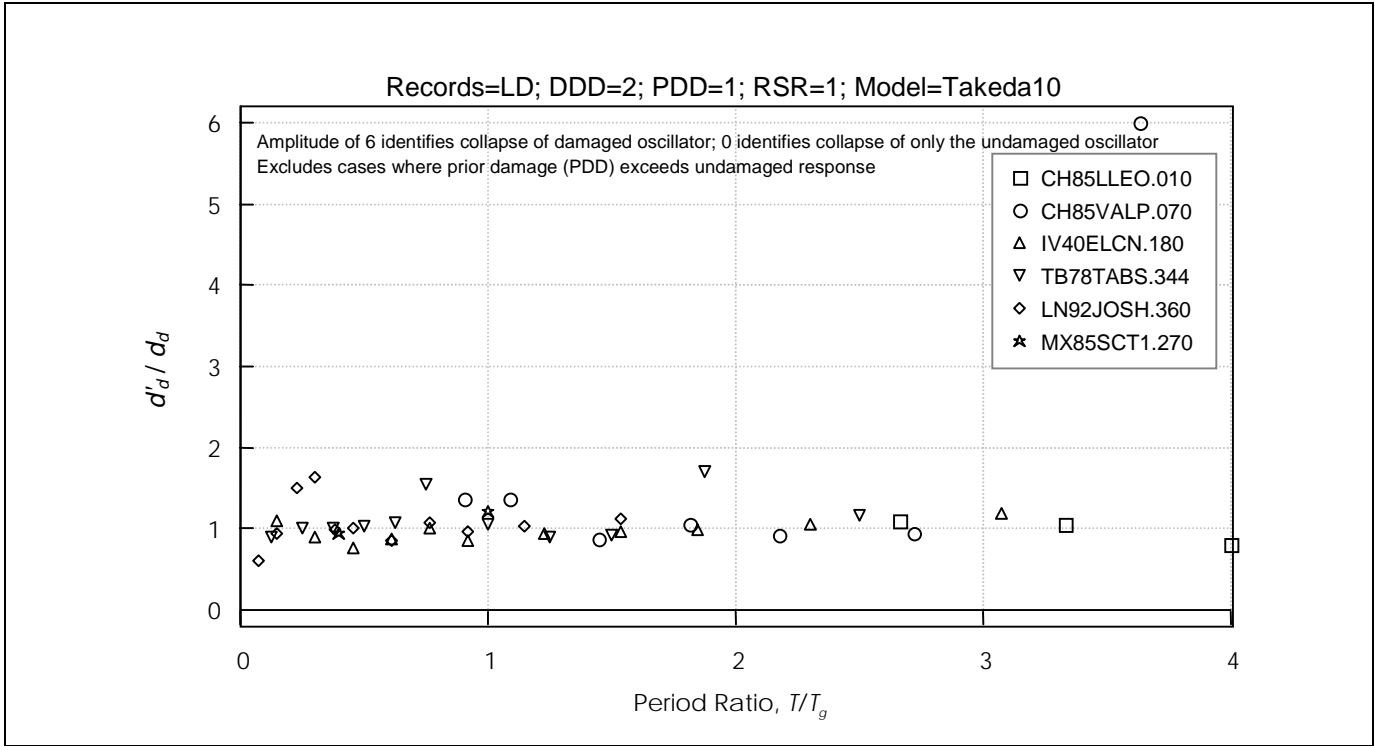


Figure 6-52 Effect of Cracking on Displacement Response of Takeda10 Model for Long-Duration Records (DDD= 8 and PDD=1)
 DDD = Design Displacement Ductility; PDD = Prior Ductility Demand; RSR = Reduced Strength Ratio

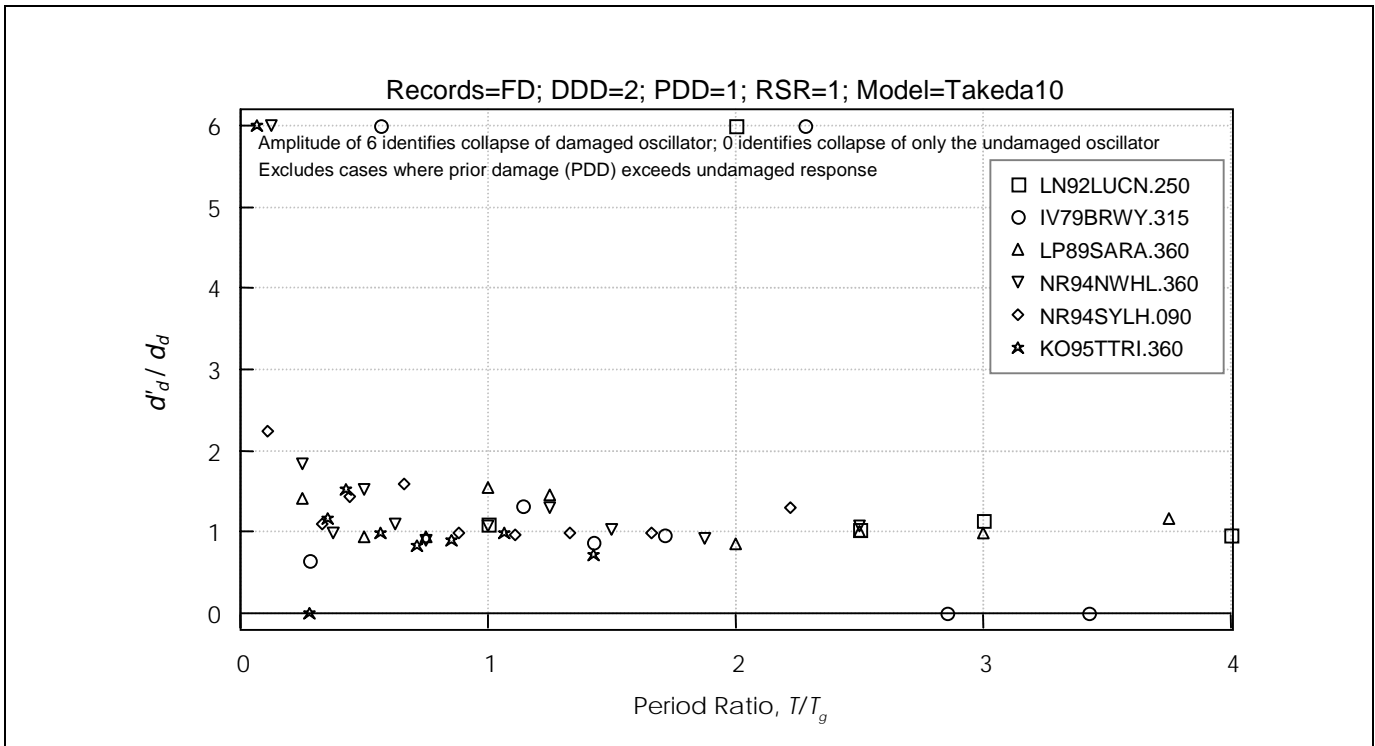


Figure 6-53 Effect of Cracking on Displacement Response of Takeda10 Model for Forward Directive Records (DDD= 8 and PDD=1)
 DDD = Design Displacement Ductility; PDD = Prior Ductility Demand; RSR = Reduced Strength Ratio

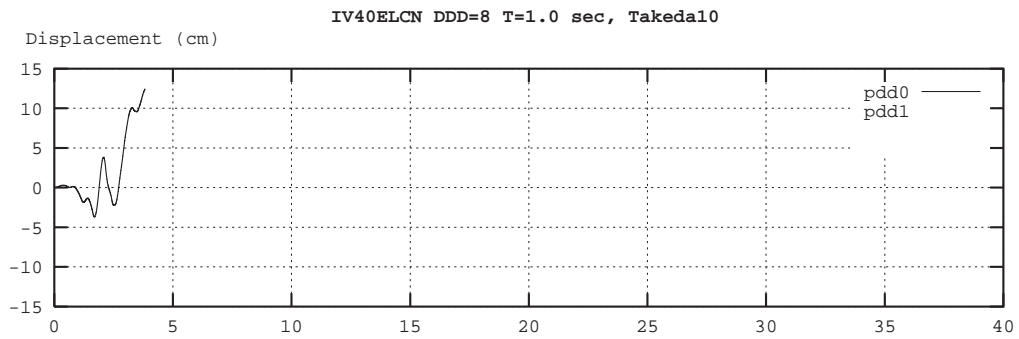


Figure 6-54 Effect of Damage on Response of Takeda10 Model to El Centro (IV40ELCN.180) for T=1.0 sec and RSR= 1 (DDD= 8)
DDD = Design Displacement Ductility

The left side of Figure 6-55 plots mean values of the ratio of damaged and undamaged oscillator peak displacement response, d'_d/d_d , as a function of DDD and PDD, for RSR = 1, 0.8, and 0.6, for the Takeda5 model. The right side of this figure plots mean-plus-one standard deviation values of d'_d/d_d . Figure 6-56 plots similar data, but for the TakPinch model. Mean displacement ratios d'_d/d_d for the Takeda5 and TakPinch models are only slightly affected by PDD and DDD, for RSR = 1. Mean displacement ratios of the TakPinch oscillators increase slightly as RSR decreases.

In Figure 6-55 it can be seen that strength reduction can have a significant effect on the mean displacement ratio d'_d/d_d for the Takeda5 oscillators. However, if the damaging earthquake reduces oscillator strength, then surely the undamaged structure would experience

strength degradation during the performance-level event. Thus, the comparison of d'_d with d_d does not provide a sufficient basis to determine the effect of strength degradation on response. Comparing response of structures having reduced strength, both with and without prior ductility demands would provide more meaningful information. Comparing data for RSR = 0.6 or 0.8, one can see in Figure 6-55 that the effect of PDD is to reduce the mean displacement ratio for Takeda5 oscillators. The capacity curve developed for a structure should incorporate strength degradation when it is anticipated.

The above discussion has focused on mean ratios of d'_d/d_d . Variability of this ratio, plotted as mean plus one standard deviation values on the right sides of Figures 6-55 and 6-56, indicates that response of a

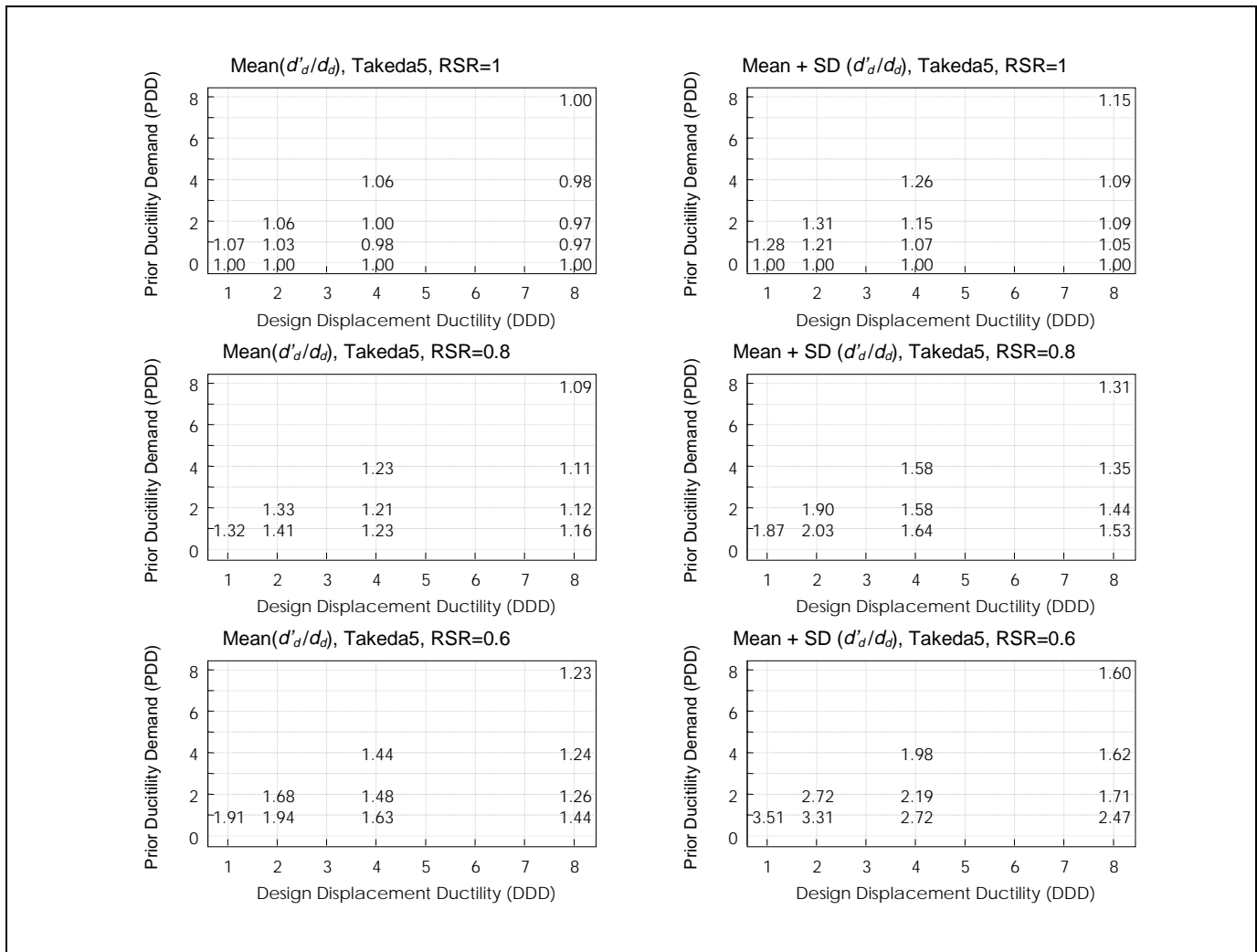


Figure 6-55 Mean and Standard Deviation Values of d'_d/d_d for Takeda5 Model.

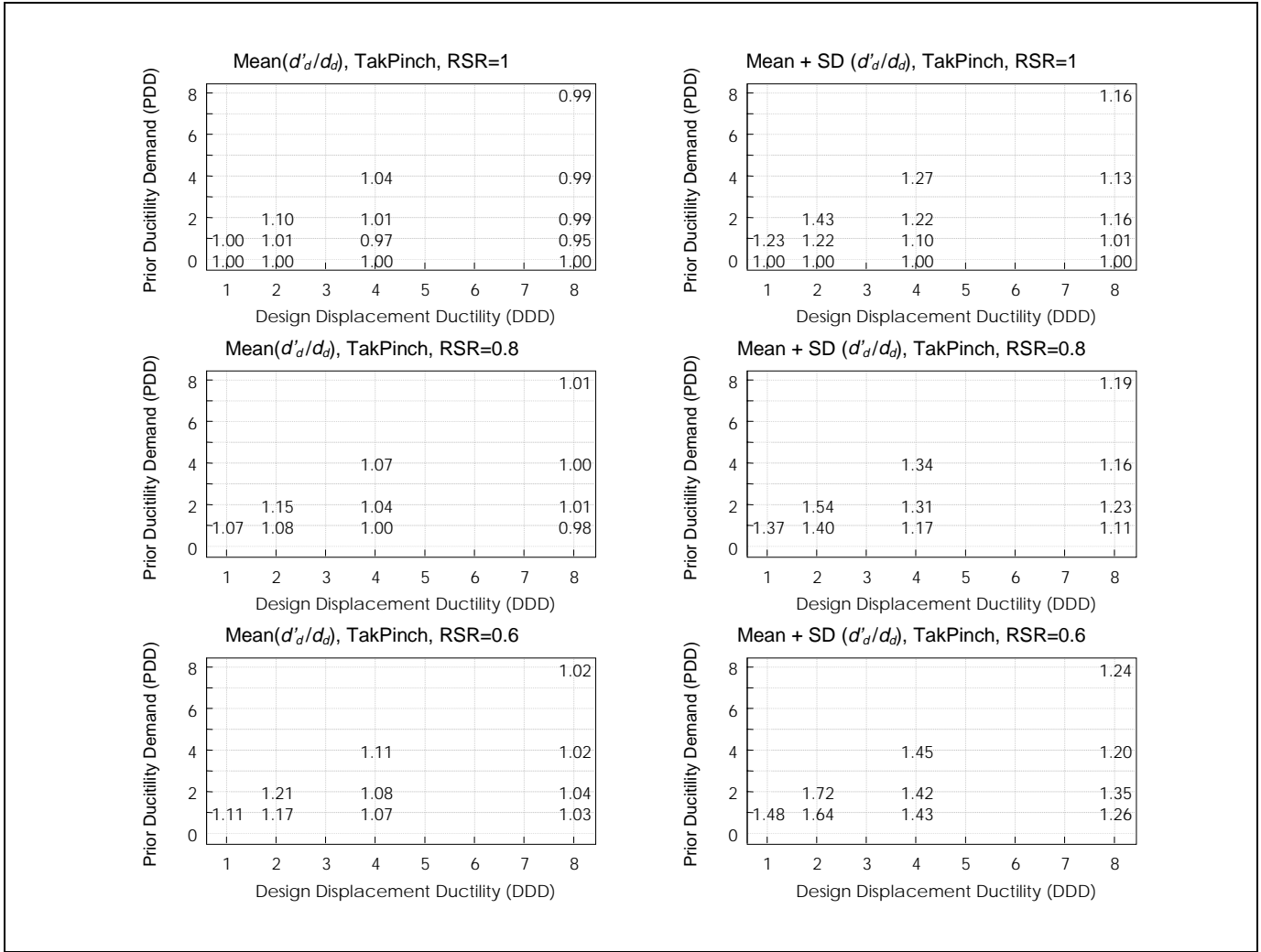


Figure 6-56 Mean and Standard Deviation Values of d'_d/d_d for TakPinch Model.

damaged structure to a given earthquake varies relative to the response in the initially-undamaged state. However, this variability is insignificant in the context of variability arising from other sources. For example, the hysteresis model and earthquake ground motion have a greater effect on response displacements than the variability arising due to prior damage. Figures 6-32 to 6-34 indicate how different the peak displacement response of undamaged Takeda and bilinear models can be to a given earthquake.

Figure 6-57 shows the percentage of Takeda10 oscillators that reached their collapse displacement. It can be observed that 10% or more of those structures designed to achieve a displacement ductility of two collapsed. This indicates the need to ensure that structures having negative post-yield stiffnesses remain nearly elastic if collapse is to be avoided. Strength

reduction tends to increase the tendency of the oscillators to collapse. No clear trend emerges as to the effect of PDD on the tendency of these oscillators to collapse.

6.5 Nonlinear Static Procedures

6.5.1 Introduction

Nonlinear static analysis is used to estimate inelastic response quantities without undertaking the effort required for inelastic dynamic analyses. Several methods are presently in use. No consensus has emerged as to the applicability and relative accuracy of the methods, which are collectively known as nonlinear static procedures (NSP). These procedures each focus

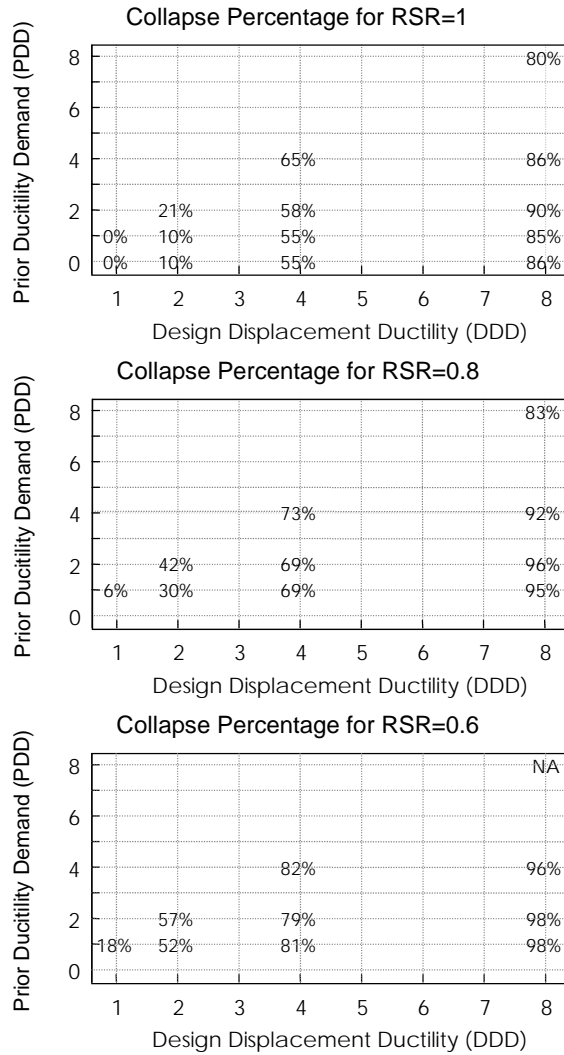


Figure 6-57 Percent of Takeda10 Oscillators that Collapsed

on different parameters for determining estimates of peak displacement response. Consequently, NSP displacement estimates may be affected to different degrees by differences in hysteretic model, initial stiffness, lateral strength, and post-yield stiffness.

Section 6.5.2 describes three nonlinear static methods; displacement coefficient, secant, and capacity spectrum methods. Differences among the methods and the implications for estimating displacements are discussed in Section 6.5.3. Assumptions made to extend the methods to cases with prior damage are discussed in Section 6.5.4. Displacement estimates obtained using

NSP are compared with values computed from dynamic analyses in Section 6.6.

6.5.2 Description of Nonlinear Static Procedures

The methods are briefly described in this section for cases assumed to correspond most closely to the dynamic analysis framework of Section 6.3.3, representing wall buildings at the collapse prevention performance level. The reader is referred to FEMA 273 for greater detail on the displacement coefficient method, and to ATC-40 for greater detail on the secant and capacity spectrum methods. The displacement

coefficient method described here is the same as in FEMA 273.

6.5.2.1 Displacement Coefficient Method

The displacement coefficient method estimates peak inelastic displacement response as the product of a series of coefficients and the elastic spectral displacement. The peak displacement estimate, d_d , is given by

$$d_d = C_0 C_1 C_2 C_3 S_a \left(\frac{T_e}{2\pi} \right)^2 \tag{6-2}$$

where coefficients C_0 through C_3 modify the spectral displacement, given by the product of the elastic spectral acceleration, S_a , and $(T_e/2\pi)^2$, where T_e is an effective period based on the effective stiffness determined using the construction of Figure 6-58. In the above, C_0 relates the spectral displacement and the expected roof displacement, and is set at 1 for SDOF systems. The coefficient C_1 accounts for the amplification of peak displacement for short-period systems, is set at 1 for $T_e > T_g$, and is computed as follows for $T_e < T_g$:

$$C_1 = \frac{1}{R} + \left(1 - \frac{1}{R} \right) \frac{T_g}{T_e} \tag{6-3}$$

where R = the strength-reduction factor, given by the ratio of the elastic base shear force and the effective

yield strength, F_{ye} , illustrated in Figure 6-58. An optional limit of 2 on C_1 was not applied in the analyses described here.

The coefficient C_2 accounts for the type of hysteretic response. At the collapse prevention performance level, C_2 varies linearly between 1.5 at 0.1 sec and 1.2 at T_g , and remains at 1.2 for T_e greater than T_g .

The coefficient C_3 accounts for increases in displacements that arise when $P-\Delta$ effects are significant. Because the dynamic analyses did not include second-order effects, C_3 was assigned a value of 1. However, the Takeda 10 models had a negative post-yield stiffness of 10 percent, which approximates $P-\Delta$ effects

6.5.2.2 Secant Method

The secant method assumes that the peak displacement response of a nonlinear system can be estimated as the peak response of an elastic system having increased period. An idealized lateral-force/displacement curve for the structure is developed using a static “pushover” analysis. The elastic response of the structure is computed using a response-spectrum analysis, using initial component stiffness values. The resulting elastic displacements are used to obtain revised stiffness values for the components, set equal to the secant stiffness defined at the intersections of the component force/displacement curves and the elastic displacements obtained from the response-spectrum analysis. Using these revised stiffness values, another response-spectrum analysis is performed, and iterations continue

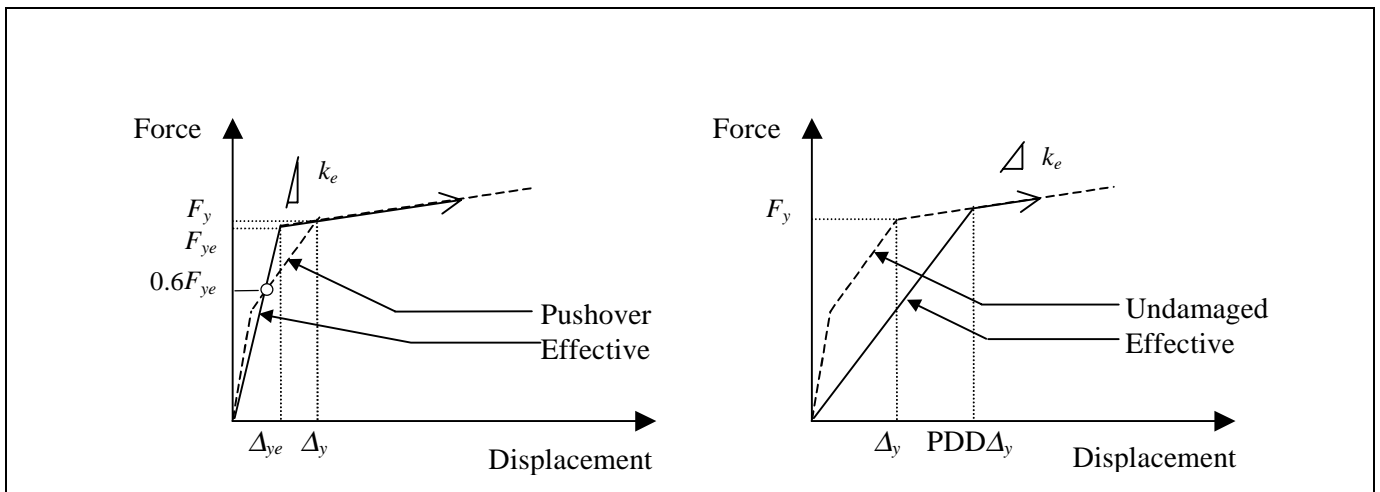


Figure 6-58 Construction of Effective Stiffness for use with the Displacement Coefficient Method

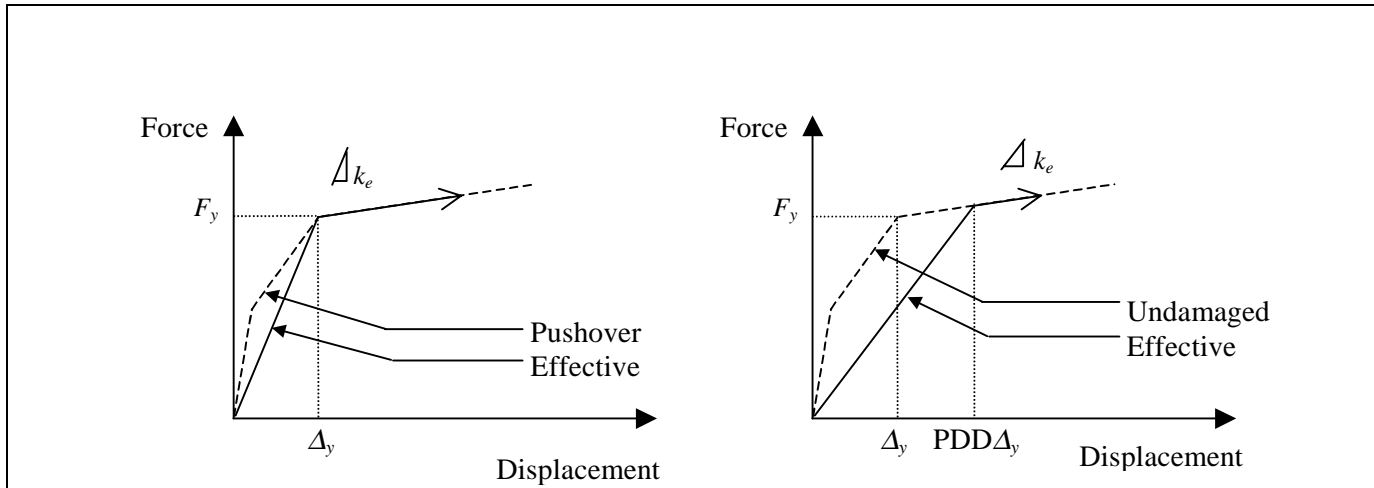


Figure 6-59 Initial Effective Stiffness and Capacity Curves Used in the Secant and Capacity Spectrum Methods

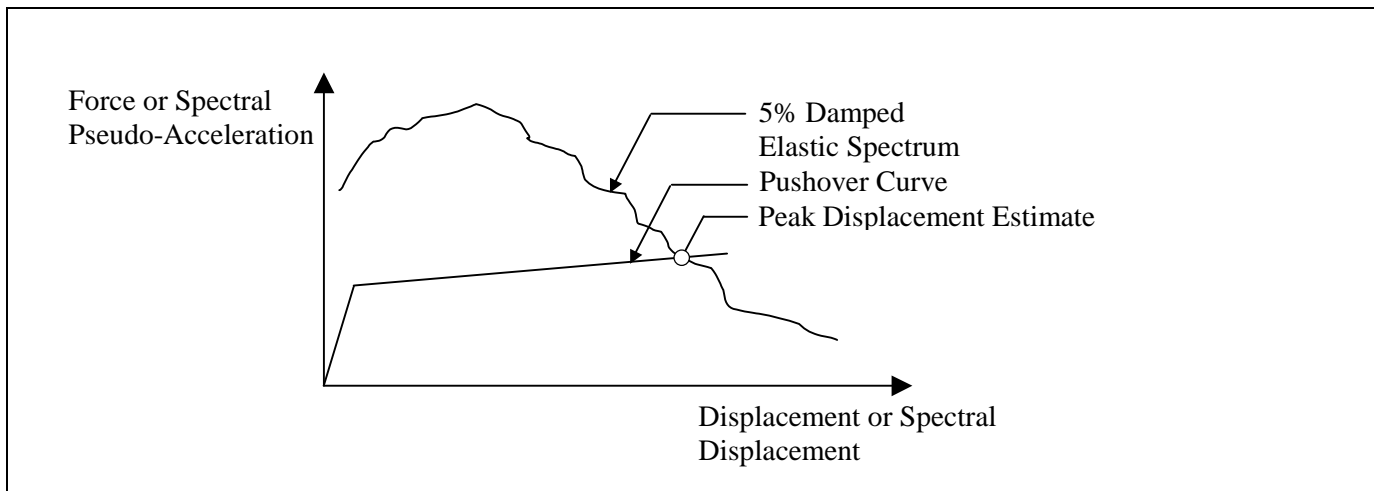


Figure 6-60 Schematic Depiction of Secant Method Displacement Estimation

until the displacements converge. All response-spectrum analyses are made for 5% damping in the secant method, as described in ATC-40.

For SDOF structures, the secant method can be implemented in spectral pseudo-acceleration–spectral displacement space, much like the capacity spectrum method. The force/displacement curve may be determined using the constructions of Figure 6-59 for both the undamaged and damaged oscillators. This curve is plotted together with the elastic response spectrum for 5% damping in Figure 6-60. An estimate of peak displacement is indicated in the figure. For the undamaged oscillators, an initial estimate of peak displacement response is the peak response of an elastic oscillator having stiffness equal to the initial stiffness of the oscillator. The intersection of the previous displacement estimate with the idealized force/displacement curve of the structure defines a new secant

stiffness. This stiffness may be used to obtain a revised estimate of peak displacement response. These iterations continue until satisfactory convergence occurs. This is shown schematically in Figure 6-61.

6.5.2.3 Capacity Spectrum Method

Like the secant method, the capacity spectrum method assumes that the peak displacement response of a nonlinear system can be estimated by an elastic system having reduced stiffness. The difference is that the elastic spectral-response values are modified to reflect increases in damping associated with inelastic response. A lateral force “pushover” curve is developed for the structure and plotted on spectral pseudo-acceleration–spectral displacement coordinates. The structure is assumed to displace until it reaches an elastic demand curve that has damping that corresponds to a value based on the current displacement estimate.

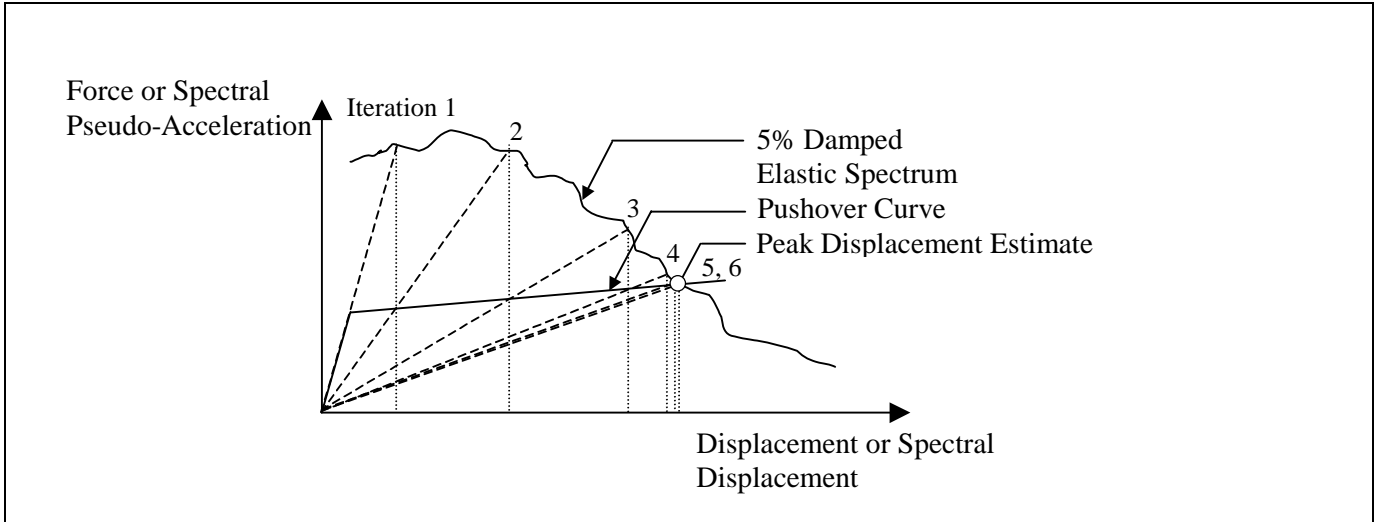


Figure 6-61 Schematic Depiction of Successive Iterations to Estimate Displacement Response Using the Secant Method for Single-Degree-of-Freedom Oscillators

The method may be implemented by successively iterating displacement response. The initial displacement is estimated using the initial stiffness of the structure and assuming elastic response for damping equal to 5% of critical damping. The intersection of the displacement estimate and the idealized force/displacement curve determines a revised estimate of the secant stiffness. Effective viscous damping is revised prescriptively, based on the displacement estimate. This calculation represents the increase in effective damping with increased hysteretic losses. The iterations continue until satisfactory convergence is obtained. Figure 6-62 illustrates the application of the method.

6.5.3 Comments on Procedures

From the above descriptions, it is clear that there are fundamental differences among the various NSPs. The displacement coefficient method primarily relies on the initial effective stiffness to determine a baseline spectral displacement, and it considers strength to a lesser extent for short-period structures.

The secant and capacity spectrum methods are insensitive to initial stiffness (for structures that yield), and displacement estimates depend primarily on yield strength and post-yield stiffness. Effective damping varies with displacement amplitude in the capacity

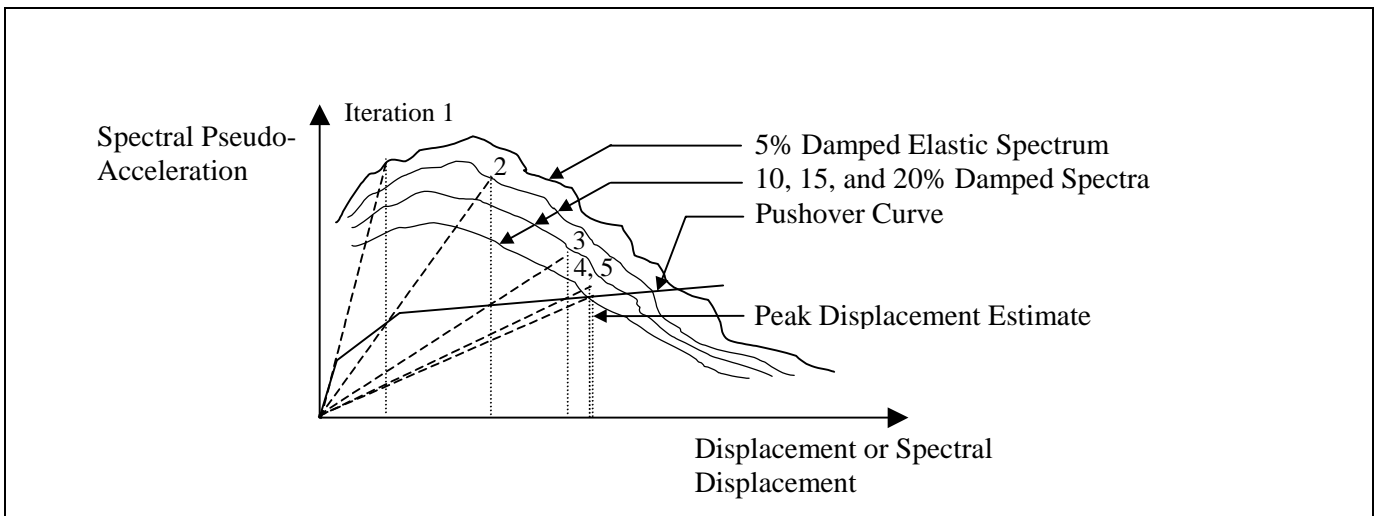


Figure 6-62 Schematic Depiction of Successive Iterations to Estimate Displacement Response Using the Capacity Spectrum Method

spectrum method, while it is invariant in the secant method. In the form presented in ATC-40, secant method displacement estimates are independent of hysteretic model. Through changes in coefficient C_2 , changes in the force/displacement model may be incorporated in the displacement coefficient method. Differences in hysteresis model are accounted for in the capacity spectrum method adjusting effective damping for three “structural behavior types.”

6.5.4 Application of Procedures to Undamaged and Damaged Oscillators

Each procedure presumes that a smoothed, elastic design response spectrum is to be used in practice. To avoid uncertainties in interpretation of results, the actual pseudo-acceleration spectra were used in place of a smoothed approximation in this study. For the capacity spectrum method, the actual pseudo-acceleration spectra were computed for a range of damping levels, and the spectral reduction factors that are prescribed for use with smoothed design spectra were not employed. These modifications introduce some scatter in the resulting displacement estimates that would not occur if smoothed spectra had been used. Thus, some “smoothing” of the data may be appropriate when interpreting the results.

The NSPs were developed for use with undamaged structures. In this study, the NSPs were applied to the initially-damaged structures using the assumptions described below, representing one of many approaches that can be taken. Recommended procedures for estimating displacements are described in Section 4.4 of FEMA 306.

For the displacement coefficient method, the capacity curve was obtained by the procedure described in FEMA 273. For the uncracked oscillators, a bilinear curve was fit, crossing at 60% of the bilinear curve yield strength. For the damaged oscillators, the effective period of vibration was set at the initial period of the damaged oscillators. Displacements were amplified by the factor C_1 without imposing the optional limit of 2 specified in the provisions.

The secant method was applied iteratively. For undamaged oscillators, the initial stiffness was the yield-point secant stiffness. For damaged oscillators, it was set at the secant stiffness obtained at the displacement imposed by prior ductility demands. The

initial stiffness of the damaged oscillators therefore reflected the previous damage.

The capacity spectrum method was also applied iteratively, beginning with the same initial oscillator stiffness used in the secant method. Effective damping was determined by using the yield point of the undamaged oscillators. The capacity spectrum method was implemented for an intermediate “building characteristic,” identified as Type B. This type is considered to represent average existing buildings subjected to short-duration motions and new buildings subjected to long-duration motions. For this type, effective damping is limited to 29% of critical damping.

For both the capacity spectrum and the secant stiffness methods, 10 iterations were performed for each structure. These iterations generally converged on a single result, and differences in successive approximations were typically less than 1%. On occasion, differences in successive approximations were large, suggesting a lack of convergence due to the jagged nature of the actual (not smoothed) spectra. Where these differences occurred, the displacement estimate at the tenth iteration was retained.

6.6 Comparison of NSP and Dynamic Analysis Results

6.6.1 Introduction

In evaluating the utility of the NSPs, attention may be directed at two estimates. The first is peak displacement response; it could be expected that an acceptable procedure would estimate the peak displacement response, d_d , of a nonlinear system within acceptable limits of accuracy. Second, it is possible that a procedure may be systematically biased, and hence may estimate displacement response poorly while providing reasonable estimates of displacement ratio; that is, the ratio of damaged structure displacement to undamaged structure displacement, d'_d/d_d . These response indices, d_d and d'_d/d_d , are examined in detail in the following sections for Takeda oscillators designed for bilinear DDDs of 8.

6.6.2 Displacement Estimation

Peak displacement response of the undamaged Takeda oscillators was estimated for each earthquake record. The ratio of the peak displacement estimate from NSP

and the value computed for each Takeda5 oscillator, at each period and for each ground motion record, is plotted in Figure 6-63 for $DDD = 8$ and $RSR = 1$. The log scale plots the ratio of estimated and computed displacement, $d_{d,NSP}/d_d$. Plots are presented for each ground motion category and for each NSP.

In Figure 6-63, it can be observed that the ratio of the estimated and computed displacements, $d_{d,NSP}/d_d$, can vary significantly, ranging from less than 0.3 to more than 100. At any period ratio, the ratio $d_{d,NSP}/d_d$ may approach or exceed an order of magnitude. Because the trends tend to be consistent for each ground motion record, the jaggedness of the actual spectra does not appear to be the source of most of the variability.

Figure 6-64 plots mean values of ratios $d_{d,NSP}/d_d$ determined for each NSP, for all ground motions and all DDD values. Results for short- and long-period Takeda5 oscillators are plotted separately. In Figure 6-64, it can be observed that the NSP procedures tend to overestimate, in a mean sense, the displacements computed for the short-period Takeda5 oscillators for all DDD . Takeda oscillators having $DDD = 1$ often displaced less than their bilinear counterparts because the Takeda oscillators had initial stiffness equal to twice that of their bilinear counterparts. The difference in initial stiffness explains the tendency of the NSP methods to overestimate displacements for low DDD . This is particularly true for the secant method estimates of short-period oscillators, for which mean ratios exceeded six for DDD greater than 1. The period ratio, T_e/T_g , marking the boundary of the elevated estimates tends to be less than one, possibly reflecting the effective increase in period of Takeda5 oscillators as their stiffness reduces (Figure 6-63).

Figure 6-64 indicates that each NSP tends to overestimate the displacement response of short-period oscillators and that the capacity spectrum method is most accurate for long-period Takeda5 oscillators, in a mean sense. Nevertheless, Figure 6-63 indicates the substantial variability in displacement estimates and the potential to overestimate or underestimate displacements with all methods. A single estimate cannot capture the breadth of response variability that may occur at a given site.

Based on Figures 6-63 and 6-64, the coefficient and capacity spectrum methods appear to be reasonably accurate and to have the least scatter. The secant method

tended to overestimate displacement and exhibited more scatter in values of $d_{d,NSP}/d_d$.

6.6.3 Displacement Ratio Estimation

The ratio of damaged oscillator displacement, d'_d , and the displacement of the corresponding Takeda oscillator having no initial damage, d_d , was estimated using the NSP methods for each Takeda oscillator/earthquake pair, as described in Section 6.5.4. This estimated displacement ratio is compared with the ratio computed from the dynamic analyses in Figures 6-65 through 6-73.

It can be observed that simple application of the displacement coefficient method using the initial stiffness of the undamaged oscillator to calculate d_d and using the reduced stiffness of the damaged oscillator to calculate d'_d almost always overestimates the effects of damage for the cases considered.

Application of the secant and capacity spectrum methods, using the initial and reduced stiffness values, typically led to nearly identical displacement estimates: estimates of d'_d/d_d were often approximately equal to one. Figures 6-68 through 6-73, which might appear to testify to the success of the methods, instead tend more to represent the inverse of the d'_d/d_d as computed for the Takeda models. Figures 6-38 through 6-40 indicate that computed values of d_d/d'_d should tend to be around one, decreasing slightly for small periods.

The preceding plots examine the effectiveness of the methods, as implemented here, for estimating the consequences of prior ductility demand. It is also of interest to examine the effectiveness of the methods in accounting for strength loss. To do this, the ratio of the displacement obtained with $RSR = 0.6$ to that with $RSR = 1.0$ was evaluated for the nonlinear Takeda5 oscillators having $DDD = 8$ and $PDD = 1$, in order to compare the NSP estimates of the displacement ratio with the displacement ratio computed for the nonlinear Takeda5 oscillators. The upper plots in Figures 6-74 through 6-82 show the estimated displacement ratio for one of the three NSPs, and the lower plots of these figures normalize this displacement ratio by the displacement ratio computed for the Takeda5 oscillators. It can be observed that the NSP methods tend to account correctly for the effect of strength reduction on displacement response, in a mean sense.

(Text continued on page 177)

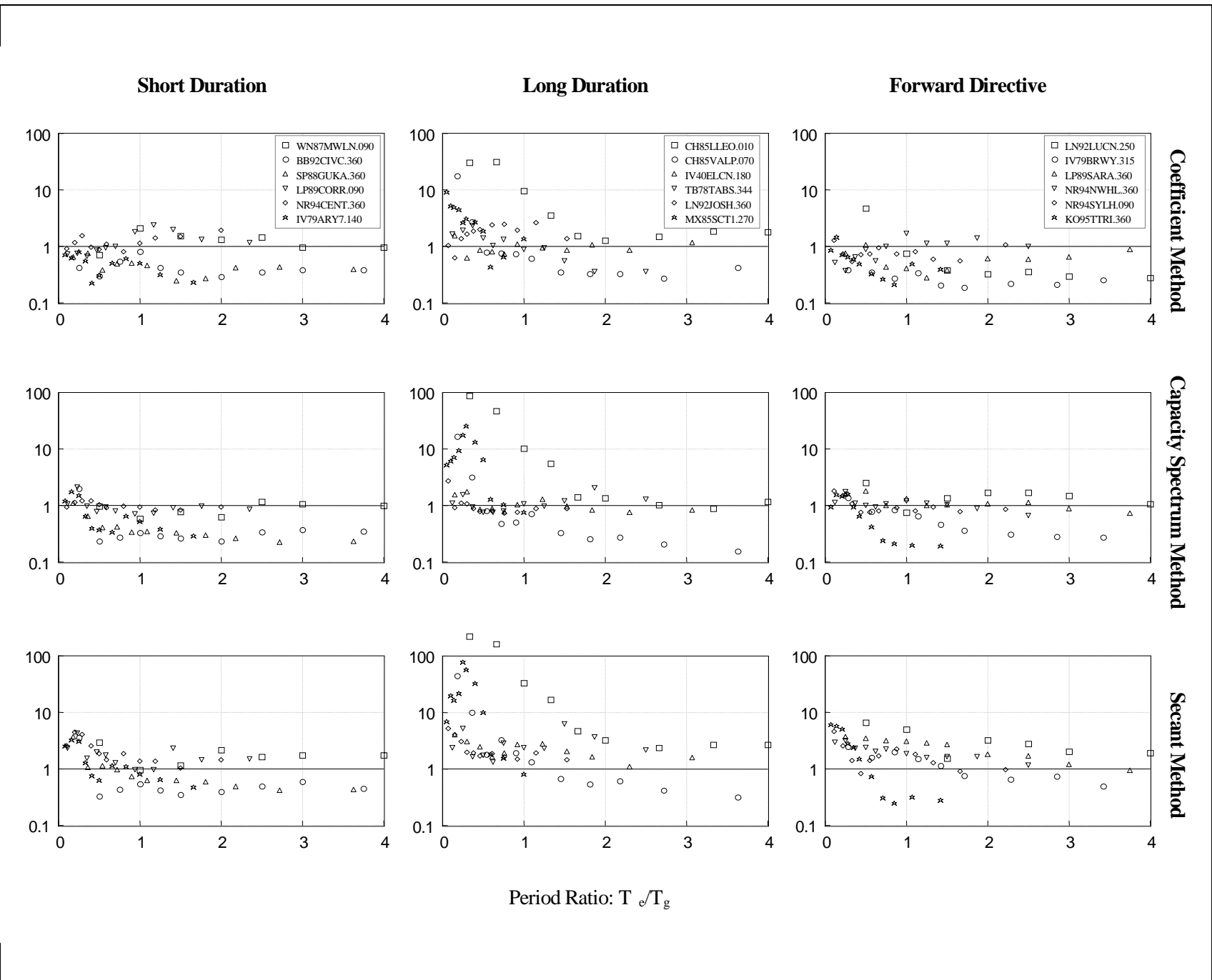


Figure 6-63

Values of d_{nsp}/d_d for the Takeda5 Model

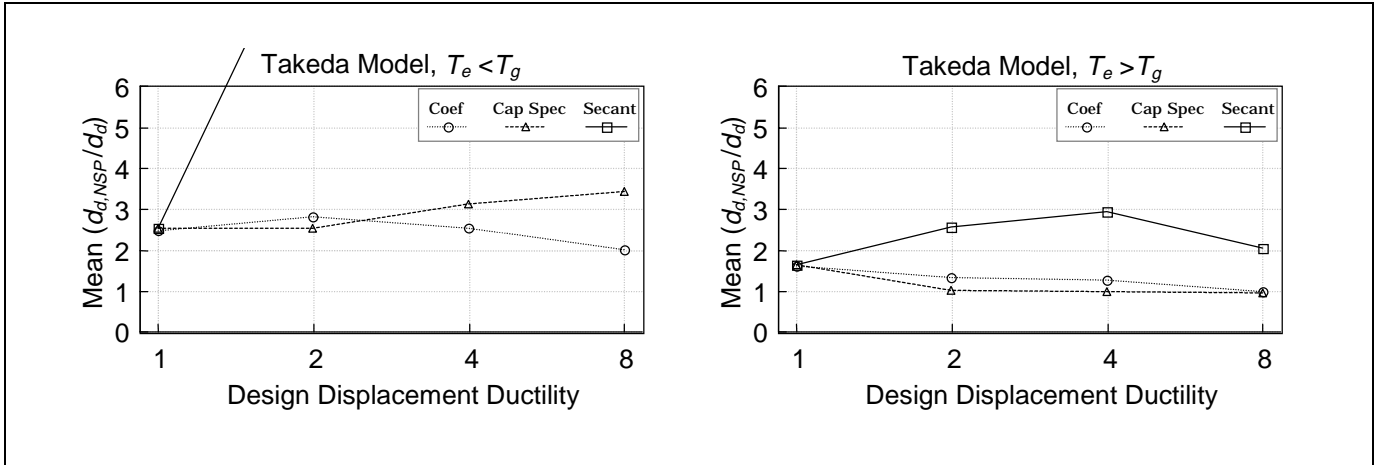


Figure 6-64 Mean values of $d_{d,NSP}/d_d$ for all ground motions for each NSP method, for short and long-period Takeda5 Models. See text in Section 6.6.2.

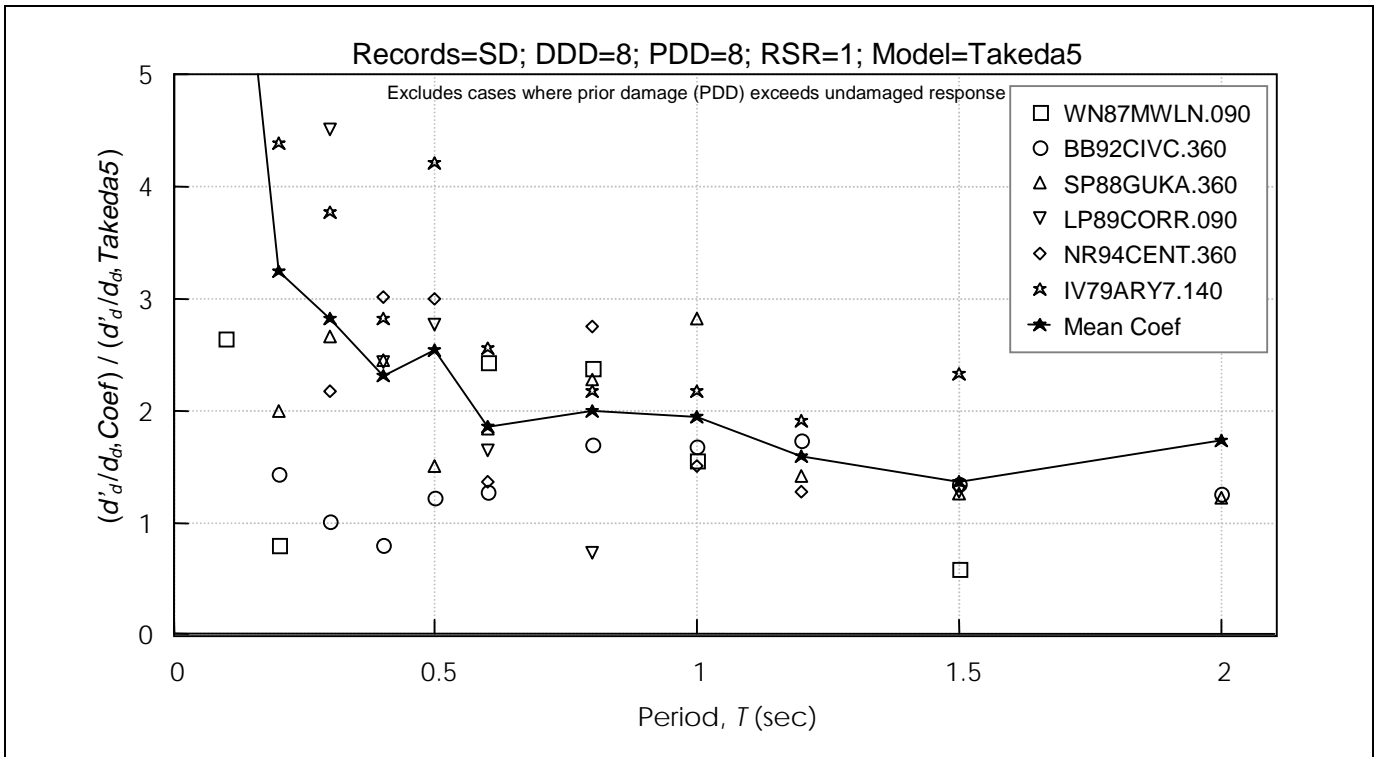


Figure 6-65 Coefficient Method Estimates of Ratio of Damaged and Undamaged Oscillator Displacement Normalized by Computed Ratio, for Short-Duration Records
 DDD = Design Displacement Ductility; PDD = Prior Ductility Demand; RSR = Reduced Strength Ratio

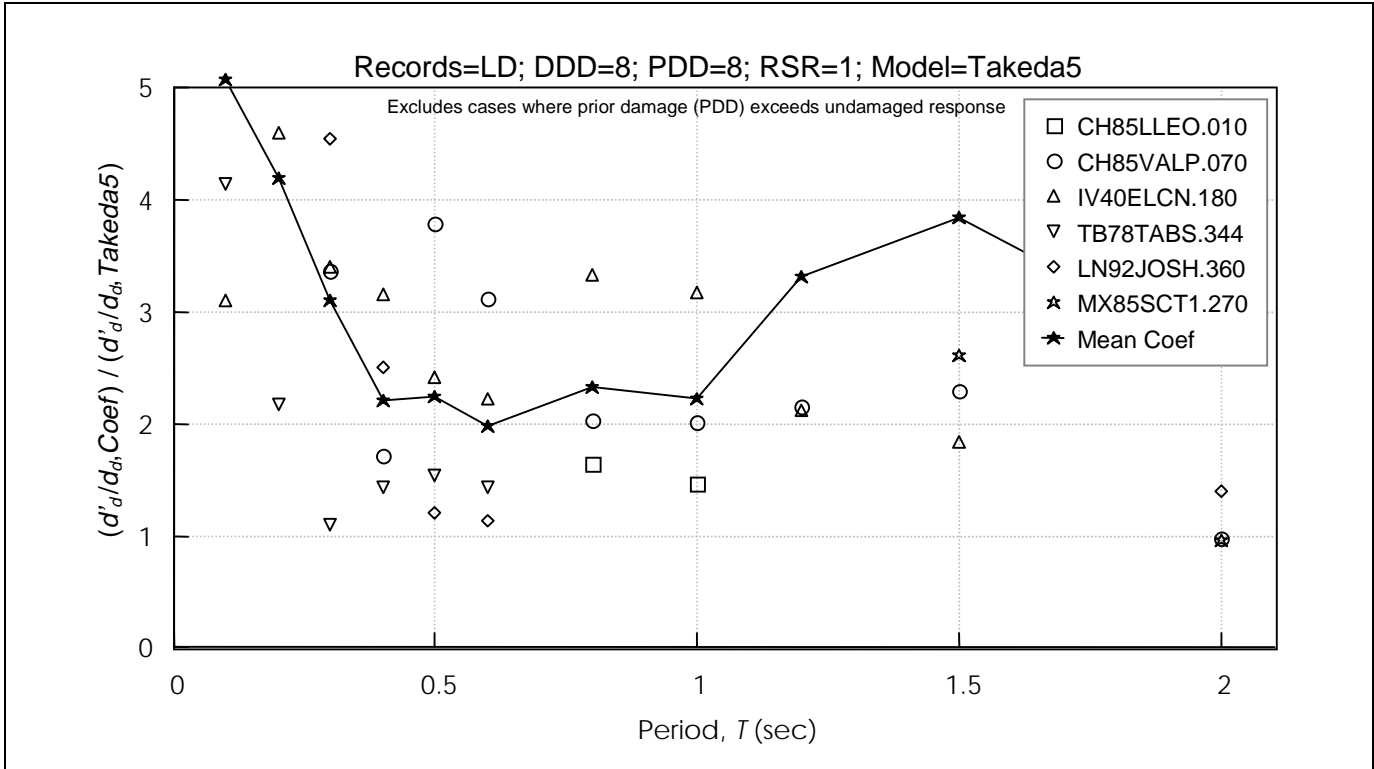


Figure 6-66 Coefficient Method Estimates of Ratio of Damaged and Undamaged Oscillator Displacement Normalized by Computed Ratio, for Long-Duration Records
 DDD = Design Displacement Ductility; PDD = Prior Ductility Demand; RSR = Reduced Strength Ratio

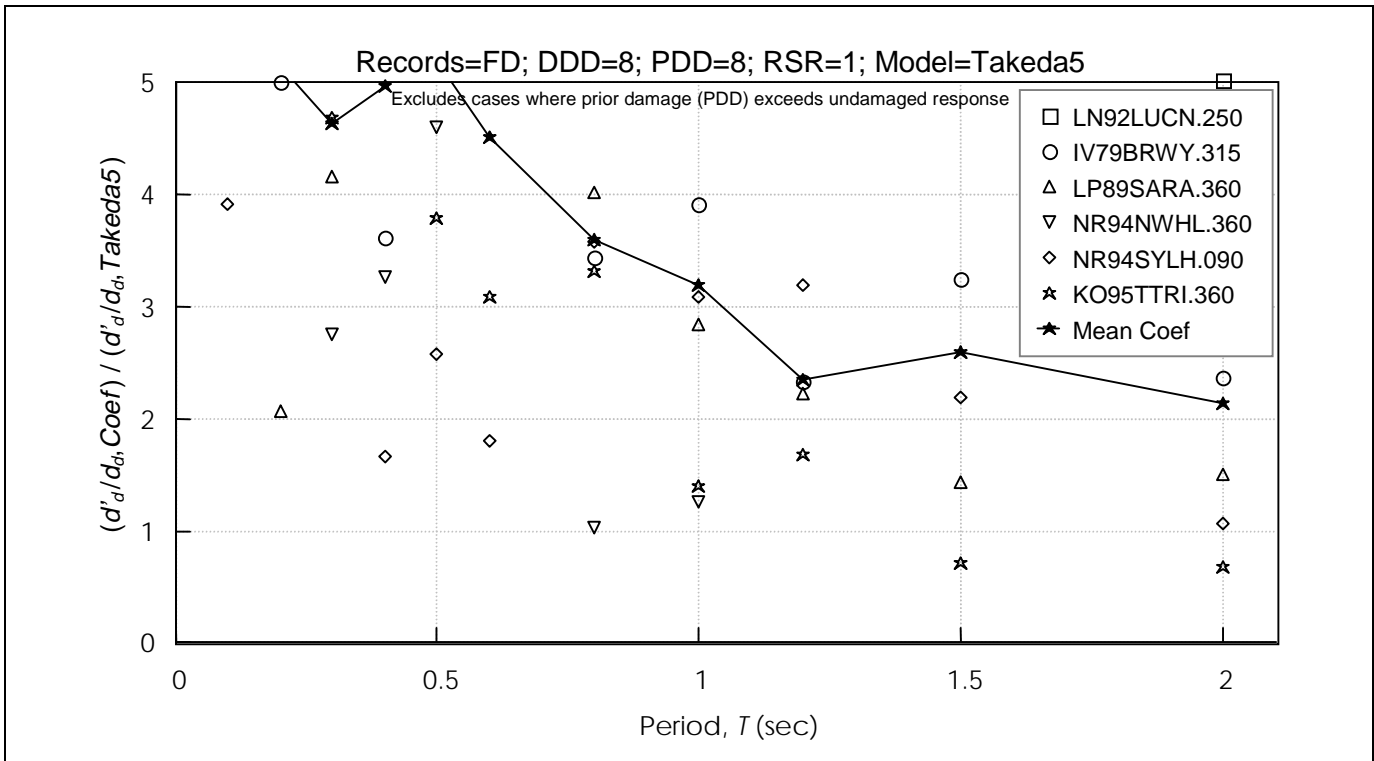


Figure 6-67 Coefficient Method Estimates of Ratio of Damaged and Undamaged Oscillator Displacement Normalized by Computed Ratio, for Forward Directive Records
 DDD = Design Displacement Ductility; PDD = Prior Ductility Demand; RSR = Reduced Strength Ratio

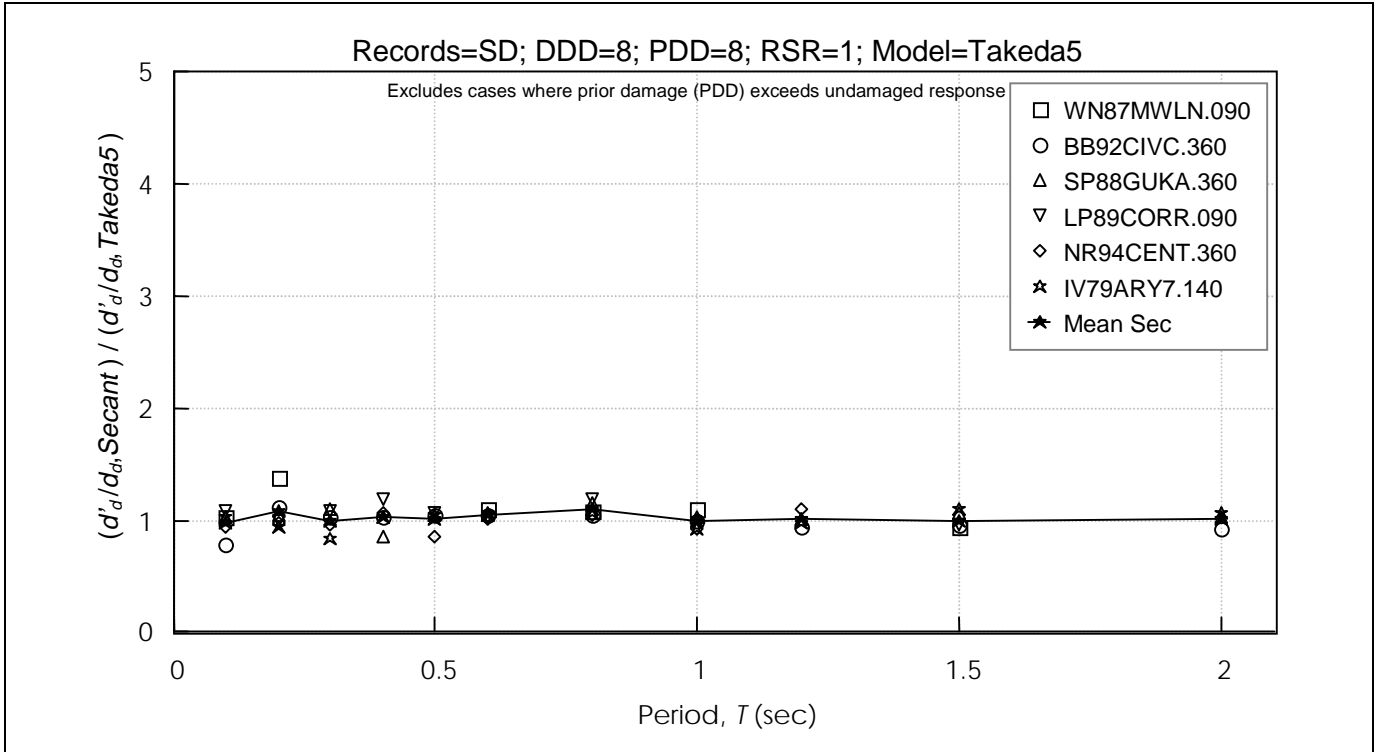


Figure 6-68 Secant Method Estimates of Ratio of Damaged and Undamaged Oscillator Displacement Normalized by Computed Ratio, for Short-Duration Records
 DDD = Design Displacement Ductility; PDD = Prior Ductility Demand; RSR = Reduced Strength Ratio

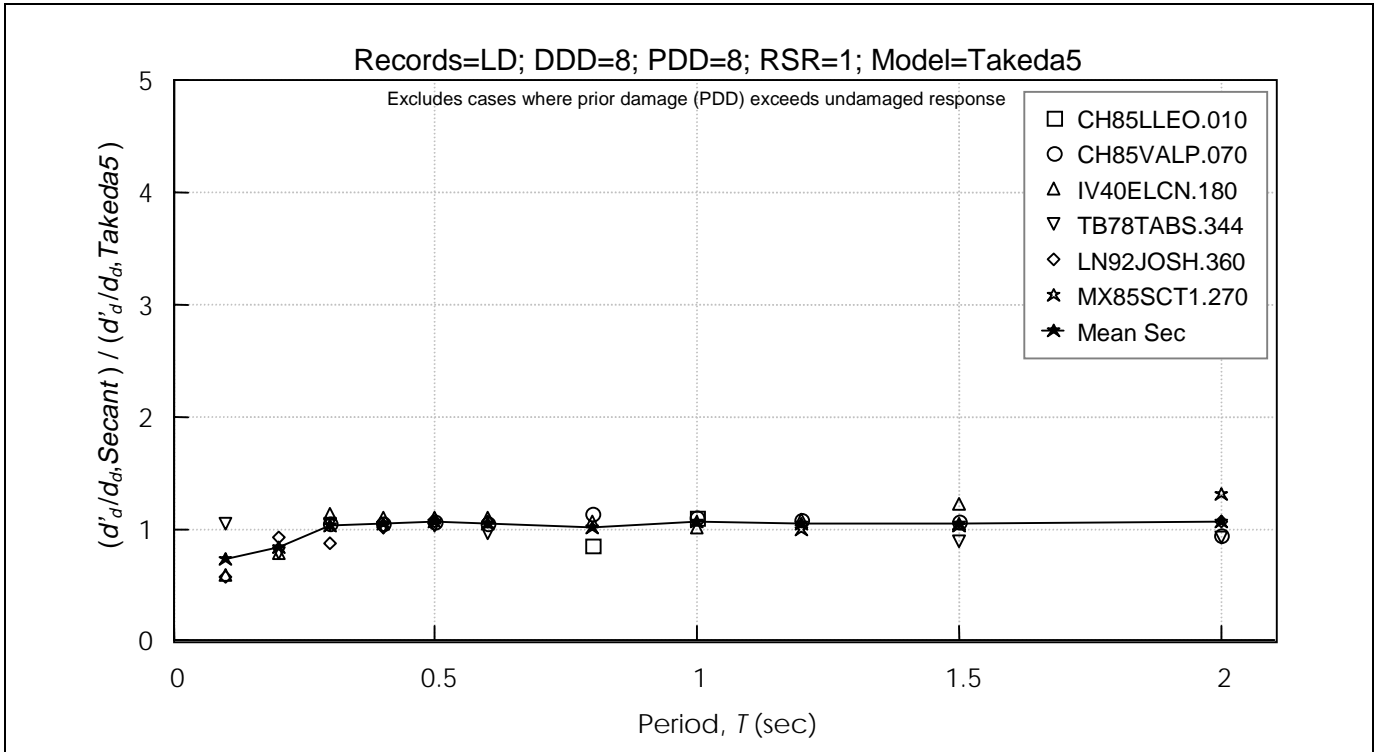


Figure 6-69 Secant Method Estimates of Ratio of Damaged and Undamaged Oscillator Displacement Normalized by Computed Ratio, for Long-Duration Records
 DDD = Design Displacement Ductility; PDD = Prior Ductility Demand; RSR = Reduced Strength Ratio

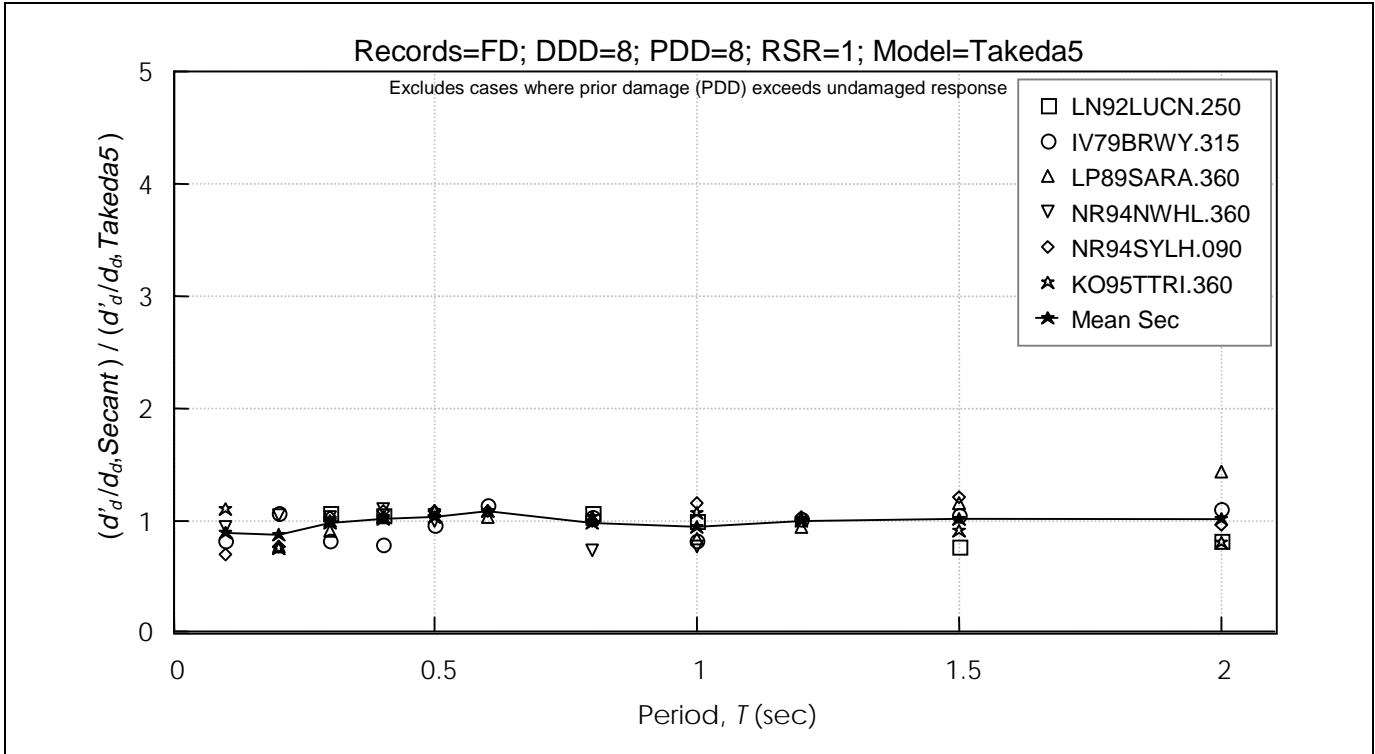


Figure 6-70 Secant Method Estimates of Ratio of Damaged and Undamaged Oscillator Displacement Normalized by Computed Ratio, for Forward Directive Records
 DDD = Design Displacement Ductility; PDD = Prior Ductility Demand; RSR = Reduced Strength Ratio

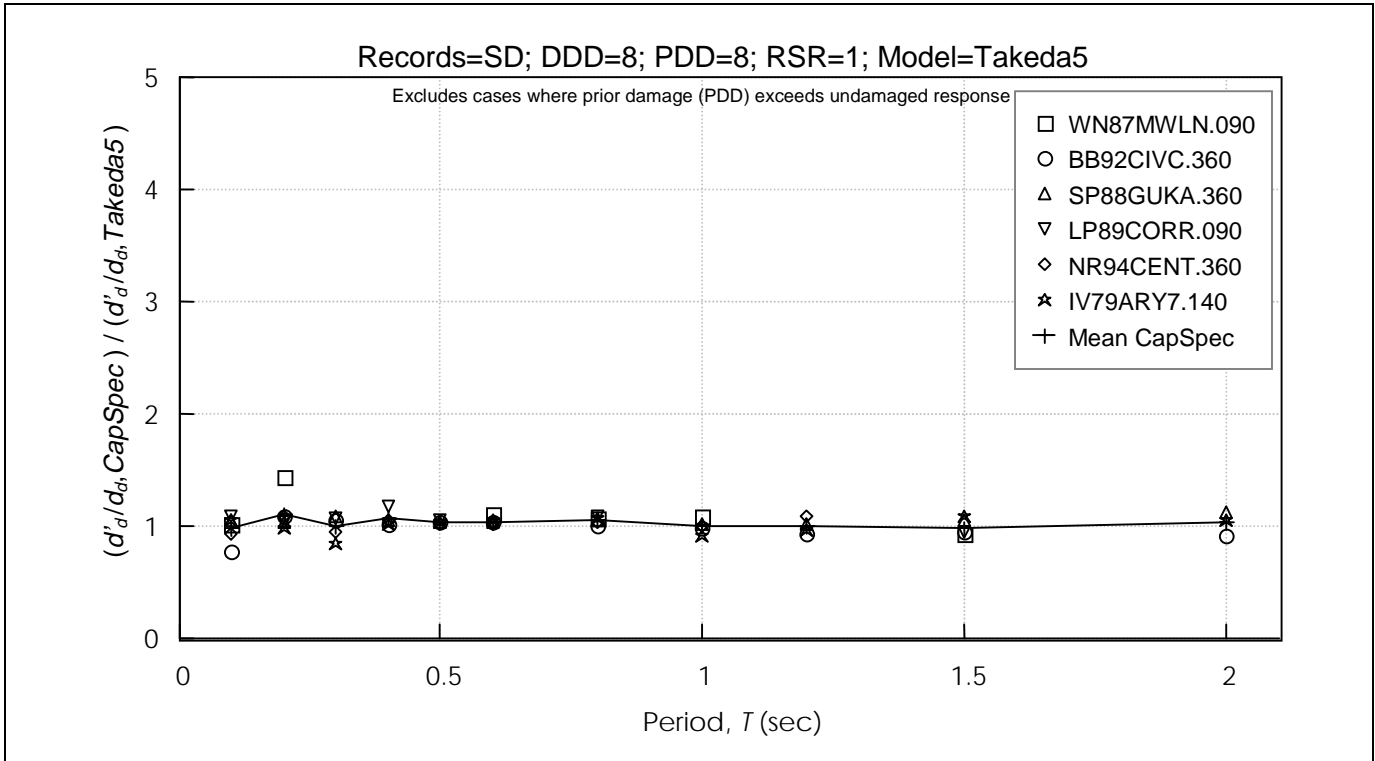


Figure 6-71 Capacity Spectrum Method Estimates of Ratio of Damaged and Undamaged Oscillator Displacement Normalized by Computed Ratio, for Short-Duration Records
 DDD = Design Displacement Ductility; PDD = Prior Ductility Demand; RSR = Reduced Strength Ratio

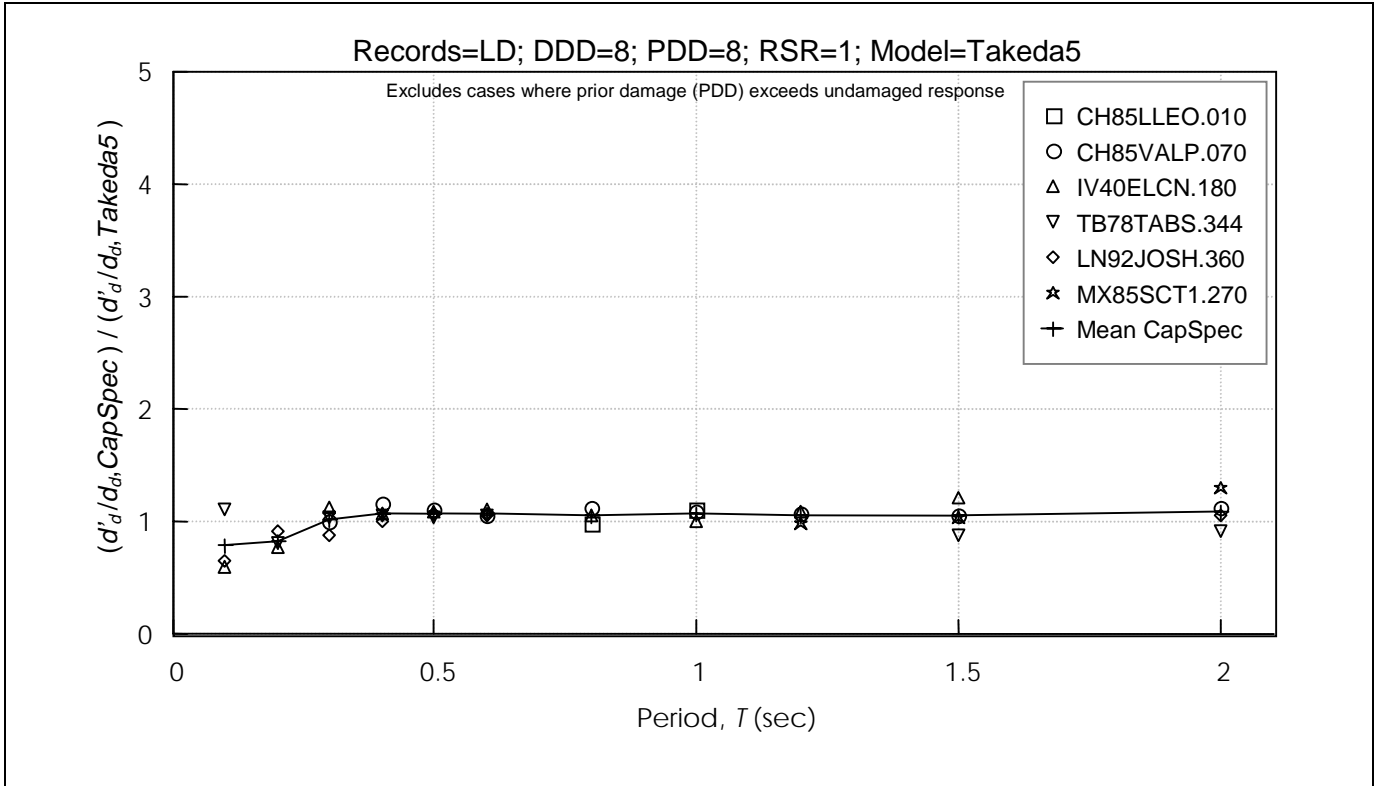


Figure 6-72 Capacity Spectrum Method Estimates of Ratio of Damaged and Undamaged Oscillator Displacement Normalized by Computed Ratio, for Long-Duration Records
 DDD = Design Displacement Ductility; PDD = Prior Ductility Demand; RSR = Reduced Strength Ratio

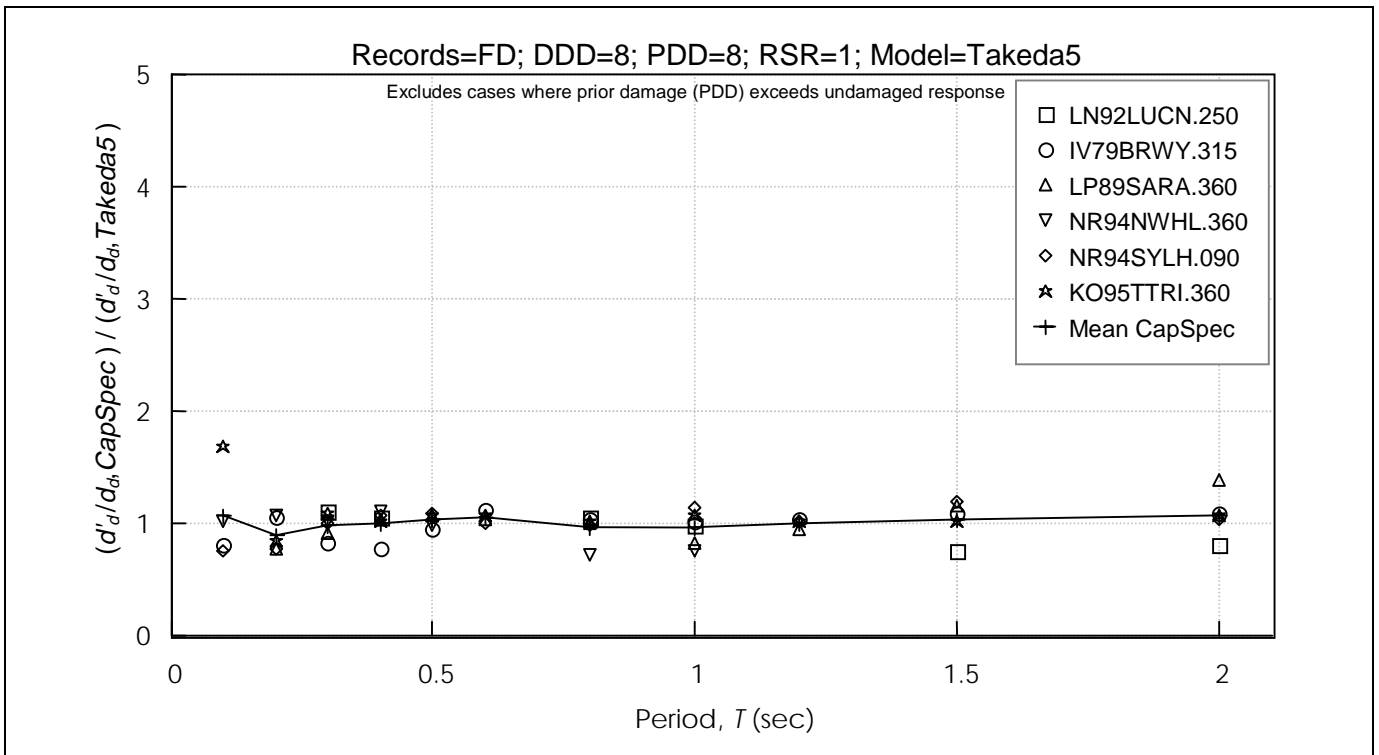


Figure 6-73 Capacity Spectrum Method Estimates of Ratio of Damaged and Undamaged Oscillator Displacement Normalized by Computed Ratio, for Forward Directive Records
 DDD = Design Displacement Ductility; PDD = Prior Ductility Demand; RSR = Reduced Strength Ratio

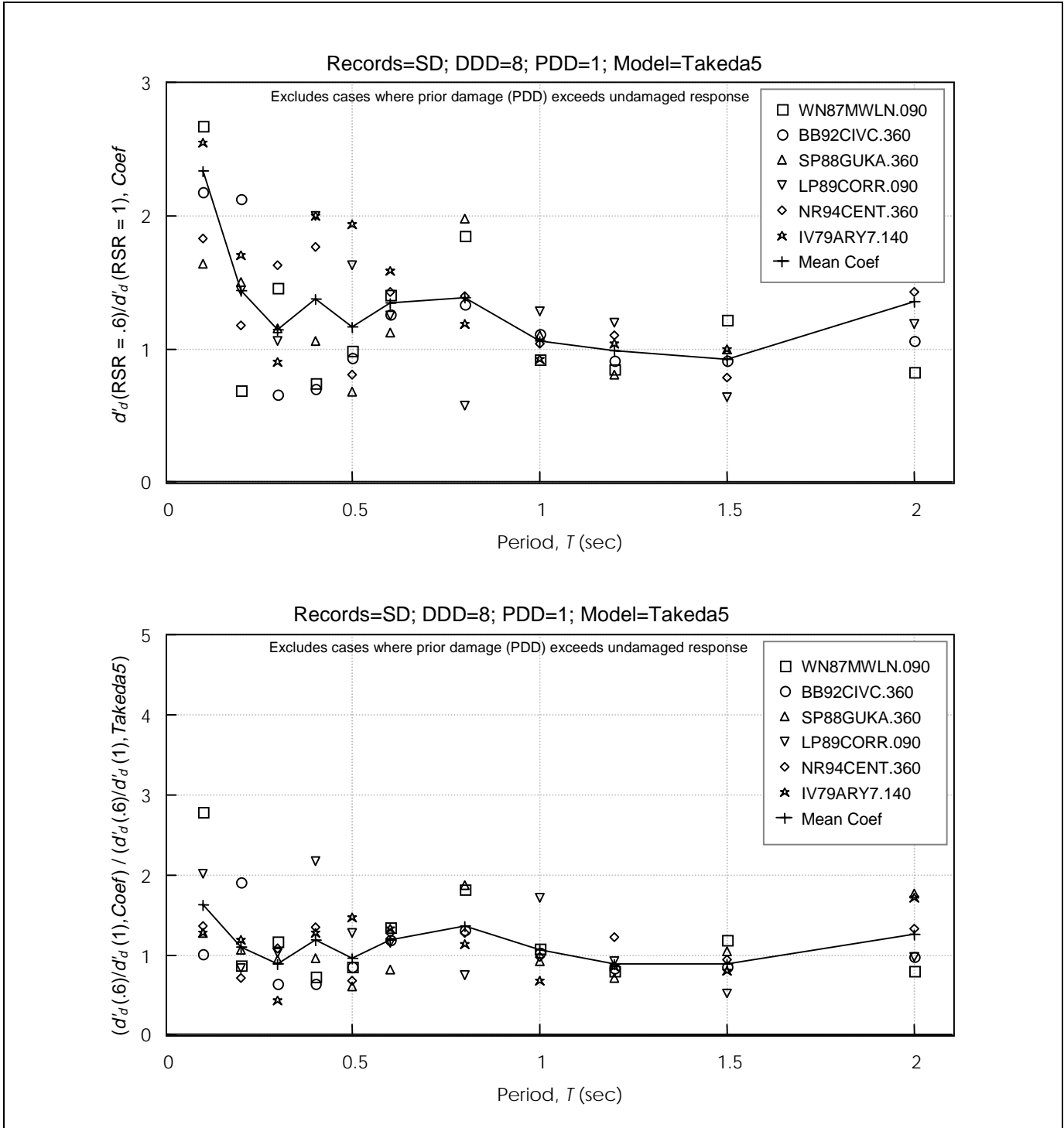


Figure 6-74 Coefficient Method Estimates of Displacement Ratio of RSR=0.6 and RSR=1.0 Takeda5 Oscillators having DDD= 8 and PDD= 1
 DDD = Design Displacement Ductility; PDD = Prior Ductility Demand; RSR = Reduced Strength Ratio

Chapter 6: Analytical Studies

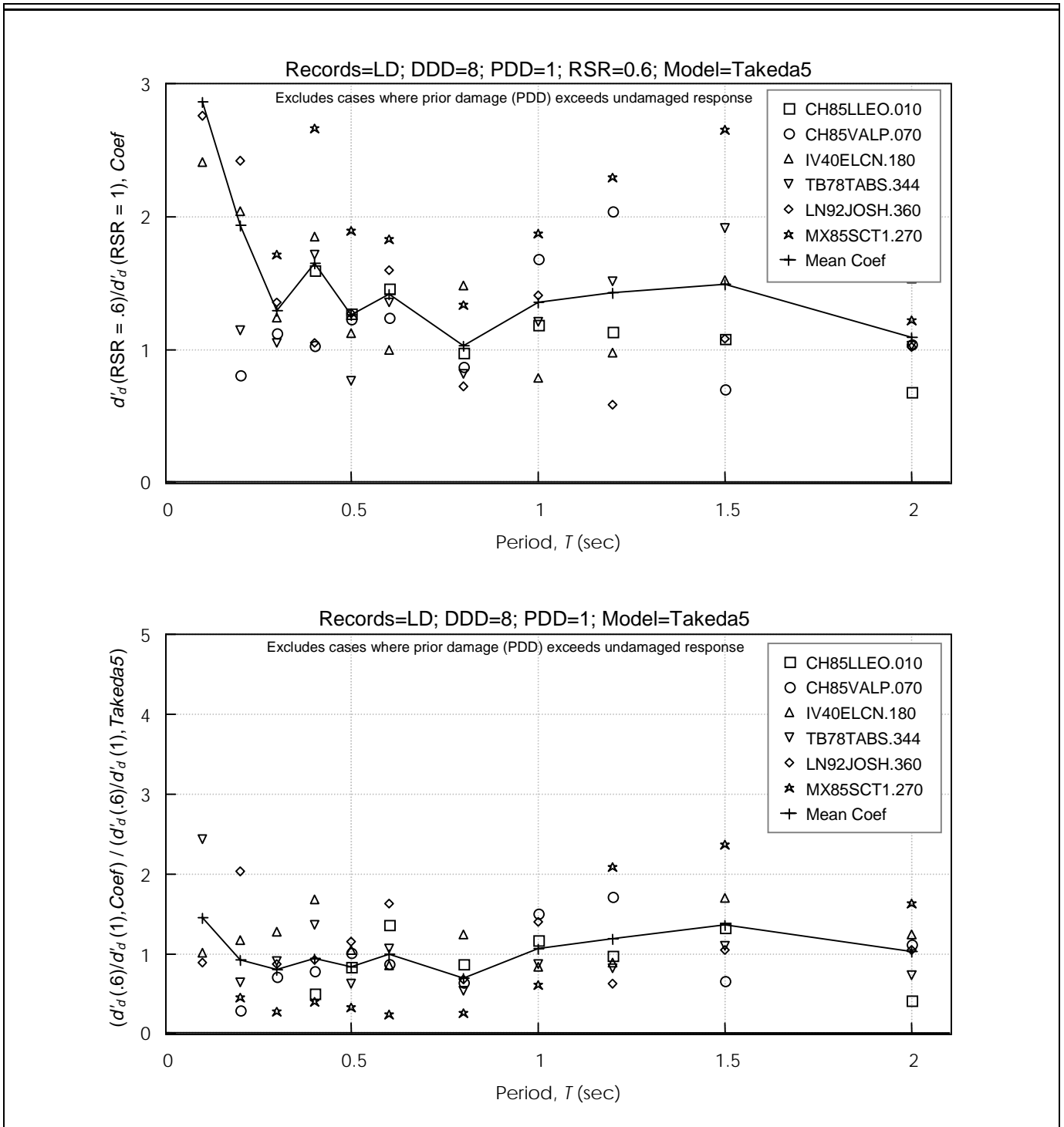


Figure 6-75 Coefficient Method Estimates of Displacement Ratio of RSR=0.6 and RSR=1.0 Takeda5 Oscillators having DDD= 8 and PDD= 1
 DDD = Design Displacement Ductility; PDD = Prior Ductility Demand; RSR = Reduced Strength Ratio

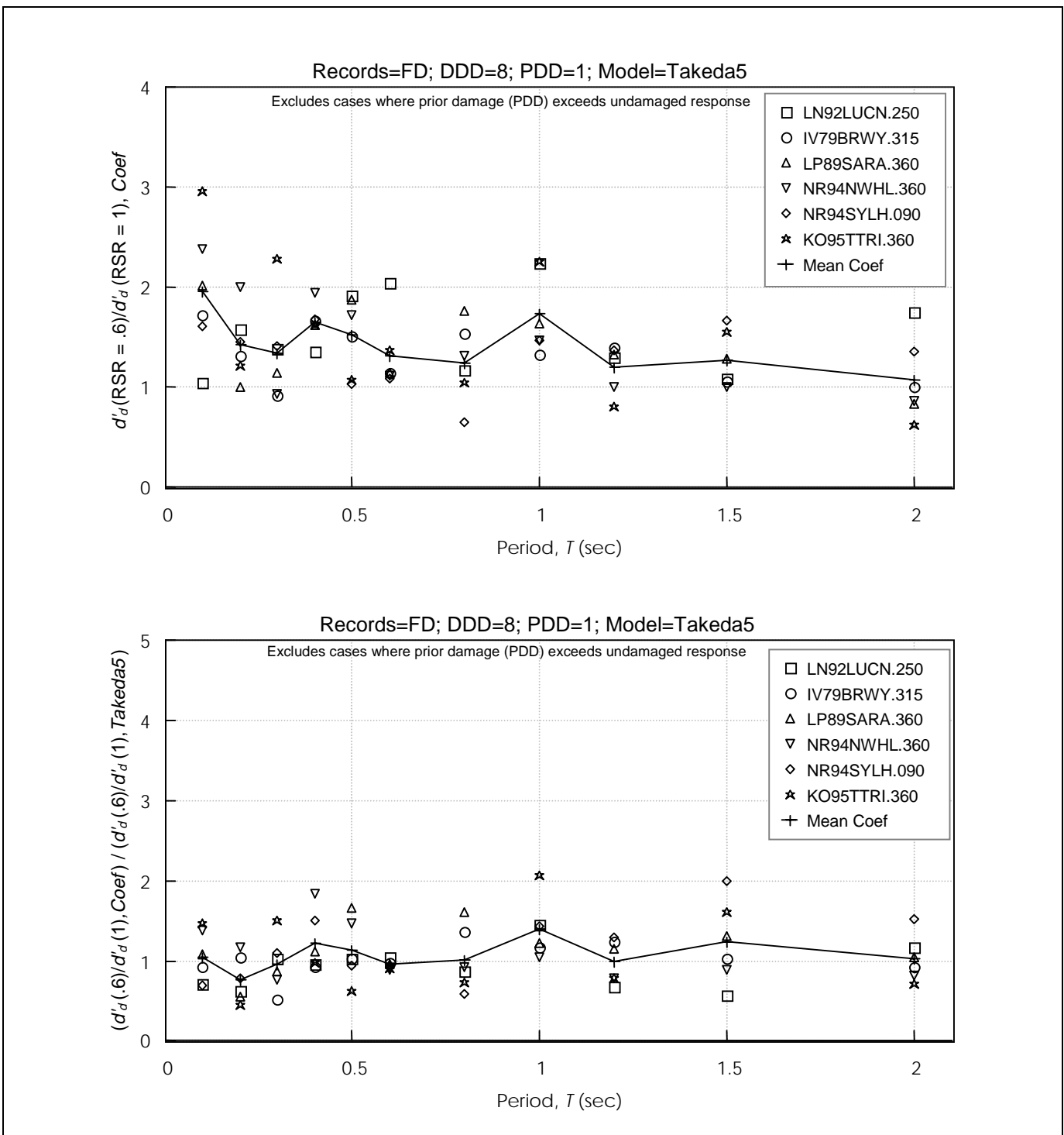


Figure 6-76 Coefficient Method Estimates of Displacement Ratio of RSR=0.6 and RSR=1.0 Takeda5 Oscillators having DDD= 8 and PDD= 1
 DDD = Design Displacement Ductility; PDD = Prior Ductility Demand; RSR = Reduced Strength Ratio

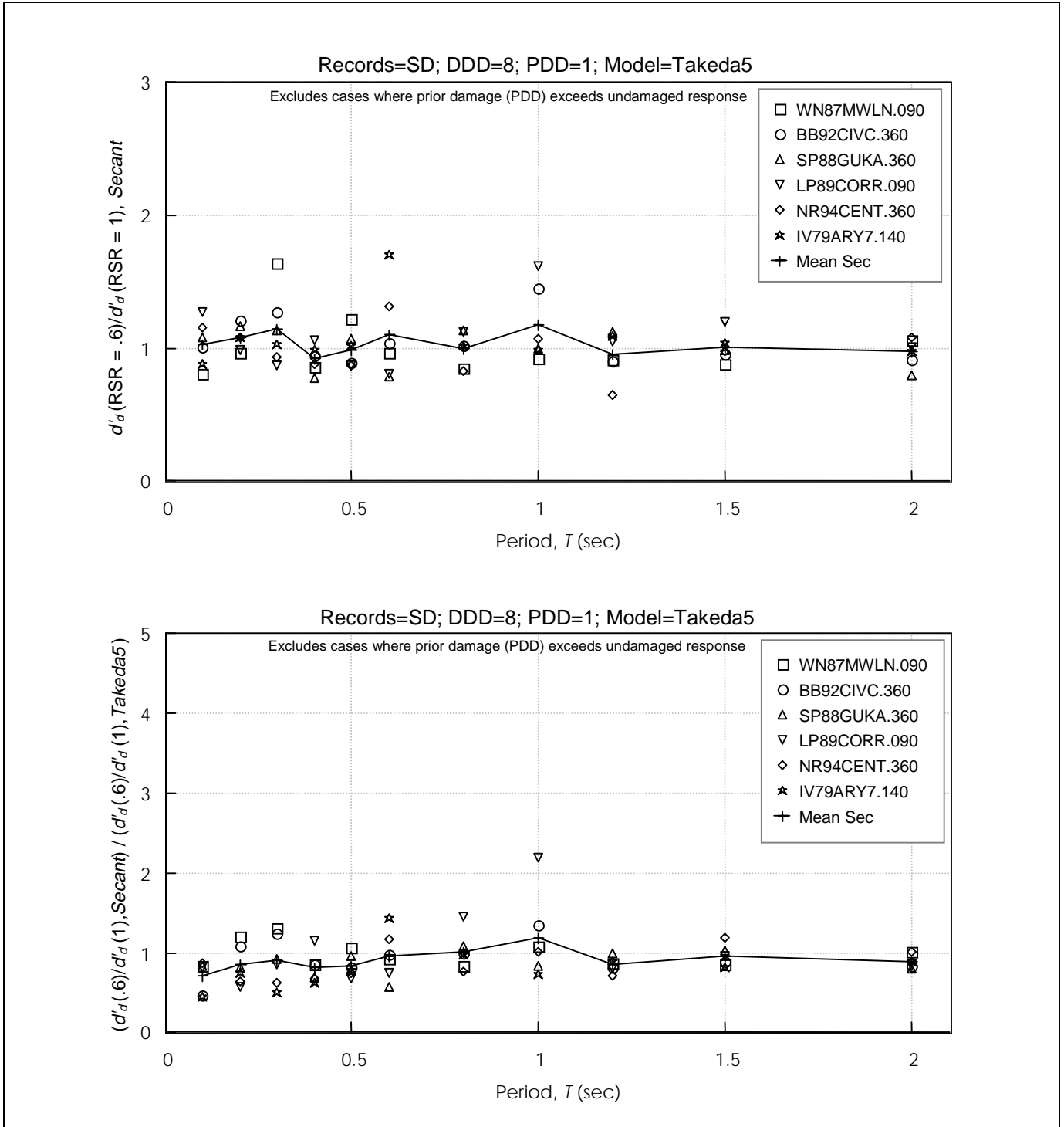


Figure 6-77 **Secant Method Estimates of Displacement Ratio of RSR=0.6 and RSR=1.0 Takeda5 Oscillators having DDD= 8 and PDD= 1**
DDD = Design Displacement Ductility; PDD = Prior Ductility Demand; RSR = Reduced Strength Ratio

Chapter 6: Analytical Studies

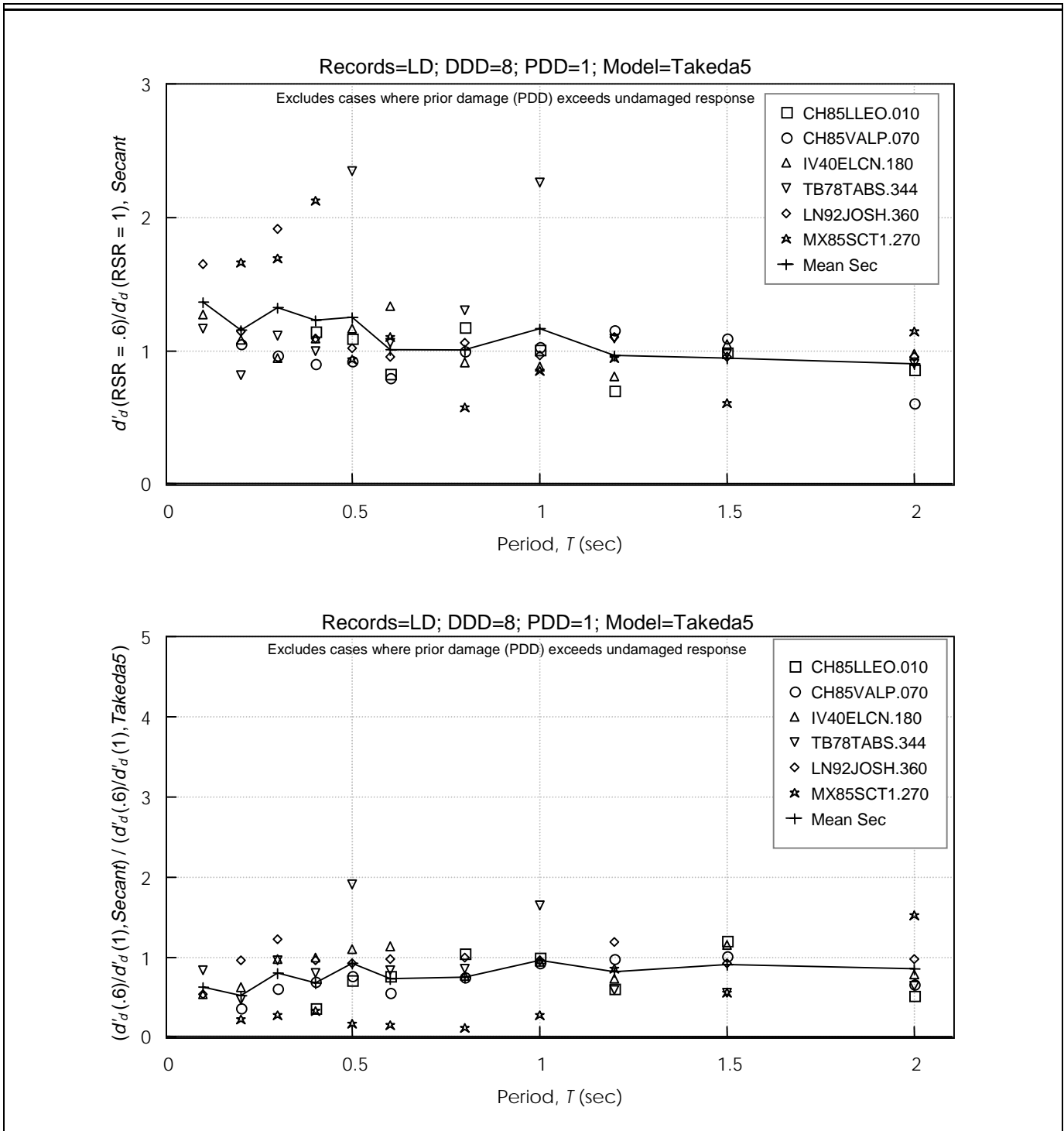


Figure 6-78 Secant Method Estimates of Displacement Ratio of RSR=0.6 and RSR=1.0 Takeda5 Oscillators having DDD= 8 and PDD= 1
 DDD = Design Displacement Ductility; PDD = Prior Ductility Demand; RSR = Reduced Strength Ratio

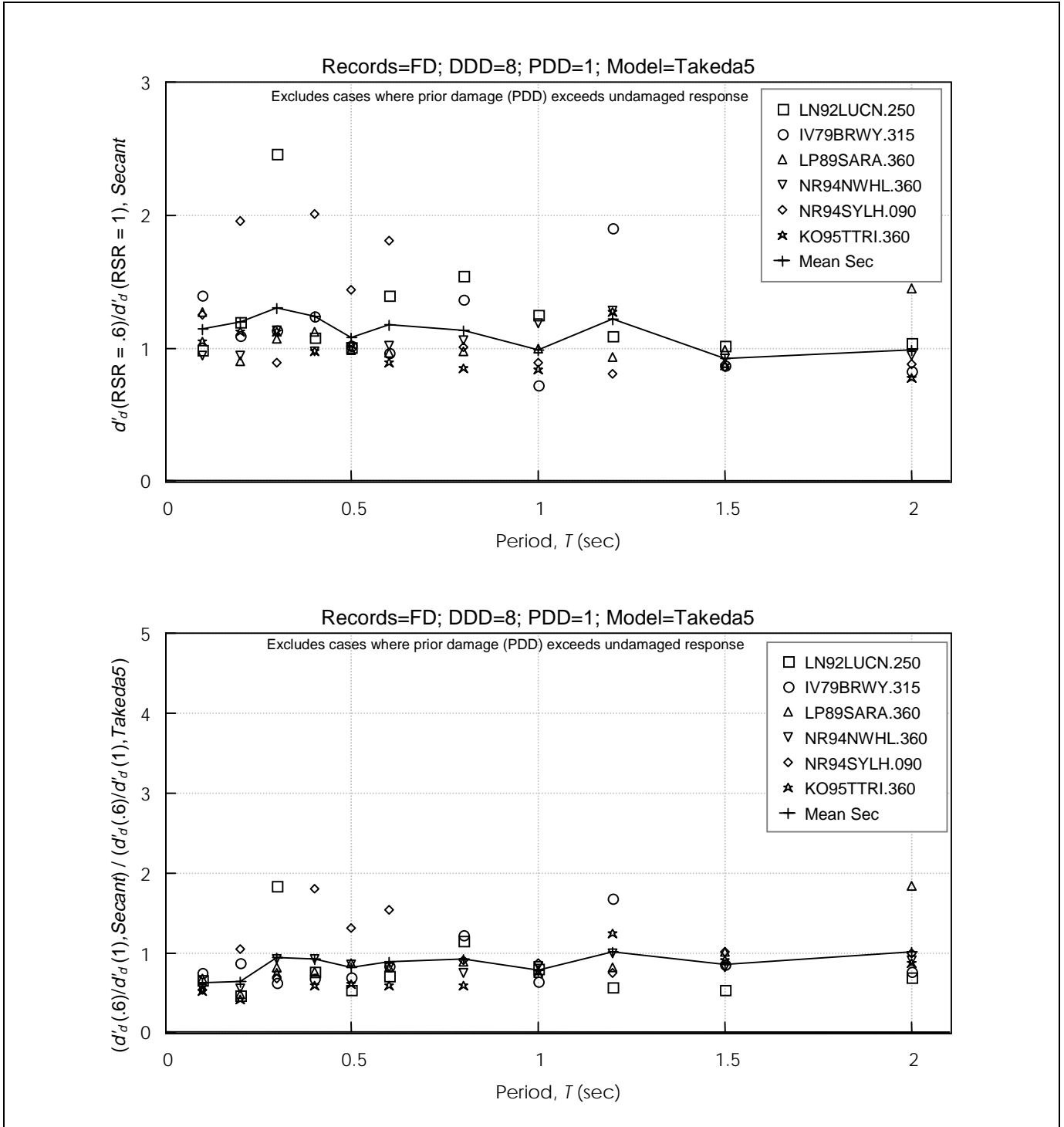


Figure 6-79 **Secant Method Estimates of Displacement Ratio of RSR=0.6 and RSR=1.0 Takeda5 Oscillators having DDD= 8 and PDD= 1**
DDD = Design Displacement Ductility; PDD = Prior Ductility Demand; RSR = Reduced Strength Ratio

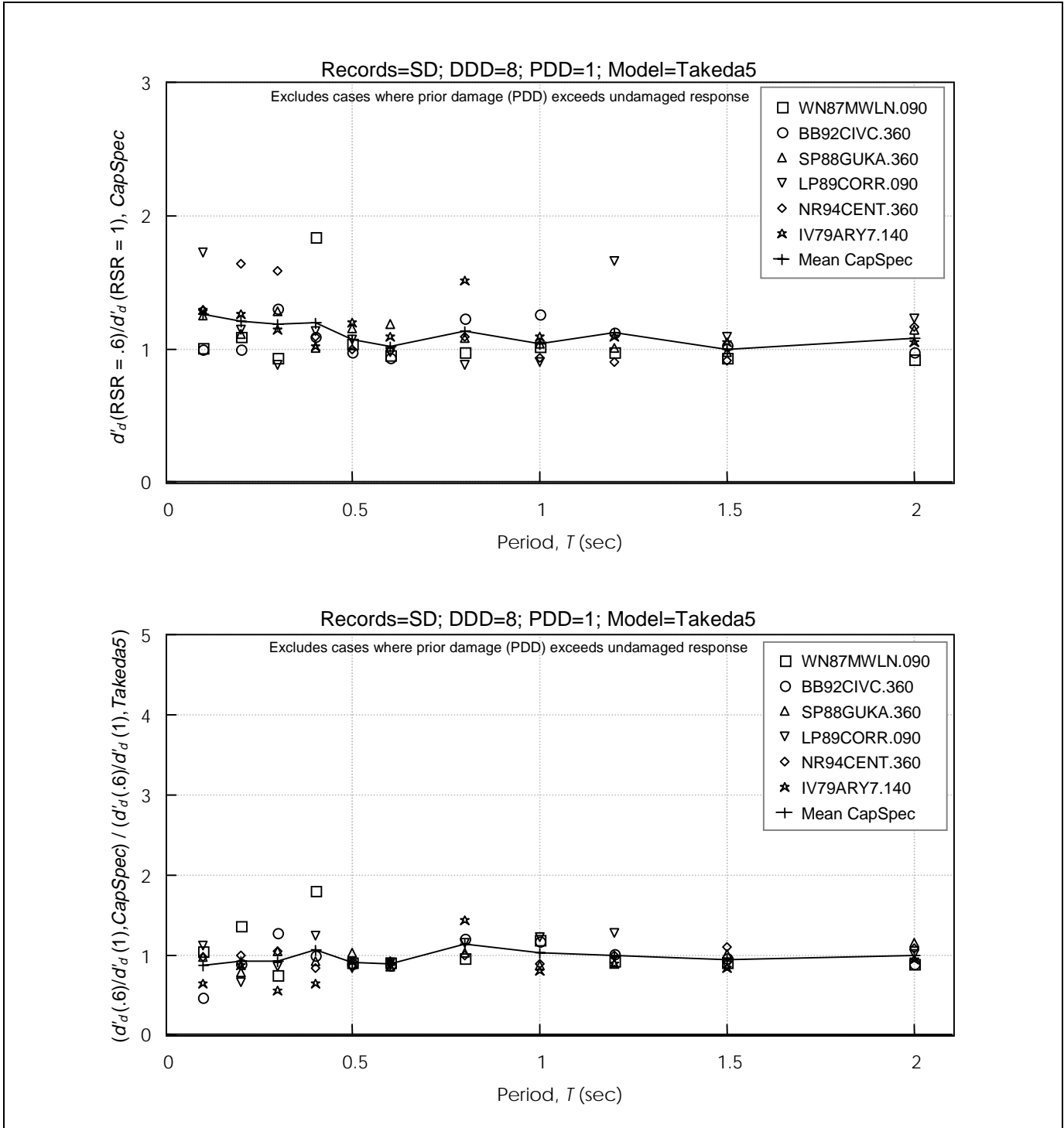


Figure 6-80 Capacity Spectrum Method Estimates of Displacement Ratio of RSR=0.6 and RSR=1.0 Takeda5 Oscillators having DDD= 8 and PDD= 1
 DDD = Design Displacement Ductility; PDD = Prior Ductility Demand; RSR = Reduced Strength Ratio

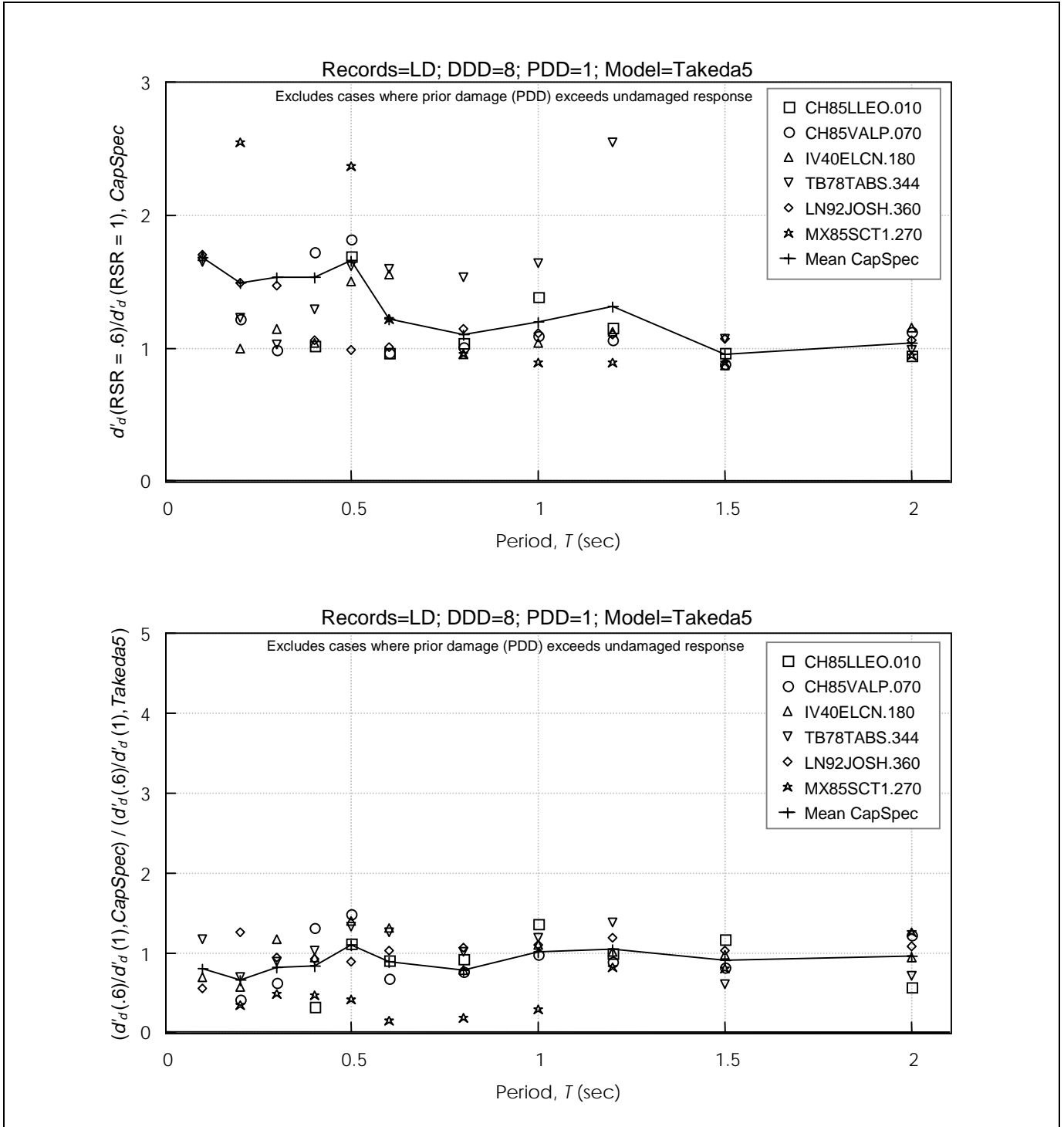


Figure 6-81 Capacity Spectrum Method Estimates of Displacement Ratio of RSR=0.6 and RSR=1.0 Takeda5 Oscillators having DDD= 8 and PDD= 1
 DDD = Design Displacement Ductility; PDD = Prior Ductility Demand; RSR = Reduced Strength Ratio

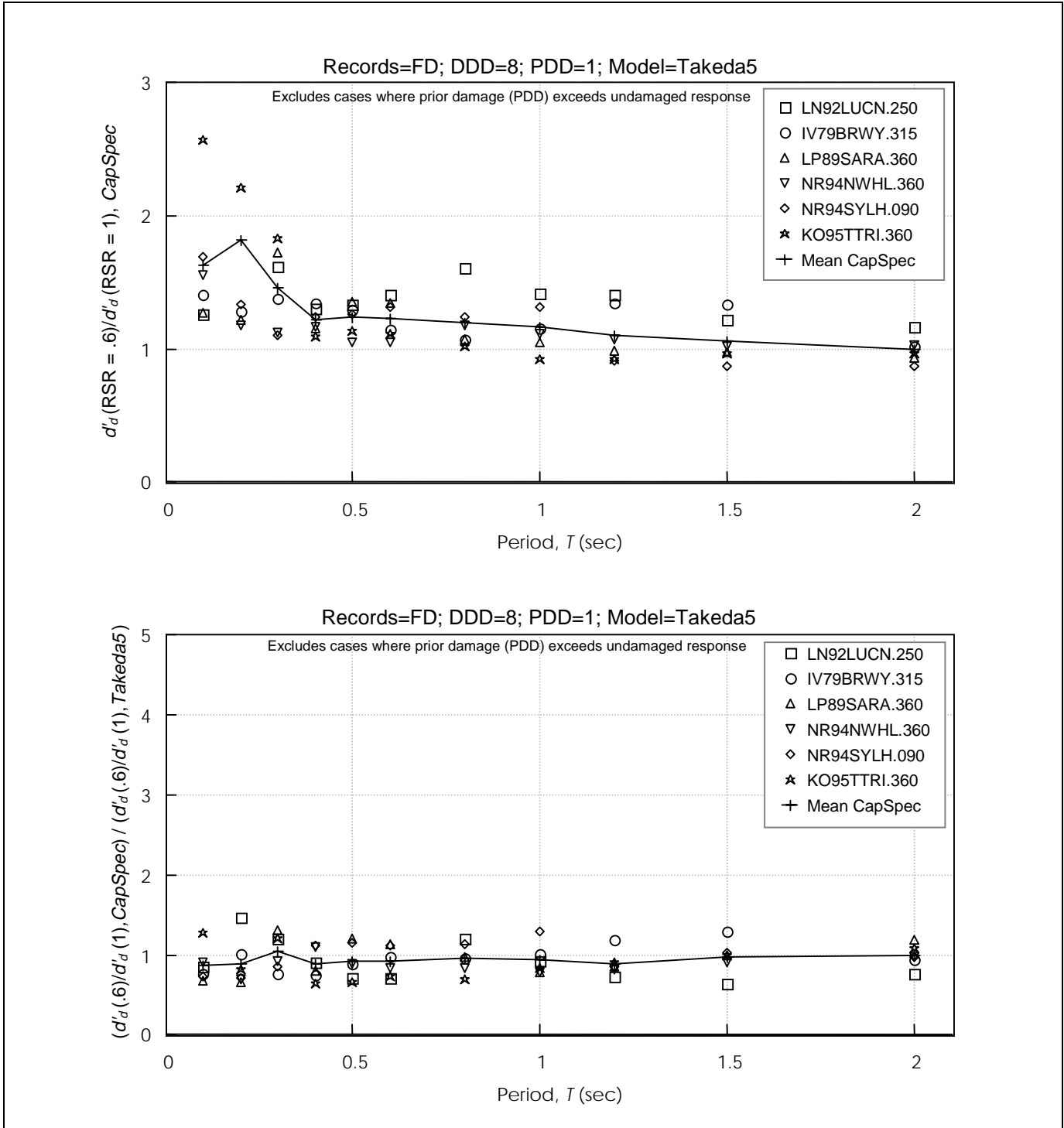


Figure 6-82 Capacity Spectrum Method Estimates of Displacement Ratio of RSR=0.6 and RSR=1.0 Takeda5 Oscillators having DDD= 8 and PDD= 1
 DDD = Design Displacement Ductility; PDD = Prior Ductility Demand; RSR = Reduced Strength Ratio

6.7 Conclusions and Implications

The analyses presented indicate that the displacement response characteristics of the ground motions generally conform to expectations based on previous studies. Forward-directivity motions may have larger displacement response in the long-period range than would be predicted by the equal-displacement rule. The strength-reduction factor, R , appropriate for forward-directivity motions may need to be reduced somewhat relative to other classes of motion if ductility demands are to be held constant.

The displacements of the Takeda oscillators were sometimes several-fold greater or less than those of the bilinear oscillators. Although it is fundamentally important to consider displacements in seismic response, variability of the response estimates as affected by ground motions and hysteresis model must also be considered.

Previous damage, modeled as prior ductility demand, did not generally cause large increases in displacement response when the Takeda models with positive post-yield stiffness were exposed to performance-level earthquakes associated with life safety or collapse prevention. Prior ductility demands were found to cause mean changes in displacement response ranging from -3% to $+10\%$ for the Takeda5 and TakPinch oscillators having no strength degradation (Figures 6-55 and 6-56). PDDs of 8 often caused a slight decrease in the displacement response computed using the Takeda5 and TakPinch models; response infrequently was 20% to 30% or more higher than that for the undamaged oscillator.

For oscillators having cyclic strength degradation, represented by the TakPinch oscillators, the effect of strength degradation was generally to increase the mean displacement response, but only by a few percent. The mean increase was larger for the structures having lower DDD, reaching as much as 21% for oscillators having $RSR = 0.6$. This result merely indicates that strength degradation tends to cause displacement response to increase relative to undamaged or nondegrading systems. Further examination revealed that increasing PDD increases or decreases the mean response of TakPinch systems with strength degradation by only a few percent (Figure 6-56). The weaker oscillators, represented by larger DDD, are more likely to exhibit damage in a real earthquake, and to have smaller increases in displacement due to prior ductility demands.

While prior damage causes relatively small changes in mean displacement response relative to undamaged structures, it also introduces some variability in displacement response. Variability in response is inherent in earthquake-resistant design, and the variability introduced by prior damage should be considered in the context of variability arising from different ground motions, choice of hysteretic models, modeling assumptions, and other sources. For example, Figures 6-32 to 6-34 illustrate the degree to which different earthquakes can cause bilinear and Takeda oscillators of equal strength to have substantially different peak displacement response. Thus, the variability in response introduced by prior damage is not considered significant.

Three NSPs for estimating peak displacement response were applied to the Takeda oscillators. Significant variability in the estimated displacements, when compared with the values calculated from nonlinear dynamic analysis, underscores the difficulty in accurately estimating response of a SDOF system to a known ground motion. The accuracy of the NSP estimates is compared in Figure 6-63. In Figure 6-64 it can be observed that the capacity spectrum and coefficient methods are more accurate, in a mean sense, than the secant method, and that all methods tend to overestimate the displacement response of short-period Takeda5 oscillators.

The NSPs were also used to estimate the change in displacement caused by a prior earthquake. Given the relatively small effect of damage on peak displacement response, it appears that damaged structures should be modeled similar to their undamaged counterparts, in order to obtain identical displacement estimates for performance events that are stronger than the damaging event. This results in damage having no effect on the displacement response, which closely approximates the analytical results.

The accuracy with which an NSP accounts for strength reduction was explored. It was found that each NSP was reasonably able to capture the effect of strength reduction.

The above findings pertain to systems characterized by ductile flexural response having degrading stiffness, with and without pinching. Systems with negative post-yield stiffness were prone to collapse, even with DDD of 2. Such systems should remain nearly elastic if their collapse is to be avoided.

6.8 References

- Araki, H., Shimazu, T., and Ohta, Kazuhiko, 1990, "On Residual Deformation of Structures after Earthquakes," *Proceedings of the Eighth Japan Earthquake Engineering Symposium—1990*, Tokyo, Vol. 2, pp. 1581-1586. (In Japanese with English abstract.)
- ATC, 1996, *Seismic Evaluation and Retrofit of Concrete Buildings*, Applied Technology Council, ATC-40 Report, Redwood City, California.
- ATC, 1997a, *NEHRP Guidelines for the Seismic Rehabilitation of Buildings*, prepared by the Applied Technology Council (ATC-33 project) for the Building Seismic Safety Council, published by the Federal Emergency Management Agency, Report No. FEMA 273, Washington, D.C.
- ATC, 1997b, *NEHRP Commentary on the Guidelines for the Seismic Rehabilitation of Buildings*, prepared by the Applied Technology Council (ATC-33 project) for the Building Seismic Safety Council, published by the Federal Emergency Management Agency, Report No. FEMA 274, Washington, D.C.
- Boroschek, R.L., 1991, *PCNSPEC Manual, (Draft)*, Earthquake Engineering Research Center, University of California at Berkeley.
- Cecen, H., 1979, *Response of Ten-Story Reinforced Concrete Model Frames to Simulated Earthquakes*, Doctoral Thesis, Department of Civil Engineering, University of Illinois at Urbana.
- Fajfar, P. and Fischinger, M., 1984, "Parametric Study of Inelastic Response to Some Earthquakes Recorded in Southern Europe," *Proceedings of the Eighth World Conference on Earthquake Engineering*, Vol. 4, pp. 75-82.
- Humar, J., 1980, "Effect of Stiffness Degradation on Seismic Response of Concrete Frames," *Proceedings of the Seventh World Conference on Earthquake Engineering*, Vol. 5, pp. 505-512.
- Iwan, W.D., 1973, "A Model for the Dynamic Analysis of Deteriorating Structures," *Proceedings of the Fifth World Conference on Earthquake Engineering*, Vol. 2., pp. 1782-1791.
- Iwan, W.D., 1977, "The Response of Simple Stiffness Degrading Systems," *Proceedings of the Sixth World Conference on Earthquake Engineering*, Vol. 2, pp. 1094-1099.
- Kawashima, K., Macrae, G., Hoshikuma, J., and Nagaya, K., 1994, "Residual Displacement Response Spectrum and its Application," *Journal of Structural Mechanics and Earthquake Engineering*, Japan Society of Civil Engineers, No. 501, pp. 183-192. (In Japanese with English abstract.)
- Lepage, A., 1997, *A Method for Drift Control in Earthquake-Resistant Design of RC Building Structures*, Doctoral Thesis, Department of Civil Engineering, University of Illinois at Urbana.
- Mahin, S.A., 1980, "Effects of Duration and After-shocks on Inelastic Design Earthquakes," *Proceedings of the Seventh World Conference on Earthquake Engineering*, Vol. 5, pp. 677-679.
- Mahin, S.A., and Lin, J., 1983, *Construction of Inelastic Response Spectra for Single-Degree-of-Freedom Systems—Computer Program and Applications*, Earthquake Engineering Research Center, University of California at Berkeley, Report No. UCB/EERC-83/17, Berkeley, California.
- Mahin, S.A., and Boroschek, R., 1991, *Influence of Geometric Nonlinearities on the Seismic Response and Design of Bridge Structures*, Background Report to California Department of Transportation, Sacramento, California.
- Minami, T., and Osawa, Y., 1988, "Elastic-Plastic Response Spectra for Different Hysteretic Rules," *Earthquake Engineering and Structural Dynamics*, Vol. 16, pp. 555-568.
- Miranda, E., 1991, *Seismic Evaluation and Upgrading of Existing Buildings*, Doctoral Thesis, Department of Civil Engineering, University of California, Berkeley.
- Moehle, J.P., Browning, J., Li, Y.R., and Lynn, A., 1997, "Performance Assessment for a Reinforced Concrete Frame Building," (abstract) *The Northridge Earthquake Research Conference*, California Universities for Research in Earthquake Engineering, Richmond, California.
- Nakamura, T., and Tanida, K., 1988, "Hysteresis Model of Restoring Force Characteristics of Reinforced Concrete Members," *Proceedings of the Ninth World Conference on Earthquake Engineering*, Paper 6-4-7, Vol. VI.
- Nasser, A.A., and H. Krawinkler, H., 1991, *Seismic Demands for SDOF and MDOF Systems*, John A. Blume Earthquake Engineering Center, Stanford University, Report No. 95, Stanford, California.

- Newmark, N.M., and Riddell, R., 1979, "A Statistical Study of Inelastic Response Spectra," *Proceedings of the Second U.S. National Conference on Earthquake Engineering*, pp. 495-504.
- Otani, S., 1981, "Hysteresis Models of Reinforced Concrete for Earthquake Response Analysis," *Journal (B)*, Faculty of Engineering, University of Tokyo, Vol. XXXVI, No. 2, pp. 125 - 159.
- Palazzo, B., and DeLuca, A., 1984, "Inelastic Spectra for Geometrical and Mechanical Deteriorating Oscillator," *Proceedings of the Eighth World Conference on Earthquake Engineering*, Volume IV, pp. 91-98.
- Parducci, A., and Mezzi, M., 1984, "Elasto-Plastic Response Spectra of Italian Earthquakes Taking into Account the Structural Decay," *Proceedings of the Eighth World Conference on Earthquake Engineering*, Volume IV, pp. 115-122.
- Paulay, T. and Priestley, M.J.N., 1992, *Reinforced Concrete and Masonry Buildings: Design for Seismic Resistance*, Wiley & Sons, New York.
- Qi, X., and Moehle, J.P., 1991, *Displacement Design Approach for Reinforced Concrete Structures Subjected to Earthquakes*, Earthquake Engineering Research Center, Report No. UCB/EERC 91/02, University of California at Berkeley, Berkeley, California.
- Rahnama, M., and Krawinkler, H., 1995, "Effects of P-Delta and Strength Deterioration on SDOF Strength Demands", *Proceedings of the 10th European Conference on Earthquake Engineering*, Vol. 2, pp. 1265-1270.
- Riddell, R., 1980, "Effect of Damping and Type of Material Nonlinearity on Earthquake Response," *Proceedings of the Seventh World Conference on Earthquake Engineering*, Vol. 4, pp. 427-433.
- Saiidi, M., 1980, "Influence of Hysteresis Models on Calculated Seismic Response of R/C Frames," *Proceedings of the Seventh World Conference on Earthquake Engineering*, Vol. 5, pp. 423-430.
- Sewell, R.T., 1992, "Effects of Duration on Structural Response Factors and on Ground Motion Damageability," *Proceedings of the SMIP92 Seminar on Seismological and Engineering Implications of Recent Strong Motion Data*, pp. 7-1 to 7-15.
- Shimazaki, K., and M.A. Sozen, M.A., 1984, *Seismic Drift of Reinforced Concrete Structures*, Research Reports, Hasama-Gumi Ltd., Tokyo (in Japanese), and draft research report (in English).
- Somerville, P.G., Smith, N.F., Graves, R.W. and Abrahamson, N.A., 1997, "Modification of Empirical Strong Ground Motion Attenuation Relations to Include the Amplitude and Duration Effects of Rupture Directivity," *Seismological Research Letters*, Vol. 68, No. 1.
- Takeda, T., Sozen, M.A., and Nielsen, N.N., 1970, "Reinforced Concrete Response to Simulated Earthquakes," *Journal of the Structural Division*, American Society of Civil Engineers, Vol. 96, No. ST12, pp. 2557-2573.
- Wolschlag, C., 1993, *Experimental Investigation of the Response of R/C Structural Walls Subjected to Static and Dynamic Loading*, Doctoral Thesis, Department of Civil Engineering, University of Illinois at Urbana.
- Xie, L.-L., and Zhang, X., 1988, "Engineering Duration of Strong Motion and its Effects on Seismic Damage," *Proceedings of the Ninth World Conference on Earthquake Engineering*, Vol. 2, Paper 3-2-7.

7. Example Application

7.1 Introduction

This section gives an example of the use of FEMA 306 recommendations to evaluate earthquake damage in a two-story reinforced-concrete building. The example is meant to be as realistic as possible and is based on an actual structure.

7.1.1 Objectives

The example is intended to help evaluating engineers understand such issues as:

- the overall process of a FEMA 306 evaluation.
- accounting for pre-existing damage.
- how both observation and analysis are used in the evaluation procedures.
- determining and using the applicable FEMA 306 Component Damage Classification Guides, including cases where an exactly applicable damage guide is not provided.
- foundation rocking of walls, which may be a prevalent behavior mode in many structures.
- some of the ways engineering judgment may need to be applied.
- how restoration measures can be determined based on either the *direct method* or the *performance analysis method*.
- aspects of using a nonlinear static procedure of analysis (pushover analysis).
- establishing displacement capacities and demands.

Reading through the example could be the best introduction to an understanding of the FEMA 306 evaluation process. References to the applicable sections of FEMA 306 or 307 (or to other sources) are given in “bookmark” boxes adjacent to the text. Because the example is meant to be illustrative, it contains more description and explanation than would normally be contained in an engineer’s evaluation report for an earthquake-damaged building.

It should be clear from this example that the FEMA 306 recommendations for evaluating earthquake damage

must be implemented under the direction of a knowledgeable structural engineer, particularly when a performance analysis is carried out. The responsible engineer should have a thorough understanding of the principles behind the FEMA 306 recommendations and should be familiar with the applicable earthquake research and post-earthquake field observations. FEMA 307 provides tabular bibliographies and additional information on applicable research.

A fundamental tenet of the component evaluation methods presented in FEMA 306 is that the severity of damage in a structural component may not be determined without understanding the governing behavior mode of the component, and that the governing behavior mode is a function not only of the component’s properties, but of its relationship and interaction with surrounding components in a structural element. In the following sections, the evaluation of the example building emphasizes the importance of this principle. There may be a temptation among users of FEMA 306 to use the damage classification guides as simple graphical keys to damage, and to complete the analysis by simply matching the pictures in the guides to the observed damage. The example is intended to show that this is not the appropriate use of the guides. It is organized to emphasize the importance of the analytical and observation verification process that is an essential element of the evaluation procedure.

7.1.2 Organization

The example is organized as shown in the flow chart of Figure 7-1. This organization follows the overall evaluation procedure outlined in FEMA 306, beginning with a building description and observations of earthquake damage.

The building has been subjected to a previous earthquake. The damage investigation establishes the pre-existing conditions so that the loss from the recent earthquake can be evaluated. The preliminary classification of component types, behavior modes, and damage severity are made by observing the structure. It is shown, however, that classification of behavior modes, and hence damage severity, may be unclear when based on observation alone. Simple analytical tools provided in the material chapters of FEMA 306 are used to verify the expected component types and behavior modes, and damage severity is assigned accordingly. The steps required to estimate the loss by the direct method are

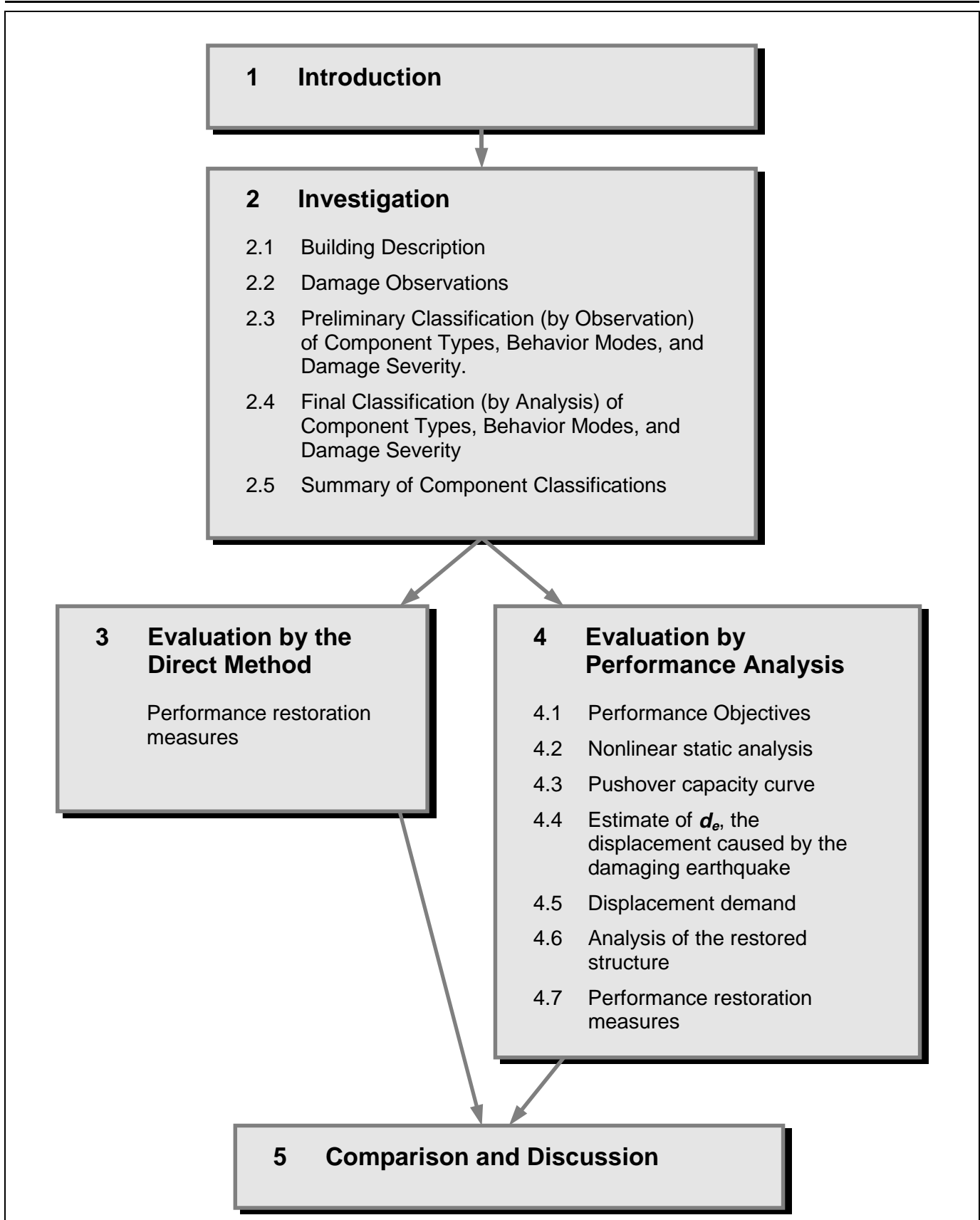


Figure 7-1 Flowchart for example

illustrated, and a relative performance analysis is carried out. It is emphasized that the direct method provides only loss estimation information, and that a relative performance analysis is required in order to make performance-based design decisions.

Damage records for all of the structural walls of the building are included. The damage records for two of the walls are discussed in detail. Damage records for the remaining walls are given at the end of the example.

7.2 Investigation

7.2.1 Building Description

The example building is a two-story concrete building located on a sloping site. The building is a “T” shape in plan with the stem of the T on the downhill side, containing a partial lower story below the other two stories. The building was designed and constructed in the late 1950s. The building is located about 3.6 miles from the epicenter of the damaging earthquake.

The overall plan dimensions of the building are 362 feet in the North-South direction by 299 feet in the East-West direction. The floor slabs cantilever about 6 feet from the perimeter columns forming exterior sun-screens/balconies. The building facade along the perimeter is set back 8 feet from the edge of the slab. For the typical floor, the interior floor area is about 62,600 square feet, and the total slab area is about 70,400 square feet. The lower level encompasses about 20,200 square feet. Floor plans are shown in Figure 7-2 and an elevation is shown in Figure 7-3. The roof of the building supports mechanical equipment.

The floors and roof are constructed with waffle slabs comprised of a 4-½ inch thick slab and 14 inch deep pans (18-½ inches total depth). Columns supporting the slabs are typically spaced at 26 feet in each direction. The interior columns are 18-inch square and the perimeter columns are 18-inch diameter. The columns are supported on spread footings.

Reinforced concrete walls in both directions of the building resist lateral forces. The walls are 12 inches thick and are cast monolithically at each end with the gravity-load-carrying columns. The walls are typically located along corridors, and the corridor side of the wall has a 1-inch thick plaster coat. The typical solid wall configuration and reinforcement are shown in Figure 7-4.

In the lower level there are several reinforced concrete masonry (CMU) walls that are framed between the ground and the first floor slab (basement level) in the three-story section of the building. The CMU walls are attached to the first floor slab. However, these walls were not designed as shear-resisting elements. Because the first floor slab is anchored to the foundation in the two-story portion of the building, the contribution of the CMU walls to the lateral force resistance, particularly in the east-west direction, is minimal.

Several of the reinforced concrete walls have door openings, 7 feet 3 inches tall by 6 feet 6 inches wide, in the middle of the wall, creating a coupled wall. The typical coupled wall configuration and reinforcement are shown in Figure 7-5. In the three-story section of the building (the stem of the T), the walls are discontinued at the lower level. This lower level contains a single reinforced concrete wall in the north-south direction centered between the two walls above.

7.2.2 Post-earthquake Damage Observations

Following the damaging earthquake, the engineers performed a post-earthquake evaluation of the building. The initial survey was conducted one month after the damaging earthquake. The structural drawings for the building were reviewed. The follow-up investigations were conducted about three months following the earthquake.

Visual observation, Guide NDE1, Section 3.8 of FEMA 306

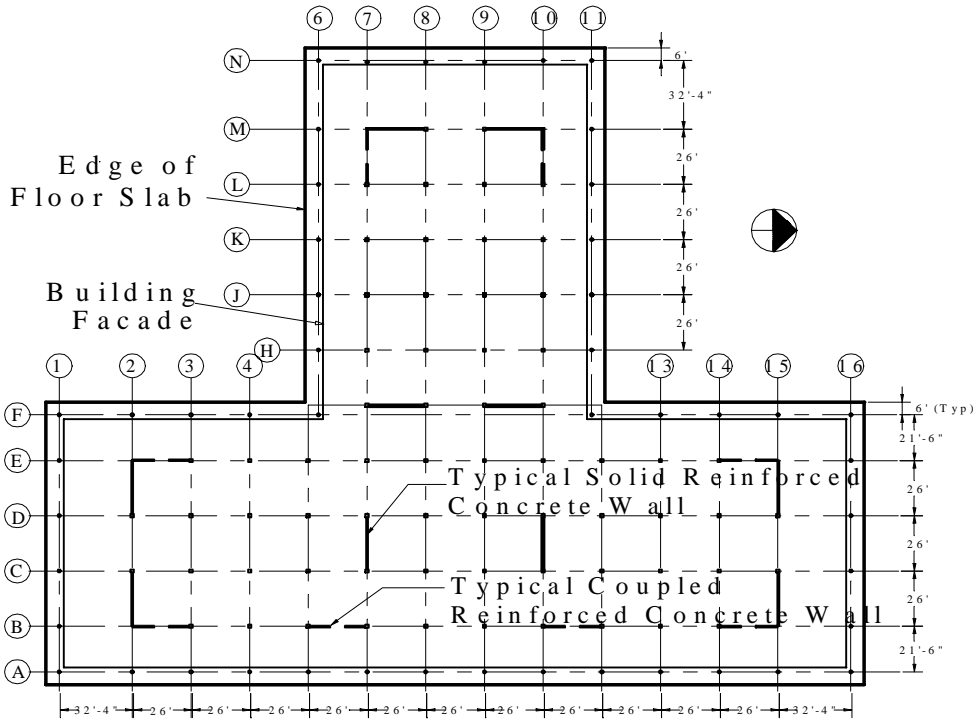
The post-earthquake evaluations were conducted using visual observation techniques on exposed surfaces of the structural elements. The sections of wall above the ceiling were typically observed only where the suspended ceiling tiles had fallen during the earthquake. Crack widths were measured at selected locations using magnifying crack comparators for most of the significant cracks in each wall.

7.2.2.1 Pre-Earthquake Conditions

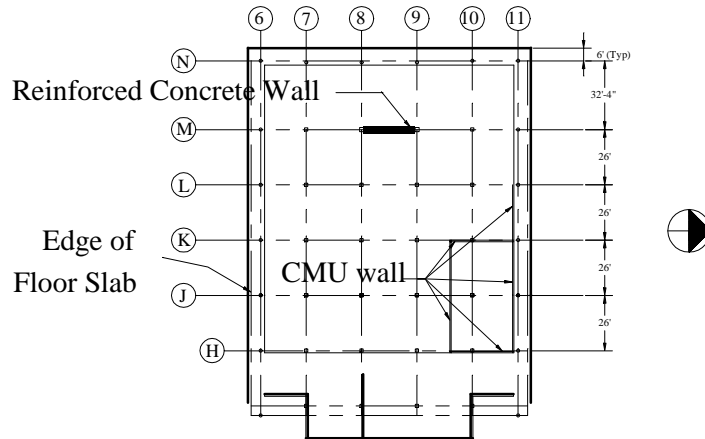
The building had experienced some cracking prior to the damaging earthquake. The pre-existing damage is judged to have been caused by a previous earthquake. The heaviest damage appeared to have been in the coupling beams. The wall cracks above the ceiling line were observed to have been repaired by epoxy injection.

Old cracks vs. new cracks, Section 3.4 of FEMA 306

Chapter 7: Example Application



a) First and Second Floor Plan



b) Basement Floor Plan

Figure 7-2 Floor Plans

Chapter 7: Example Application

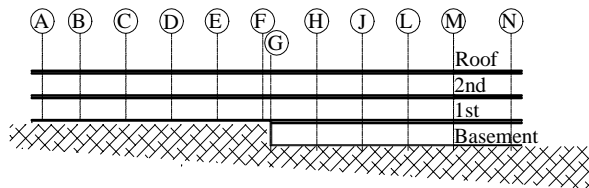


Figure 7-3 Building Cross-section

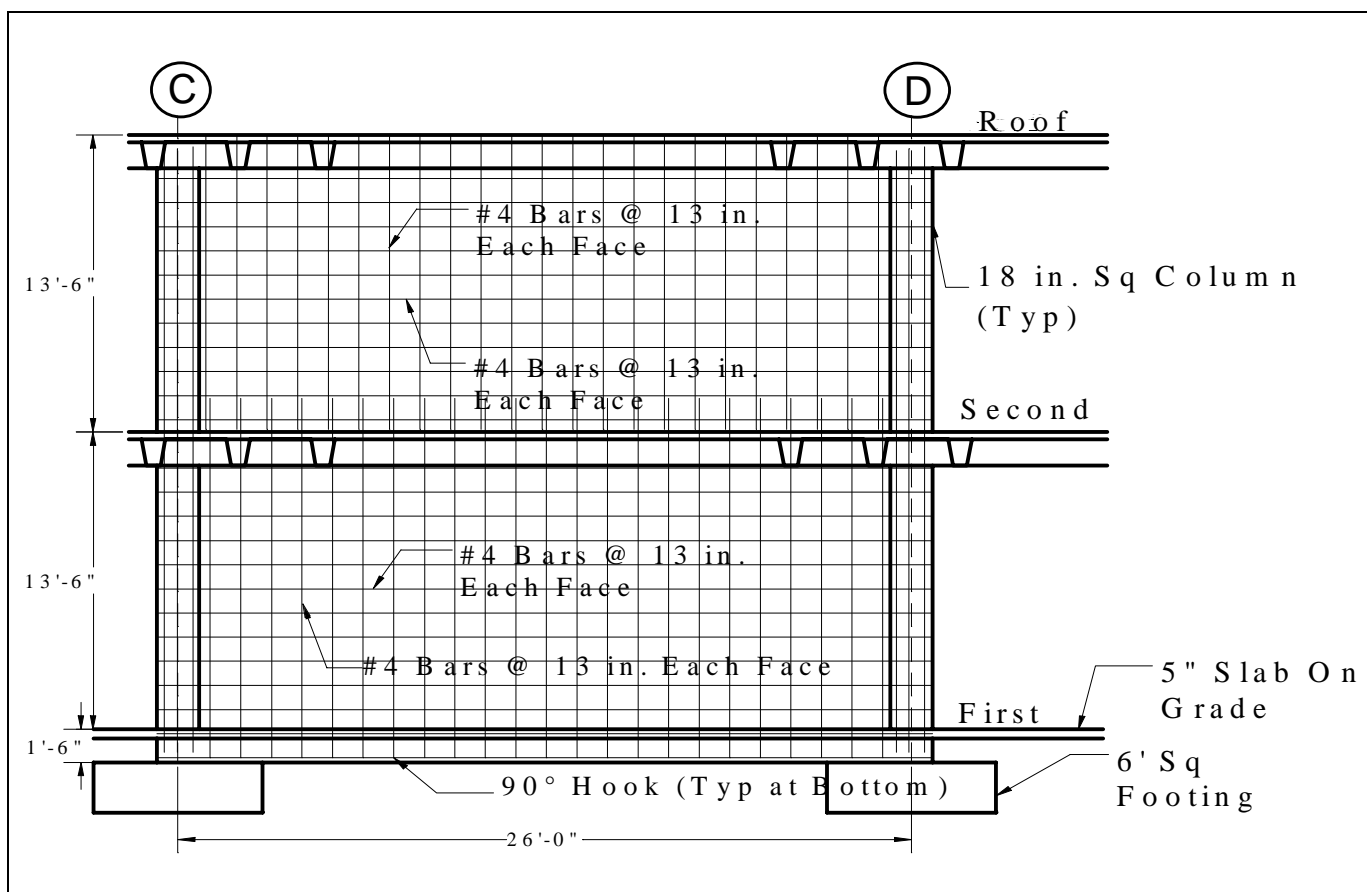


Figure 7-4 Example Solid Wall Detail (Condition at Line 7)

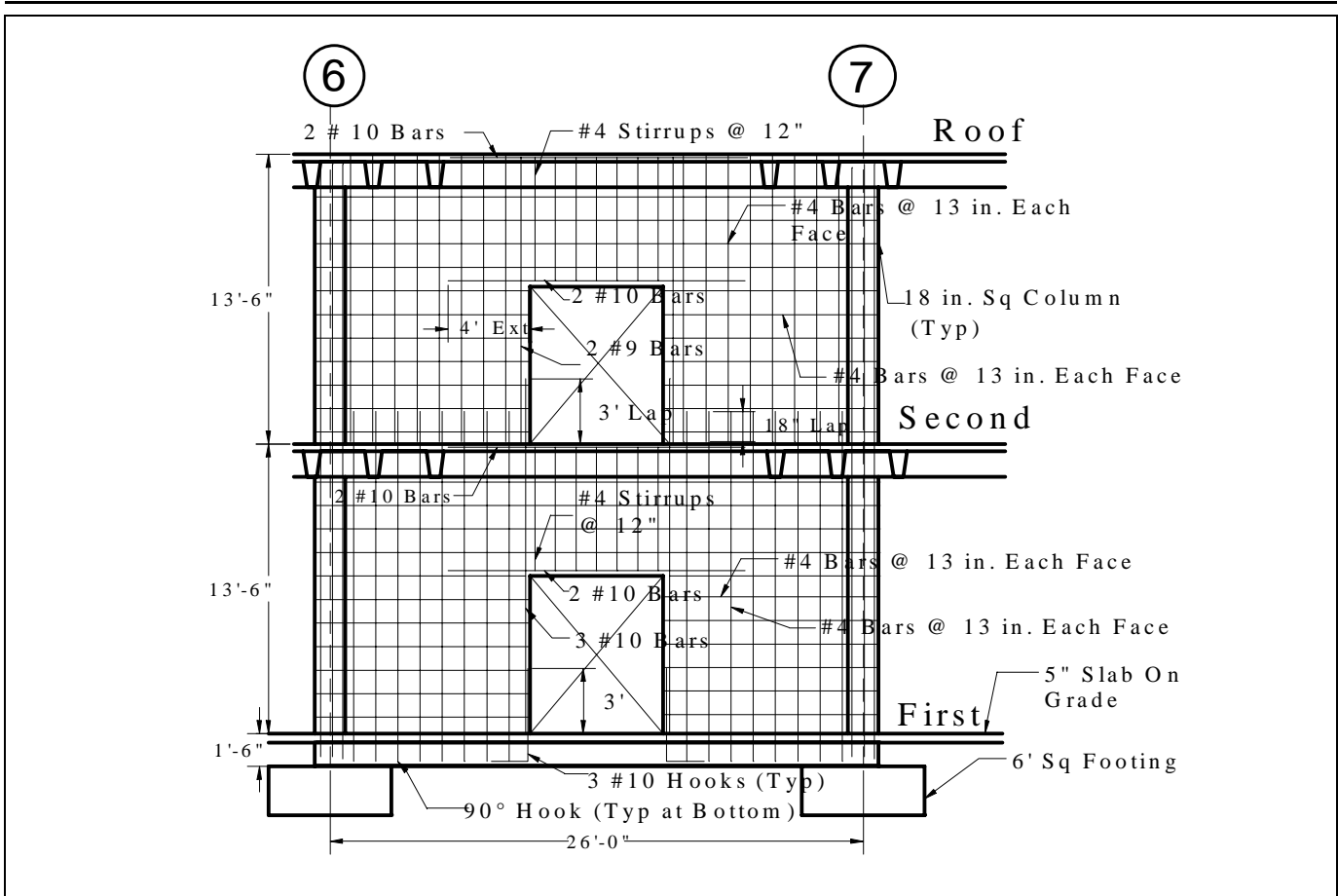


Figure 7-5 Example Coupled Wall Detail (Condition at line B)

Below the ceiling the cracks may also have been injected with epoxy. However, the architectural finishes on those surfaces obscured the evidence of the previous repairs. Many of the cracks in the plaster coat on the walls appeared to have been cosmetically repaired using a strip of fabric and plaster placed over the crack. It was not clear whether the underlying cracks in the concrete had been repaired. Therefore, the building is assumed to have some cracking prior to the damaging earthquake and the pre-existing cracking is taken into account by reducing the pre-event stiffness of the concrete walls.

7.2.2.2 Postearthquake Condition and Damage Documentation

The concrete walls experienced minor to moderate amounts of cracking. Based on the visual observations, component damage records were prepared for each of the walls in the building. These forms are included as Figures 7-6, 7-7, and in Appendix A, Component Damage Records D1 through

Documentation of damage, Section 3.7 of FEMA 306

D19. Each of the component damage records depicts the observations for both stories of a two-story wall, except for the single-story wall on the lower level shown on Record D19. All observable cracks are shown, but only those cracks found to be wider than 30 mils (1/32 inch) have the crack width, in mils, written on the component damage record at the approximate location of the measurement. Cracks found to be previously repaired with epoxy and those with pre-existing surface patches are indicated. Spalls are also noted.

The two first-story coupled walls in the stem of the T section of the building experienced heavy cracking in the coupling beams (Column lines 7 and 10, L to M, Component Damage Records D4 and D6). One of the other coupling beams (Column Line B, 14 to 15, Record D12) also experienced heavy cracking. The damage to the coupling beams included some spalling of the concrete, buckling of reinforcing bars, and cracking of the floor slab adjacent to the wall. Several walls were

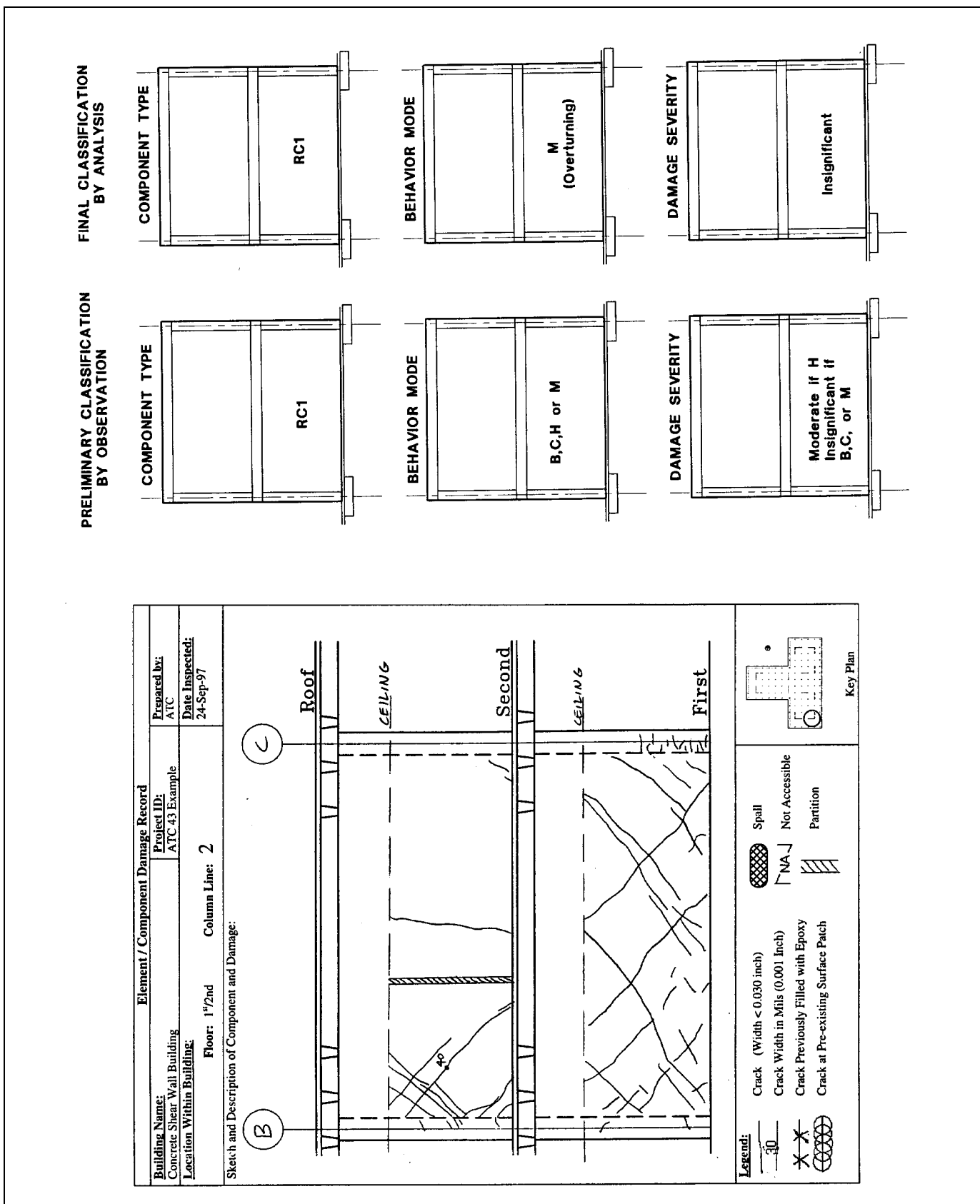


Figure 7-6 Solid Wall Example

FINAL CLASSIFICATION BY ANALYSIS

| | | | |
|-----|--|-----|-----|
| RC3 | | RC1 | |
| RC3 | | RC3 | RC1 |
| | | | |
| | | | |

| | | | |
|---|--|---|---|
| H | | N | |
| H | | H | N |
| | | | |
| | | | |

| | | | |
|---------------|--|---------------|--|
| Insignificant | | Insignificant | |
| Moderate | | Heavy | |
| | | | |
| | | | |

PRELIMINARY CLASSIFICATION BY OBSERVATION

| | | | |
|-----|--|-----|-----|
| RC3 | | RC1 | |
| RC3 | | RC3 | RC1 |
| | | | |
| | | | |

| | | | |
|--------|--|---------------|---|
| B or H | | B, C, H, or N | |
| B or H | | B or H | N |
| | | | |
| | | | |

| | | | |
|---------------------------|--|---------------------------|--|
| Insignificant or Moderate | | Insignificant or Moderate | |
| Insign. or Moderate | | Heavy | |
| | | | |
| | | | |

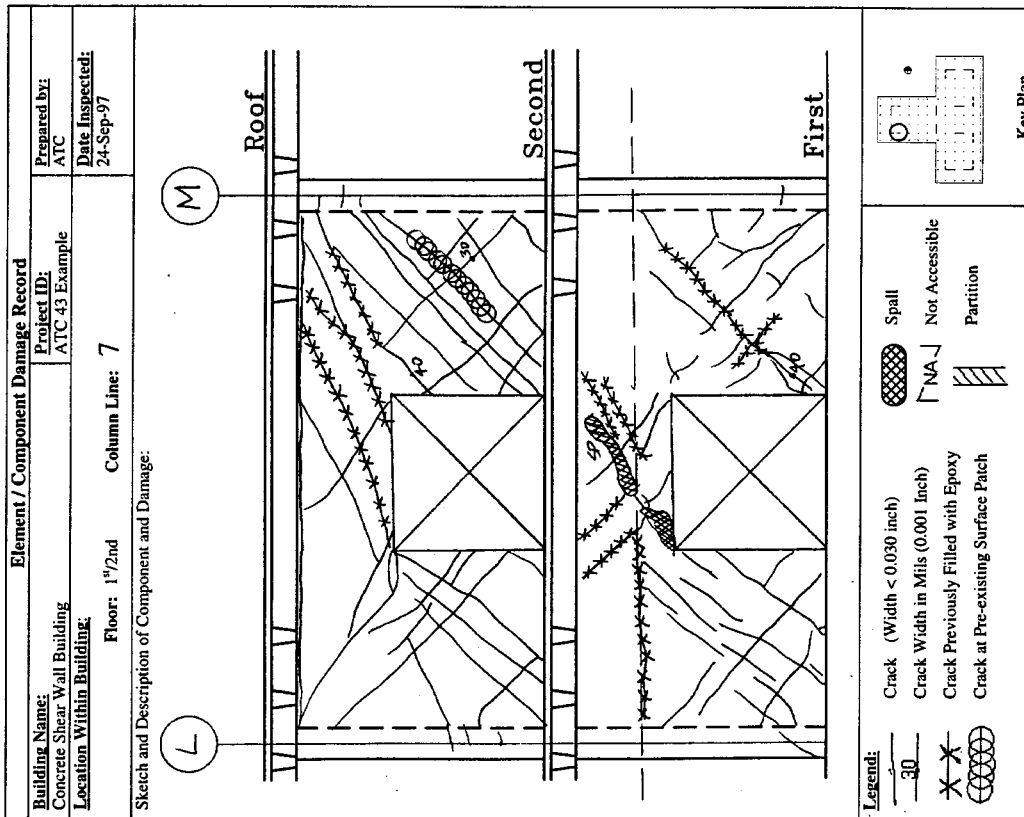


Figure 7-7 Coupled Wall Example

observed to have horizontal cracks along the interface between the top of the wall and the floor slab above.

7.2.3 Preliminary Classification (by Observation) of Component Types, Behavior Modes, and Damage Severity

The first critical step in interpreting component damage records is to identify the components within the structural element under investigation. In this case, the example building is reinforced concrete, so the summary of relevant component types is found in Sections 2.4 and 5.2.1 of FEMA 306.

Component types, Table 5-1 of FEMA 306

7.2.3.1 Component Types

The first pass in the identification process is conducted by observation, keeping in mind that the definition of a component type is not a function of the geometry alone, but of the governing mechanism of lateral deformation for the entire element or structure. Thus the identification of structural components requires consideration of the wall element over multiple floor levels. Complete diagrams showing the crack pattern over multiple floor levels such as the ones shown in the attached damage records shown in Figures 7-6, 7-7 and Damage Records D1 through D19 (Appendix A) are essential.

For the typical coupled wall elements of the example building, shown in Figure 7-7, a survey of the element geometry and the general pattern of damage suggests that the beams over the openings may be classified as weaker coupling beams (RC3), and that the wall piers flanking the openings will behave as two-story cantilever components (RC1). The thought process that leads to this conclusion includes the recognition that the beam elements are likely to be weaker than the walls on either side of the coupling beams, as well as a mental visualization of the lateral deformation of the walls and the attendant large deformation demands on the beams. As shown in Figure 7-6, the solid reinforced concrete wall component is type RC1.

Component identification, Section 2.4 of FEMA 306

7.2.3.2 Behavior Modes and Damage Severity

Once the component types have been identified, an initial classification of the behavior modes and damage severity may be made by inspecting the visible damage with reference to the component damage classification guides. Tables 5-1, 5-2, and

Behavior modes, Table 5-2 of FEMA 306

5-3 of FEMA 306 are also helpful in identifying behavior modes appropriate to the identified components.

For the typical coupled wall shown in Figure 7-7, the coupling beam component (RC3) on the second floor is observed to have light diagonal (shear) cracking, with little or no evidence of flexural cracking. As is typical of a building designed in the late 1950s, the coupling beam does not contain diagonal reinforcement, or even sufficient stirrup reinforcement, so mode A (ductile flexure) may be safely eliminated. The diagonal cracks then suggest that the behavior mode may be either mode B (flexure/diagonal tension) or mode H (preemptive diagonal tension). At the first floor coupling beams, the damage is more severe, but the behavior mode still appears to be either B or H.

In the first floor coupling beam, identification of the damage severity is relatively straightforward: the observed damage would be classified as Heavy regardless of the behavior mode. In many cases, however, the damage severity level may depend on the behavior mode. In the second floor coupling beam, for example, the damage would be classified as Insignificant if the behavior mode is identified as B (flexure followed by diagonal tension), but as Moderate if the behavior mode is identified as H (preemptive diagonal tension).

Component Guides, Section 5.5 of FEMA 306

Similarly, the wall piers of the coupled walls (RC1) have light diagonal cracking, which may be indicative of early stages of mode B (flexure/diagonal tension), early stages of mode C (flexure/diagonal compression) or more advanced stages of mode H (preemptive diagonal tension). In the first two cases, damage would be classified as Insignificant, while in the last case, damage would be classified as Moderate.

It is often not possible to distinguish between the different behavior modes, and hence the damage severity, without some analysis. This is particularly important for lower levels of damage where different modes may look very much alike, but which have different response at higher levels of damage. Consider, for example, modes B and H. The flexural cracks that initiate mode B response may have closed and become nearly invisible. The light diagonal cracking that occurs at the outset of both modes B and H will then be indistinguishable from one another, and only analysis of the section will differentiate the two modes, and hence the severity of damage. In other cases, the differences between modes are of less impor-

Verification loop, Figure 1-3 of FEMA 306

tance. Modes B and C are physically different, but have a similar effect on the stiffness, strength, and deformation capacity of the component at all levels of damage severity.

7.2.4 Final Classification (by Analysis) of Component Type, Behavior Mode and Damage Severity

In the previous section, component type, behavior mode, and damage severity were preliminarily defined based only on observation. In this section, those definitions are verified by calculation. In practice, iterations between observation and analysis may be needed to interpret correctly the seismic response and damage.

7.2.4.1 Expected Strength

The expected pre-earthquake strengths for each of the components were calculated using the FEMA 306 Section 3.6 procedures. The design concrete strength was shown on the drawings to be 3000 psi. According to the discussion in FEMA 306, Section 5.3.2, expected concrete strengths ranging from 1.0 to 2.3 times the specified strength are not unrealistic. In the example building, concrete strength was suspect, so tests were conducted which revealed that expected strength was, in fact, near the specified strength. For the purposes of the following analysis an expected strength of 3000 psi was assumed. Based on the drawing notes, reinforcing bars had a specified yield strength of 40 ksi. The expected strength of the reinforcing bars was assumed to be greater than the nominal yield strength by a factor of 1.25, so a value of 50 ksi was used for the yield strength in all calculations. If, during the course of the analysis, it becomes difficult to reconcile analytically determined behavior modes with observed damage, assumed values for material strength may need to be re-evaluated or verified through tests.

Expected strength, Section 3.6 of FEMA 306

There are two typical element types in the lateral-force-resisting system, solid walls and coupled walls. The following sections describe the details of the calculations and methodology used to classify the components of these elements.

7.2.4.2 Example 1 – Solid Wall (2B-2C)

Once a preliminary damage classification has been made by visual observation, it will generally be neces-

sary to perform some analysis to distinguish between behavior modes that are different but visually similar. As a first example, consider the damage record for the wall shown in Figure 7-6. The wall is 12 inches thick with 18-inch square boundary elements at each end. The wall length from center to center of the boundary elements is 26 feet, and the story height is 13 feet-6 inches. Note that the wall is L-shaped in plan and has a 26-foot return along line B.

Component Type. The definition of this wall as a single RC1 component (isolated wall or stronger wall pier) is easily and intuitively verified by sketching the inelastic deformation mechanism for the wall and its surrounding structure. The slabs framing into the wall clearly do not have the stiffness or strength to force a “weaker wall” type of behavior. The wall is therefore a single component with a height of 27 feet.

Behavior Mode. The preliminary classification identified four possible behavior modes for this component that were consistent with the component type and the observed damage: mode B (flexure/diagonal tension), mode C (flexure/diagonal compression), mode H (preemptive diagonal tension), and mode M (foundation rocking). For each of these behavior modes, Component Guides provide, in addition to the visual description of the different behavior modes, guidance in the analytical steps required to verify a particular behavior mode. See for example the Component Damage Classification Guide RC1B under “How to distinguish behavior mode by analysis”. Based on the recommendations of the guide, the shear associated with the development of the maximum strength in flexure, diagonal tension, web crushing, and foundation rocking were calculated. Calculation results are summarized in Table 7-1. Selected details of the calculations are provided in the box on 192.

Component guides, RC1B, RC1C, and RC2H, Section 5.5 of FEMA 306

The relationship between capacities of the different potential behavior modes defines the governing component behavior mode. Initially, consider the first five modes listed in Table 7-1, temporarily neglecting the overturning (foundation rocking) response. Because the wall is flanged, its response depends on the direction of seismic force, and the flexural capacity must be calculated for each direction. It is possible that a different behavior mode will govern in each of the two different loading directions. In this example, the diagonal tension strength at low ductility is less than the flexural strength

Table 7-1 Capacity of Potential Behavior Modes for Typical Solid Wall (2B-2C)

| Behavior Mode | Shear Capacity (kips) | FEMA 306 Reference | Comments |
|--|-----------------------|--------------------|--|
| Flexure (modes A & B) – flange in compression $M_e = 31,300$ k-ft | 1570* | Sect. 5.3.5 | All distributed reinforcement is included in the calculation of flexural strength, as is the contribution of the flange reinforcement. |
| Flexure (A & B) – flange in tension $M_e = 44,600$ k-ft | 2230* | Sect. 5.3.5 | |
| Diagonal Tension (B & H) – at low flexural ductility | 1350 | Sect. 5.3.6b | Low ductility implies $\mu \leq 2$ and high ductility implies $\mu \geq 5$, but for this example the exact displacement ductility is not important. Capacity at high ductility does not govern, since flexural yielding does not occur. |
| Diagonal Tension (B) – at high flexural ductility | 851 | Sect. 5.3.6b | |
| Web crushing (C) | 2560 | Sect. 5.3.6c | |
| Overturning (M) – flange in compression $M_e = 6,860$ k-ft | 343 | Sect. 5.2.6 | When the flange is in tension, the vertical load includes dead load contribution of flange. |
| Overturning (M) – flange in tension $M_e = 18,000$ k-ft | 923 | Sect. 5.2.6 | |

* Shear associated with development of the moment strength

in either loading direction, so mode H (preemptive diagonal tension) appears to be the governing the behavior mode. In either direction, web crushing can be eliminated as a potential behavior mode since its capacity is greater than that of all of the other modes. In the absence of overturning, mode H would therefore be selected as the behavior mode for this component.

Additional calculations indicate, however, that foundation rocking (overturning of the wall and its foundation) will occur before the other failure modes can develop. This is indicated in the last two rows of Table 7-1, where overturning capacity with the flange in compression is shown to be less than other behavior modes. As shown in the example calculations (see sidebar), the foundation rocking capacity is based on the static overturning force associated with all tributary gravity loads. In reality, there are a number of factors that would increase the force required to overturn the wall, so the calculated value may be a lower bound. For example, as the foundation lifts, it will pick up an increasing tributary area of the surrounding slabs, thus increasing the

restoring force. However, the overturning value calculated is sufficiently less than the other behavior modes to suggest that damage will be limited by rocking on the foundation. Mode M is therefore the behavior mode for the wall.

Damage Severity. The identification of the rocking behavior mode is important, because the damage severity is different for mode M than for mode H. While there is no explicit Component Damage Classification Guide provided for the rocking mode—the component may be considered as roughly analogous to the portion of a flexural wall (mode A) above the plastic hinge region—there is a ductile fuse in the structure below the component in question that will prevent the development of the brittle, force-controlled behavior mode H by limiting the development of additional seismic force. Using this analogy, and Component Guide RC1A, the damage severity is classified as Insignificant. Without the rocking mechanism, the behavior mode would be classified as H, and the damage severity would be Moderate rather than Insignificant. It is important to note

Chapter 7: Example Application

EXAMPLE CALCULATIONS FOR DIFFERENT BEHAVIOR MODES EXAMPLE 1 – SOLID WALL

Flexure:

The boundary elements at each end of the wall have 4-#10 and 7-#11 bars. The vertical wall reinforcement is #4 bars at 13" on center in each face. An approximation of the flexural capacity with the flange in compression may be made, assuming that all the steel in the tension boundary and all the wall vertical steel is yielding, as follows:

$$M_{e(comp.)} = \underbrace{A_s f_{ye} l_{wall}}_{(15.3) 50 (26)} + \underbrace{A_{sv} f_{ye} l_{wall} / 2}_{(9.2) 50 (13)} + \underbrace{P_{DL(wall)} l_{wall} / 2}_{(419) 13}$$

$$= 31,300 \text{ k-ft}$$

With the flange in tension the capacity increases because of the yielding of the wall vertical reinforcing in the effective flange width assumed to be one half the effective wall height (M/V) plus the wall thickness, or about ten feet. The capacity also increases because of the additional dead load resistance of the flange. An approximation of the flexural capacity with the flange in tension is then:

$$M_{e(ten.)} = M_{e(comp.)} + \underbrace{A_{sv} f_{ye} l_{wall}}_{(3.8) 50 (26)} + \underbrace{P_{DL(flange)} l_{wall}}_{(320) 26}$$

$$= 31,317 + 44,600 \text{ k-ft}$$

These approximations for moment capacities were checked using strain compatibility calculations and found to be acceptable. Using an M/V ratio of 20 ft the shear forces associated with the moment capacities are 1570 k (flange in compression) and 2230 k (flange in tension).

Diagonal Tension (Shear Strength):

In order to include the effect of axial load on shear strength, and the potential degradation of the shear in plastic hinge zones, the equations recommended in Section 5.3.6b of FEMA 306 were used to calculate the diagonal tension strength.

$$V_n = V_c + V_s + V_p$$

An M/V ratio of 20 feet was used (approximately 0.75 times the component height) based on the analysis results for shear and moment.

$$A_s = 41.2 \text{ in}^2$$

$$A_g = 4176 \text{ in}^2$$

$$\rho_s = 0.0098$$

Thus Equations 5-3 and 5-4 of FEMA 306 yield

$$\alpha = 1.5 \quad k_{rc} = 3.5 \text{ (low ductility)}$$

$$\beta = 0.7 \quad k_{rc} = 0.6 \text{ (high ductility)}$$

and the concrete contribution (Equation 5-2) becomes

$$V_c = \alpha \beta k_{rc} \sqrt{f'_{ce}} b_w (0.8l_w)$$

$$V_c = 605 \text{ kips at low ductility demand}$$

$$V_c = 104 \text{ kips at high ductility demand}$$

The steel contribution is given by Equation 5-5:

$$V_s = \rho_n f_{ye} b_w h_d$$

where $\rho_n = .00256$, $f_{ye} = 50 \text{ ksi}$, $b_w = 12"$, and h_d is limited by the component height of 27'-0". Thus

$$V_s = 498 \text{ kips}$$

The axial load contribution is given by Equation 5-6. Considering only the structure dead load tributary to the wall (419 kips) V_p becomes

$$V_p = \frac{(l_w - c) N_u}{(2M / V)} = 264 \text{ kips (flange in compression)}$$

$$= 249 \text{ kips (flange in tension)}$$

NOTE: $c = 16.8 \text{ in.}$ (flange in compression), $c = 33 \text{ in.}$ (flange in tension)

Therefore, Equation 5-1 for the diagonal tension strength gives a value of 1352 kips at low ductility demand, and 851 kips at high ductility demand, both with the flange in tension.

Diagonal Compression (Web Crushing):

The web crushing strength is given by Equation 5-7. This equation requires an estimate of the drift ratio to which the component is subjected, with increasing drift corresponding to a decrease in capacity. An upper bound estimate of 1 percent drift is assumed, to get a lower bound on the web crushing strength:

$$V_{wc} = \frac{1.8 f'_{ce} b_w (0.8l_w)}{1 + \left(600 - 2000 \frac{N_u}{A_s f'_{ce}} \right) \delta} = 2560 \text{ kips}$$

Foundation Rocking (Overturning):

The static overturning calculation includes not only the dead weight of the wall and tributary slabs at the 2nd floor and roof, but also a tributary area of the slab on grade (496 kips total) and the foundation weight (16 kips per footing). When the wall flange is in tension, the weight of the flange and additional DL are included.

$$V_{or} = \frac{1}{(M / V)} M_{or} = \frac{1}{20} (496k(26' / 2) + 16k(26'))$$

$$= 343 \text{ kips (flange in compression)}$$

$$V_{or} = \frac{1}{(M / V)} M_{or}$$

$$= \frac{1}{20} (496k(26' / 2) + 446k(26') + 16k(26'))$$

$$= 923 \text{ kips (flange in tension)}$$

that the damage severity is not a function of the observed crack pattern alone – the governing behavior mode must be known before a judgement of the damage severity can be made.

7.2.4.3 Example 2 – Coupled Wall (7L-7M)

As an example of the second typical wall element type, consider the damage record for the coupled wall shown in Figure 7-7. Like the solid wall example, the wall is 12 inches wide with 18-inch-square boundary elements at each end. However, there is a 6'-6" wide by 7'-3" tall opening in the center of the wall at each floor. The wall length from center to center of the boundary elements is 26 feet, and the story height is 13'-6". The coupled wall has an L-shaped plan with a 26-foot flange along line M. The coupling beam and wall are similar to the example shown in Figure 7-5, except that this particular coupled wall is discontinuous below the first floor and is supported on 24-inch-square reinforced-concrete columns at the basement.

Component Type. Visual observation leads to the division of this structural element into two RC1 wall piers and two RC3 coupling beams. Analysis will verify that the beams are weaker than the walls, and thus that the initial classification is valid.

Behavior Mode. In the preliminary classification, the coupling beams were designated by observation as

mode B (flexure / diagonal tension) or mode H (preemptive diagonal tension), and the wall piers were designated as mode B (flexure / diagonal tension), mode C (flexure / diagonal compression), mode H (preemptive diagonal tension), or mode N (individual pier rocking). As in the first example, the shears associated with the development of the maximum strength in flexure, diagonal tension, and web crushing were calculated, with results summarized in Tables 7-2 and 7-3. Selected details of the calculations are provided for reference on pages 196 through 198.

Looking first at the RC3 coupling beam component, the calculation results shown in Table 7-2 indicate that the shear strength will be reached before the development of the moment strength, even at low ductility levels, so the behavior mode H (preemptive diagonal tension) governs.

For the RC1 wall pier components, the calculations and discussions that follow show that behavior mode N, individual pier rocking, governs the seismic response. For the piers of the coupled wall, which discontinue below the first floor and are supported on basement columns, this behavior mode involves the yielding in flexure of the basement columns and the coupling beams reaching their capacity in shear. The wall pier rotates about the supporting column in a manner similar to

Table 7-2 Capacity of Potential Behavior Modes for Typical Coupling Beam

| Coupling Beams RC3 Behavior Mode | Limiting Component Shear (kips) | FEMA 306 Reference | Comments |
|--|---------------------------------|--------------------|---|
| Flexure (mode A) $M_e = 1210$ k-ft | 373* | Sect. 5.3.5 | Note that slab reinforcement was ignored in the calculation of the beam flexure capacity. Since preemptive shear governs ($242 < 373$), this is irrelevant. A more accurate calculation would be warranted if the capacities in the different modes were similar. |
| Diagonal Tension (B and H) – at low flexural ductility | 242 | Sect. 5.3.6b | Governing capacity |
| Diagonal Tension (B) – at high flexural ductility | 137 | Sect. 5.3.6b | This capacity does not govern since flexural yielding does not occur. |
| Sliding Shear (D) | 150 | Sect. 5.3.6c | This mode is unlikely since it typically occurs after flexural yielding. Such yielding is not expected since preemptive diagonal tension governs over flexural response. |

* Component shear in beam associated with development of the component moment strength

Chapter 7: Example Application

Table 7-3 Shear Capacities for Potential Behavior Modes of Wall Pier (RC1) Components in Coupled Wall

| Potential Behavior Mode | Limiting Component Shear (kips) | FEMA 306 Reference | Notes |
|--|---------------------------------|--------------------|--|
| <u>Flexure(mode A)</u> | See notes* | Sect. 5.3.5 | *In example calculations, moment capacities are compared to moment demands corresponding to mode N. Flexure is shown not to govern. |
| <u>Diagonal Tension (mode B and H) at Low Flexural Ductility</u> RC1@7L-load to east RC1@7L-load to west RC1@7M-load to east RC1@7M-load to west | 690 311 328 692 | Sect. 5.3.6b | Limiting shears are compared to those for behavior mode N. To consider redistribution of lateral forces, the sum of shears for the two wall piers is considered. |
| <u>Diagonal Tension (mode B) at High Flexural Ductility</u> RC1@7L-load to east RC1@7L-load to west RC1@7M-load to east RC1@7M-load to west | 470 163 166 472 | Sect. 5.3.6b | These capacities do not govern, since flexural yielding does not occur. |
| <u>Web Crushing (mode C)</u> RC1@7L-load to east RC1@7M-load to west | 1710 1810 | Sect. 5.3.6c | Web crushing not applicable for low axial load or tension. |
| <u>Rotation about Column (mode N)</u> RC1@7L-load to east RC1@7L-load to west RC1@7M-load to east RC1@7M-load to west | 330 300 300 330 | | Shear in piers is limited by capacity of coupling beam (RC3) components. |

foundation rocking. Free body diagrams corresponding to this mechanism and behavior mode are shown in the example calculations that follow.

Comparison of the moment demands corresponding to the behavior mode N to moment capacities of the wall pier sections is shown in the example calculations. The moment demands are well below the moment capacities, indicating that flexural yielding will not occur. This eliminates modes B (flexure/diagonal tension) and C (flexure/diagonal compression) as possible behavior modes.

The limiting component shears associated with possible behavior modes for the wall piers are summarized in Table 7-3. The table verifies that the web crushing (diagonal compression) can be eliminated as a possible behavior mode because the capacity is much higher than that corresponding to other behavior modes. Behavior mode H, preemptive diagonal tension, is investigated by comparing the limiting shears to those of mode N.

Diagonal tension capacities at high ductility are only relevant for the combined flexure/diagonal tension behavior mode, which will not occur since flexural

yielding and the consequent degradation of the V_c component of shear strength does not occur. The relevant diagonal tension capacities are those at low ductility.

The diagonal tension capacities of 311k (RC1@7L-load to west) to 328k (RC1@7M-load to east) for the wall piers subject to axial tension are similar to the shear demands in the pier rotation mode after failure of the coupling beams; however, there is significant capacity of 690k (RC1@7L-load to east) to 692k (RC1@7M-load to west) in diagonal tension on the corresponding compression sides of the wall. A diagonal tension failure cannot fully develop on one side of the coupled wall without transferring lateral forces to the other side of the wall. Considering that shear can be transferred as axial forces in the coupling beam and slab according to the stiffness and strength of each wall pier, the sum of wall pier component strengths on each side of the coupled wall can be used to determine the governing behavior mode. For the individual pier rotation behavior, the associated total shear demand is 630k on the coupled wall element. For a diagonal tension behavior mode occurring in both wall piers, the associated shear capacity is 1003k to 1018k. Diagonal tension failure will not govern, since the pier rotation behavior mode occurs at a lower total lateral load. Thus, the results of the analytical calculations indicate the pier rotation (N) is the governing behavior mode for the RC1 components. This analytical conclusion agrees with field observation. The degree of diagonal cracking observed in the wall pier RC1 components is consistent with substantial shear stress, but less than that which might be expected for diagonal tension failure.

Damage Severity. For the RC3 components behaving in mode H, the damage classification guides indicate that the observed damage is Moderate in the second story and Heavy in the first story coupling beam. In the wall piers, the protection of the element by a ductile mode (similar to mode N, Foundation Rocking) in surrounding components places them in an Insignificant damage category.

7.2.5 Other Damage Observations

Several of the walls were observed to have horizontal cracks just below the roof slab and/or the second-floor slab. In addition to new cracks of this type, a few walls had pre-existing horizontal cracks below the slabs, which had been repaired by epoxy injection. The widest of these horizontal cracks occurred under the roof slab of the wall on column lines 7C-7D, as shown in the Component Damage Record D3. The engineer in the field indicated that joint movement occurred at this

crack and suspected that sliding shear behavior may have occurred.

Subsequent thinking by the evaluating engineers about this observation, however, weighed against the conclusion of sliding shear behavior. The crack was not observed to extend into the boundary columns of the wall, and there was no evidence of lateral offset at the boundary columns. While the crack is located near a likely construction joint where poor construction practice can exacerbate sliding shear behavior, the crack is not located in the maximum moment region of the wall. As is indicated in FEMA 306, sliding shear behavior is most likely to occur after flexural yielding has occurred. For this wall, flexural yielding would initiate at the base of the wall where moments are at a maximum, not at the top. In any case, foundation rocking preempts flexural yielding for the typical solid wall, as indicated previously in this example. A quick calculation of sliding shear strength shows that the behavior mode is not expected to govern the wall's response.

Given this information, the damage observations are reconsidered, and it is judged that sliding movements did not occur at the horizontal crack. Therefore, the most likely explanation is that these horizontal cracks are caused by earthquake displacements in the *out-of-plane* direction of the wall. It is judged that the horizontal cracks, whose widths are less than 0.03 inches, do not significantly affect seismic response.

7.2.6 Summary of Component Classifications

7.2.6.1 Solid Walls

All wall components of the building are evaluated in a similar manner, as described in the preceding sections. In total, the building has six coupled walls plus five solid walls acting in the North-South direction, and two coupled walls plus six solid walls acting in the East-West direction. The damage records for these walls can be found in Component Damage Records D1–D19 (Appendix A).

Each solid wall is a single structural component (RC1), while each coupled wall has four components: two coupling beams (RC3) and two wall piers (RC1). Thus there are a total of 43 structural wall components in the building, as indicated in Tables 7-4 and 7-5. For each of these, the component type, behavior mode and damage severity is established as described below and shown in the tables.

**EXAMPLE CALCULATIONS FOR DIFFERENT BEHAVIOR MODES
EXAMPLE 2 – COUPLED WALL (7L-7M)**

COUPLING BEAMS

RC3 Flexure:

The moment strength of the coupling beams is calculated as discussed in FEMA 306, Section 5.3.5 using expected values for material properties ($f'_{ce} = 3000$ psi, $f_{ye} = 50$ ksi). The beams are 6'-3" deep, with 3 - #9 bars at top and bottom and #4 bars @ 13" on center at each face. The calculated moment capacity is 1210 k-ft. This capacity is determined using strain compatibility calculations that demonstrate that all longitudinal bars yield. The M/V ratio for the coupling beam is 3'-3", so the shear associated with development of the moment capacity at each end of the beam is 373 kips. Note that slab reinforcement is ignored in the calculation of the beam flexure capacity. It will be shown below that pre-emptive shear clearly governs, so this is irrelevant. However, a more accurate calculation would be warranted if the capacities in the different modes were similar.

RC3 Diagonal Tension (Shear Strength):

The equations for diagonal tension strength in Section 5.3.6b of FEMA 306 may be used for coupling beams. For beams, the axial load is not significant, thus $V_p = 0$ and Equation 5-1 becomes:

$$V_n = V_c + V_s$$

Using an M/V ratio of 3'-3" (half the clear span of the coupling beams) Equations 5-3 and 5-4 of FEMA 306 yield

$$\alpha = 1.5 \quad \rho_g = 0.0059 \quad \kappa_{rc} = 3.5, 0.6$$

$$\beta = 0.61 \quad \sqrt{f'_{ce}} = 55 \text{ psi}$$

and the concrete contribution Equation 5-2 becomes

$$V_c = \alpha \beta k_{rc} \sqrt{f'_{ce}} b_w (0.8l_w)$$

$$V_c = 127 \text{ kips at low ductility}$$

$$V_c = 22 \text{ kips at high ductility}$$

The steel contribution is given by Equation 5-5

$$V_s = \rho_n f_{ye} b_w h_d$$

where $\rho_n = .00256$ is based on the vertical (stirrup) reinforcement, $f_{ye} = 50$ ksi is the expected steel yield strength, $b_w = 12"$, and $h_d = 75"$ is the horizontal length over which vertical stirrup reinforcement contributes to shear strength, in this case the length of the coupling beam. Thus

$$V_s = 115 \text{ kips}$$

The total diagonal tension strength is then 242 kips at low ductility, and 137 kips at high ductility.

RC3 Sliding (Sliding Shear):

FEMA 306 Section 5.3.6d gives the sliding shear strength for coupling beams at moderate ductility levels as

$$V_{sliding} = 3 \left(\frac{l_n}{h} \right) \sqrt{f'_{ce}} b_w d = 150 \text{ kips}$$

This failure mode is generally associated with beams that are well reinforced for diagonal tension, and that undergo multiple cycles at a moderate ductility level. Since the pre-emptive shear failure mode governs, the sliding shear mode is not a potential failure mode.

WALL PIERS

RC1 Flexure:

The figures below show the free body diagrams of the wall for lateral forces toward the east and toward the west. In both cases it is assumed that the coupling beams and first floor slab have reached their capacities. It is also assumed that the columns beneath the first floor are yielding in flexure. These assumptions define a potential inelastic lateral mechanism for the coupled wall. If the assumed lateral mechanism for the coupled wall is correct, the flexural capacity of the RC1 components must be sufficient to generate the diagonal tension failure in the RC3 coupling beams. The moment demand diagrams for the RC1 pier components are also shown below.

The boundary elements in the wall piers at lines L and M each contain 8-#11 vertical bars. The vertical wall reinforcing comprises #4 bars at 13" on center in each face. Using strain compatibility calculations, the moment capacities at the top and bottom of the piers (between the first floor and the top of the door opening) corresponding to the appropriate axial loads are calculated.

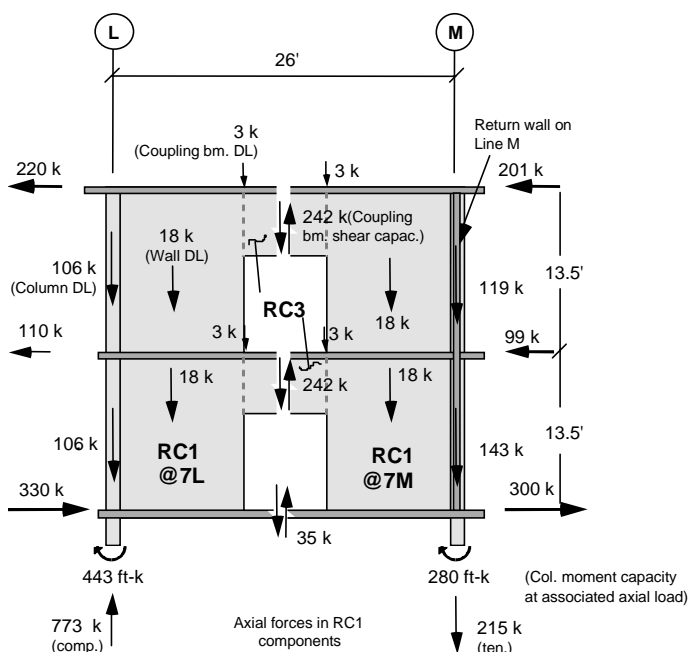
The moment capacity and demand for the RC1 components must be determined with respect to the same axis. For RC1@L the elastic centroid is selected. For RC1@M the elastic centroid of the component neglecting the return wall is used as the axis. When the return wall is in compression it contributes little to the flexural strength of the wall pier. However, when in tension, the reinforcement in the return increases moment strength. Therefore, in the capacity calculations, the vertical reinforcement in approximately 10 ft. of return is included. This distance is estimated in accordance with FEMA 306 Section 5.3.5b as 50% to 100% of the M/V for the entire wall.

The flexural demand and capacity of the RC1 components are summarized in the following table:

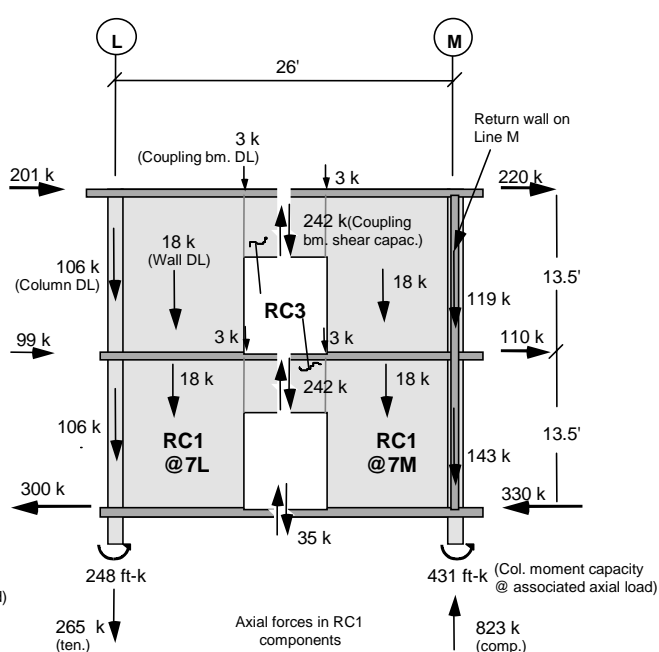
Chapter 7: Example Application

CALCULATIONS FOR EXAMPLE 2 – COUPLED WALL (continued)

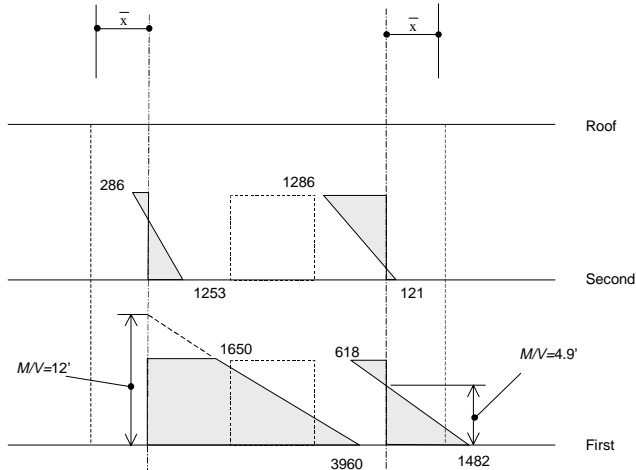
| Component | Load Direction | Location on Pier | Axial Load (k, comp.+) | Moment Capacity (k-ft) | Moment Demand (k-ft) |
|-----------|----------------|------------------|------------------------|------------------------|----------------------|
| RC1@L | East | Top | 773 | 6470 | 1650 |
| | | Bottom | 773 | 6470 | 3960 |
| | West | Top | -265 | 2190 | 428 |
| | | Bottom | -265 | 2190 | 1660 |
| RC1@M | East | Top | -215 | 2400 | 618 |
| | | Bottom | -215 | 7120 | 1480 |
| | West | Top | 823 | 6660 | 1850 |
| | | Bottom | 823 | 6660 | 4160 |



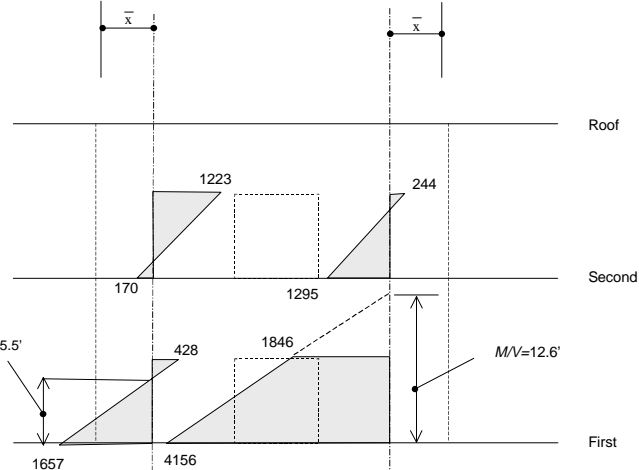
Free Body Diagram for Seismic Forces to East



Free Body Diagram for Seismic Forces to West



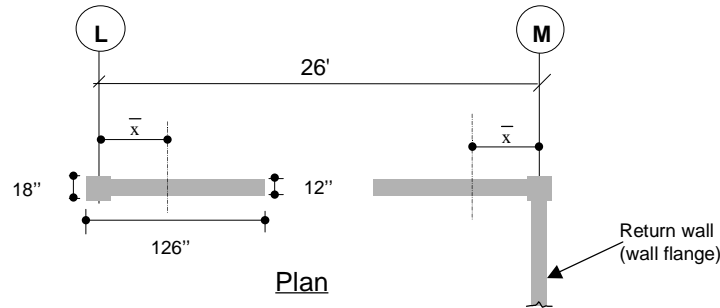
Moment Diagram (@ centroid of piers) for Load to East
(plotted on tension side in k-ft)



Moment Diagram (@ centroid of piers) for Load to West
(plotted on tension side in k-ft)

Chapter 7: Example Application

CALCULATIONS FOR EXAMPLE 2 – COUPLED WALL (continued)



Distance to the elastic centroid from gridline:

$$X = \left\{ \frac{[126(12)126/2 + 2(18)3(9)]}{[126(12) + 2(18)3]} \right\} - 9$$

$$= 50.2" \text{ or } 4.2'$$

| Comp. | Load Direct. | Axial Load (k) | V_c | Reduce for Ten. | Net V_c (k) | V_s (k) | V_p (k) | Tot. V (k) | Duct. |
|-------|--------------|----------------|-----------|-----------------|---------------|-----------|-----------|------------|-------------|
| RC1@L | East | 773 (comp.) | 265 45 | 1.0 | 265 45 | 133 | 292 | 690 470 | low high |
| | West | -265 (ten.) | 265 45 | 0.67 | 178 30 | 133 | 0 | 311 163 | low high |
| RC1@M | East | -215 (ten.) | 265 45 | 0.74 | 195 33 | 133 | 0 | 328 166 | low high |
| | West | 823 (comp.) | 265 45 | 1.0 | 265 45 | 133 | 294 | 692 472 | low high |

RC1 Diagonal Tension (Shear Strength):

The equations in Section 5.3.6 of FEMA 306 were again used to calculate the diagonal tension strength.

$$V_n = V_c + V_s + V_p$$

Using the component M/V values from the moment diagrams, Equations 5-3 and 5-4 yield

$$\alpha = 1.5 \quad \beta = 0.76 \quad \rho_g = 0.0013$$

and the concrete contribution from Equation 5-2 becomes

$$V_c = \alpha \beta k_{rc} \sqrt{f'_{ce}} b_w (0.8l_w)$$

$$V_c = 265 \text{ kips at low ductility}$$

$$V_c = 45 \text{ kips at high ductility}$$

When the component experiences net axial tension ACI 318-95, eqn. 11-8 specifies the the concrete contribution to shear strength, V_c , be reduced by the factor $1 - [N_u / (500 A_g)]$.

The steel contribution is given by Equation 5-5

$$V_s = \rho_n f_{ye} b_w h_d$$

where $\rho_n = .00256$, $f_{ye} = 50 \text{ ksi}$, $b_w = 12"$, and h_d is limited by the height of the door 7'-3". Thus

$$V_s = 133 \text{ kips}$$

The compressive axial load contribution is given by Equation 5-6.

$$V_p = \frac{(l_w - c)N_u}{\left(2 \frac{M}{V}\right)}$$

Considering all of the above contributions the diagonal tension strengths of the RC1 components are summarized in the table above:

RC1 Diagonal Compression (Web Crushing):

The web crushing strength is given by Equation 5-7. This equation requires an estimate of the drift ratio to which the component is subjected, with increasing drift decreasing the capacity. An upper bound estimate of 1% is assumed to get a lower bound on the web crushing strength:

$$V_{wc} = \frac{1.8 f'_{ce} b_w (0.8l_w)}{1 + \left(600 - 2000 \frac{N_u}{A_g f'_{ce}}\right) \delta} = 1710 \text{ kips for RC1@7L load to East}$$

$$= 1807 \text{ kips for RC1@7M load to West}$$

Web crushing is not typically an issue for low axial loads or net tension.

The typical solid walls were calculated to behave in a foundation rocking (or overturning) mode (type M). There are no damage guides for this behavior mode. However, component behavior description in FEMA 306 considers this mode to have moderate to high ductility. The damage associated with this behavior mode may not be apparent based on the observations of the walls. Damage to other structural and nonstructural elements, such as damage to the floor slab at the base or to the beams framing into the ends of the walls, should be used to assess the severity of the mode. Since there was no significant damage to the adjacent structural and nonstructural elements, the damage severity is judged to be Insignificant.

7.2.6.2 Coupling Beams

Based on calculations, the behavior mode of the coupling beams is Preemptive Diagonal Tension (Type H). Based on the damage observations and the component guides, the damage for the coupling beams with spalling, bar-buckling, and/or significant cracking was classified as Heavy. For the coupling beams with shear cracking, but no bar-buckling or significant spalling, the damage is Moderate.

7.2.6.3 Wall Piers

The walls adjacent to the coupling beams are expected to behave in a mode of individual pier rocking (type N). There are no Component Guides for this behavior mode. However, the component behavior description for this mode of behavior considers this mode to have moderate to high ductility. Similar to the solid shear walls, the lack of damage to the adjacent structural and nonstructural elements was used to classify the damage as Insignificant.

7.3 Evaluation by the Direct Method

The effects of damage are quantified by the costs associated with potential repairs (component restoration measures), which if implemented, would restore the components to their pre-event condition. In the direct method, restoration measures are considered on a component-by-component basis without an analysis of global performance. It is intended to be a simple and approximate approach. The Component Damage Classification Guides in FEMA 306 are used to determine

Hypothetical repairs for direct method, Section 4.6 of FEMA 306

the appropriate potential repairs to restore each component.

The potential repairs required to restore the structural performance and nonstructural functionality of the building include both structural and nonstructural (e.g., cosmetic) measures for each damaged component.

7.3.1 Structural Restoration Measures

7.3.1.1 Coupling Beams

As shown in Tables 7-4 and 7-5, three of the coupling beams were classified as component type RC3, behavior mode H, having Heavy damage. As recommended for this component type, behavior mode, and damage severity, the component restoration measure chosen is to replace these components. The proposed repair would be to remove the concrete at the coupling beam and a portion of the floor slab, install new reinforcing bars, and cast new concrete for the wall. The new reinforcing steel in the coupling beams would be detailed in accordance with the current provisions of the governing building code for coupled shear walls, as shown in Figure 7-8.

Damage guide for RC3H, Table 5-2 of FEMA 306

The coupling beams with Moderate damage could be repaired by epoxy injection of all diagonal shear cracks greater than 10 mils wide, since epoxy injection is recommended for structural restoration using the damage guide for RC3H. Although it is possible to inject smaller cracks, the additional cost does not justify the marginal benefit. Since cracks as large as 12 mils can be tolerated in normal concrete structures (ACI, 1994), the unrepaired cracks should not be detrimental. The length of the cracks to be injected is estimated as 100 feet.

7.3.1.2 Solid Walls

The remaining wall components are type N or M. There are no Component Guides for these modes to indicate the appropriate repairs directly. As discussed earlier, these modes have moderate to high ductility capacity. Conservatively, the damage guide for Type B, flexure / diagonal tension, is used since this is a moderate ductility mode, analogous to the actual behavior mode. The Component Guides for the type RC1B components indicate that if cracks are less than 1/16 inch, the damage can be classified as Insignificant, and therefore structural repairs are not necessary. Two of the shear wall components had cracks that exceeded 1/16 inch. This amount of cracking would be classified as Moder-

Chapter 7: Example Application

Table 7-4 Summary of Component Type, Behavior Mode, and Damage Severity for Wall Components (North-South Direction)

| Column Line | Floor | Wall Type | Component Type and Behavior Mode | Damage Severity |
|--------------------|--------------|------------------|---|------------------------|
| B / 2-3 | First-Second | Coupled | RC1N | Insignificant |
| | First | Coupled | RC3H | Moderate |
| | First-Second | Coupled | RC1N | Insignificant |
| | Second | Coupled | RC3H | Moderate |
| B / 5-7 | First-Second | Coupled | RC1N | Insignificant |
| | First | Coupled | RC3H | Moderate |
| | First-Second | Coupled | RC1N | Insignificant |
| | Second | Coupled | RC3H | Moderate |
| B / 10-12 | First-Second | Coupled | RC1N | Insignificant |
| | First | Coupled | RC3H | Moderate |
| | First-Second | Coupled | RC1N | Insignificant |
| | Second | Coupled | RC3H | Moderate |
| B / 14-15 | First-Second | Coupled | RC1N | Insignificant |
| | First | Coupled | RC3H | Heavy |
| | First-Second | Coupled | RC1N | Insignificant |
| | Second | Coupled | RC3H | Moderate |
| E / 2-3 | First-Second | Coupled | RC1N | Insignificant |
| | First | Coupled | RC3H | Moderate |
| | First-Second | Coupled | RC1N | Insignificant |
| | Second | Coupled | RC3H | Insignificant |
| E / 14-15 | First-Second | Coupled | RC1N | Insignificant |
| | First | Coupled | RC3H | Moderate |
| | First-Second | Coupled | RC1N | Insignificant |
| | Second | Coupled | RC3H | Moderate |
| G / 7-8 | First-Second | Solid | RC1M | Insignificant |
| G / 9-10 | First-Second | Solid | RC1M | Insignificant |
| M / 7-8 | First-Second | Solid | RC1M | Insignificant |
| M / 9-10 | First-Second | Solid | RC1M | Insignificant |
| M / 8-9 | Ground | Solid | RC1B | Insignificant |

Table 7-5 Summary of Component Type, Behavior Mode, and Damage Severity for Wall Components (East-West Direction)

| Column Line | Floor | Wall Type | Component Type and Behavior Mode | Damage Severity |
|-------------|--------------|-----------|----------------------------------|-----------------|
| 7 / L-M | First-Second | Coupled | RC1N | Insignificant |
| | First | Coupled | RC3H | Heavy |
| | First-Second | Coupled | RC1N | Insignificant |
| | Second | Coupled | RC3N | Moderate |
| 10 / L-M | First-Second | Coupled | RC1N | Insignificant |
| | First | Coupled | RC3H | Heavy |
| | First-Second | Coupled | RC1N | Insignificant |
| | Second | Coupled | RC3N | Moderate |
| 2 / B-C | First-Second | Solid | RC1M | Insignificant |
| 2 / D-E | First-Second | Solid | RC1M | Insignificant |
| 7 / C-D | First-Second | Solid | RC1M | Insignificant |
| 10 / C-D | First-Second | Solid | RC1M | Insignificant |
| 15 / B-C | First-Second | Solid | RC1M | Insignificant |
| 15 / D-E | First-Second | Solid | RC1M | Insignificant |

ate for type B behavior. Epoxy injection is recommended in the Component Damage Classification Guides for these cracks. Thus, for performance restoration by the direct method, these walls would have all of the cracks exceeding 1/16 inch repaired by injection with epoxy. The total length of crack to be injected is estimated at 22 feet.

Spalls (other than at the coupling beams that are being replaced) could be repaired by application of a concrete repair mortar to restore the visual appearance. The total volume of concrete spalls is estimated to be 3 cubic feet.

7.3.2 Nonstructural Restoration Measures

The wall components with visible cracks could be repaired by patching the cracks with plaster, and then painting the entire wall. This repair is only intended to restore the visual appearance of the wall. Restoration of other nonstructural characteristics, such as water tightness and fire protection, are not necessary in this instance.

In addition, many of the suspended ceiling tiles became dislodged and fell during the earthquake. The nonstructural repairs would include replacing the ceiling tiles.

7.3.3 Restoration Summary and Cost

Table 7-6 summarizes the performance restoration measures and estimated costs. Additional costs related to inspection, evaluation, design, management and indirect costs may also be involved.

7.4 Evaluation by Performance Analysis

The use of the direct method is limited to an estimate of the loss associated with the damaging earthquake. It cannot be used to evaluate actual performance. For these purposes, relative performance analysis as described in FEMA 306 is used. The basic procedure comprises a comparison of the anticipated performance of the building in future earthquakes in its pre-event, damaged, and repaired conditions. This comparison may be made for one or more performance objectives.

Chapter 7: Example Application

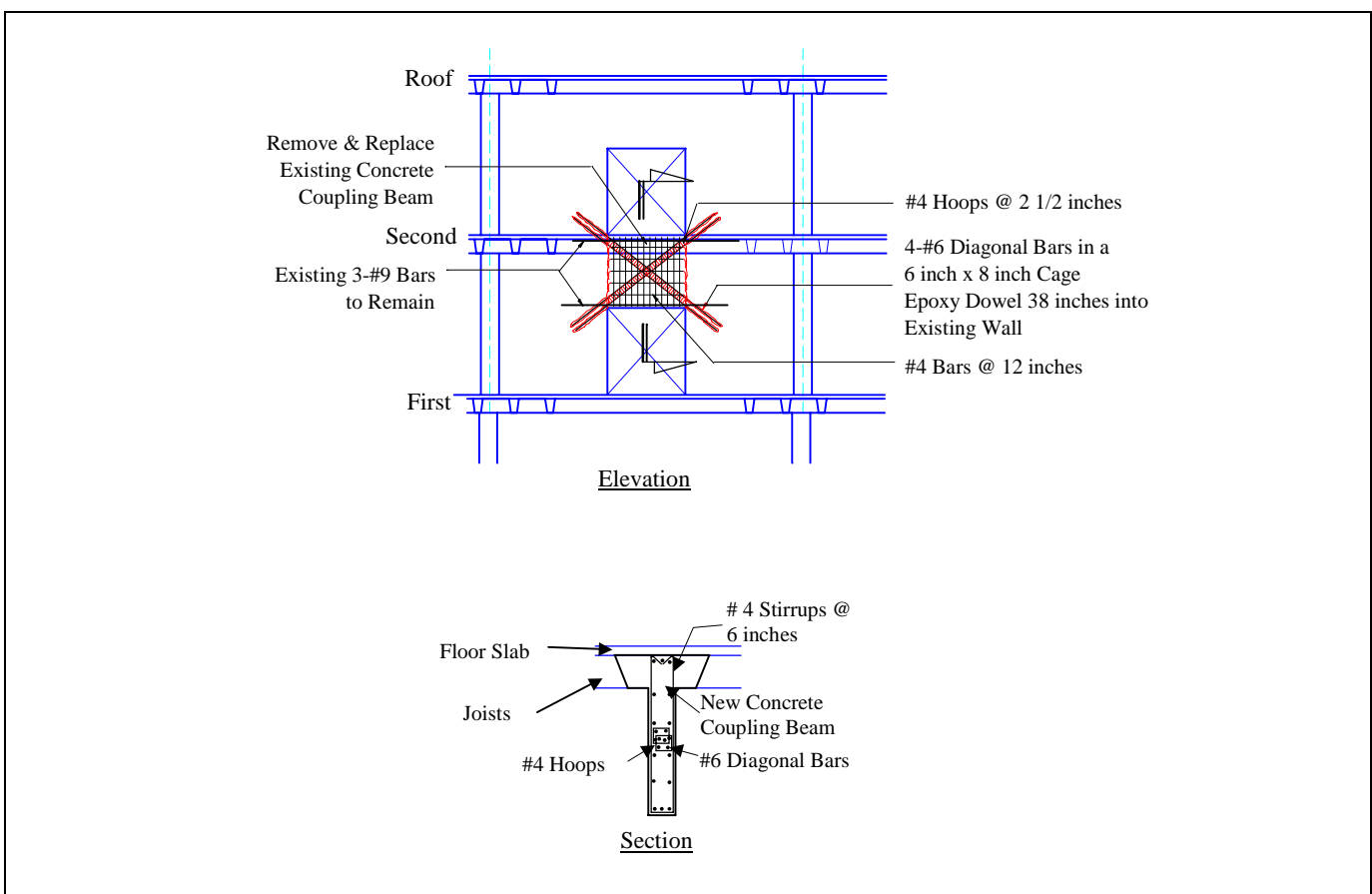


Figure 7-8 Detail of Coupling Beam Replacement

Table 7-6 Restoration Cost Estimate by the Direct Method

| Item | Unit Cost (1997 dollars) | Quantity | Cost (1997 dollars) |
|---|-----------------------------|--------------|------------------------|
| Epoxy Injection | \$25.00 /lin ft | 122 ft | \$ 3,050. |
| Coupling Beam Removal and Replacement | \$74.00 /cu ft | 122 cu ft | \$ 9,028. |
| Patch and paint walls | \$0.60 /sq ft | 10,175 sq ft | \$ 6,105. |
| Replace ceiling tiles | \$2.00 /sq ft | 15,000 sq ft | \$30,000. |
| General Conditions, Fees, Overhead & Profit (@ 30%) | | | \$14,455. |
| Total | | | \$62,638. |

7.4.1 Performance Objectives

Two performance objectives are considered in this example. The first is the *life safety* performance level, as defined in FEMA 273, for an earthquake associated with a 475-year

Performance objectives, Section 4.2 of FEMA 306

return period (10 percent probability of exceedance in 50 years) for this site. The response spectrum for this earthquake is shown in Figure 7-9. The soil at the site was determined to be type S_c . Using the available seismic data, the spectral response at short periods ($T = 0.2$ sec) for this site is 1.0 g and the spectral response at 1 second is 0.56 g.

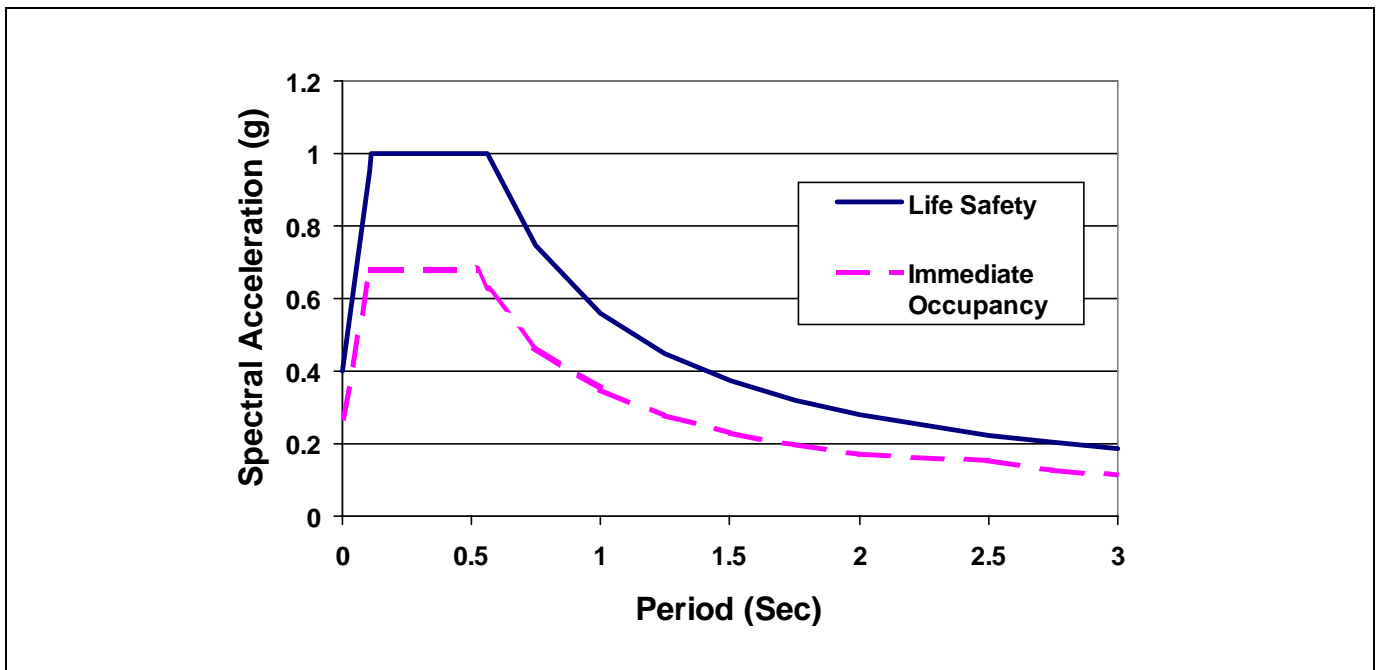


Figure 7-9 Response Spectra for Selected Performance Levels

The building was also checked for *immediate occupancy* performance level using an earthquake with a 50 percent probability of exceedance in 50 years. For this earthquake, the spectral response at short periods at this site is 0.68 g and the spectral response at 1 second is 0.35 g. The response spectra for the immediate occupancy performance level is also shown in Figure 7-9.

It should be noted that these performance objectives do not necessarily correspond to the original criteria used for design of the building.

7.4.2 Nonlinear Static Analysis

7.4.2.1 Computer Model

The building is analyzed in its pre-event, post-event and repaired conditions using a three-dimensional computer model. Modeling of the building is done using the recommendations of FEMA 273 and FEMA 306. The model is subjected to a nonlinear static (pushover) analysis to assess its force/displacement response. For this example, the analysis is run only in the East-West direction, which is the direction that experienced the most significant damage.

The computer analysis program SAP2000 (CSI, 1997) is used to model the structure. The reinforced concrete walls and coupling beams are modeled using beam elements. The beam elements are located at the center of gravity of each wall section, and are given properties

that represent the wall section stiffness. Rigid end offsets are used to model the joint regions in the coupled walls as shown in Figure 7-10. Small models of individual walls are used to verify that the beam elements used to model the walls have approximately the same stiffness and shear distribution as a model using shell elements for the walls. A three dimensional view of the global model is shown in Figure 7-11. The horizontal floor and roof diaphragms are modeled using beam elements, as shown in Figure 7-11, with lumped masses at the nodes.

The pushover analysis is conducted by applying static loads at the locations of the lumped masses in a vertical distribution pattern as described in the second option of Section 3.3.3.2 C, of FEMA 273. Sixty percent of the total lateral force is applied to the roof, thirty percent is applied at the second floor, and ten percent is applied at the first floor. The nodal loads are increased proportionally in progressive iterations. When elements reach their strength limit, their stiffness is iteratively reduced to an appropriate secant stiffness and the model is rerun at the same load level until no elements resist loads in excess of their calculated capacities. (Secant stiffness method, see side bar.)

The pushover analysis is continued to cover the displacement range of interest, which is based on a preliminary estimate of the maximum displacement demand. A global pushover curve is then produced.

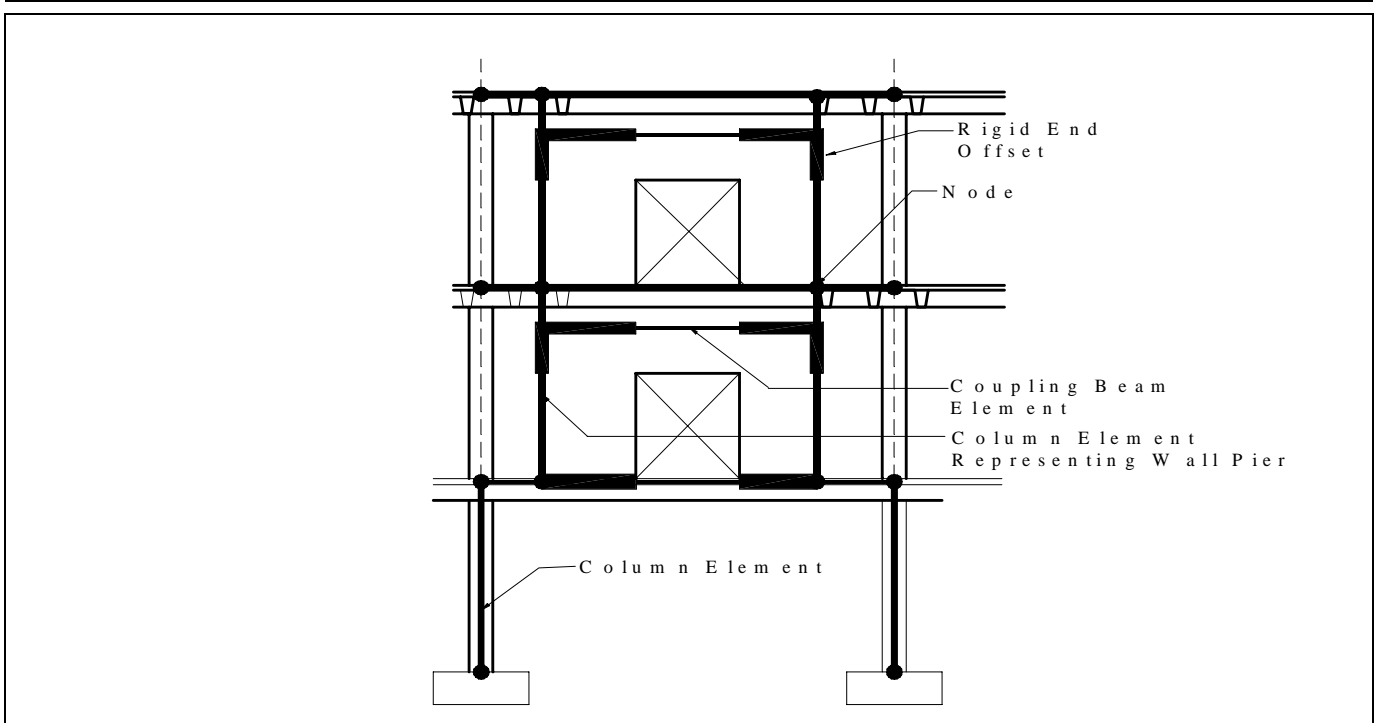


Figure 7-10 Mathematical Model of Coupled Shear Wall

7.4.2.2 Component Force-Displacement Behavior

Component force-displacement curves are developed for each of the typical wall components using the generalized force-displacement curves from Figure 6-1 of FEMA 273. The acceptance limits for the coupling beam components are based on Table 6-17 of FEMA 273 for the case of “nonconforming”, transverse reinforcement, and shear exceeding $6t_w l_w \sqrt{f'_c}$. The pre-event shear-strength-to-

Component force-displacement relations, FEMA 273 and Sections 4.3 and 4.4 of FEMA 306

chord-rotation relationship is shown in Figure 7-12(a). Also shown in this figure are the points representing the displacement limits for immediate occupancy and life safety performance.

The initial slope of the component force/deformation curves is based on the initial elastic stiffness of the component. The pre-event structure is modeled using the effective initial stiffness values recommended in Table 6-4 of FEMA 273. Walls and coupling

Component modeling for pre-event condition, Section 4.4.3.1 of FEMA 306

COEFFICIENT AND CAPACITY SPECTRUM METHODS

Either of two methods are recommended for establishing displacement demands for a nonlinear static analysis: the coefficient method and the capacity spectrum method. A description of these methods is included in ATC 40. The coefficient method is also described in FEMA 273, and the coefficient and capacity spectrum methods are described in FEMA 274. Although either method may be used, it is essential for a valid comparison that the same method be used to assess the performance of the pre-earthquake, post-earthquake, and repaired structure, as outlined in FEMA 306.

In this example, the coefficient method is used. In this method, a target displacement, d_t is calculated and compared to the displacement of a control node, generally located at the roof. The target displacement is determined by multiply-

ing a set of coefficients times a function of the effective building period and the spectral acceleration.

$$\delta_t = C_0 C_1 C_2 C_3 S_a \frac{T_e^2}{4\pi^2} g$$

To use the coefficient method, the nonlinear static analysis must be conducted in order to construct the pushover curve. The pushover curve can be presented as spectral acceleration versus spectral displacement or as base shear versus roof displacement. Once the pushover curve is constructed, an equivalent bilinear curve is fitted to approximate the actual curve. The equivalent bilinear curve is then used to obtain the effective stiffness of the building and the yield base shear needed for calculating the target displacement.

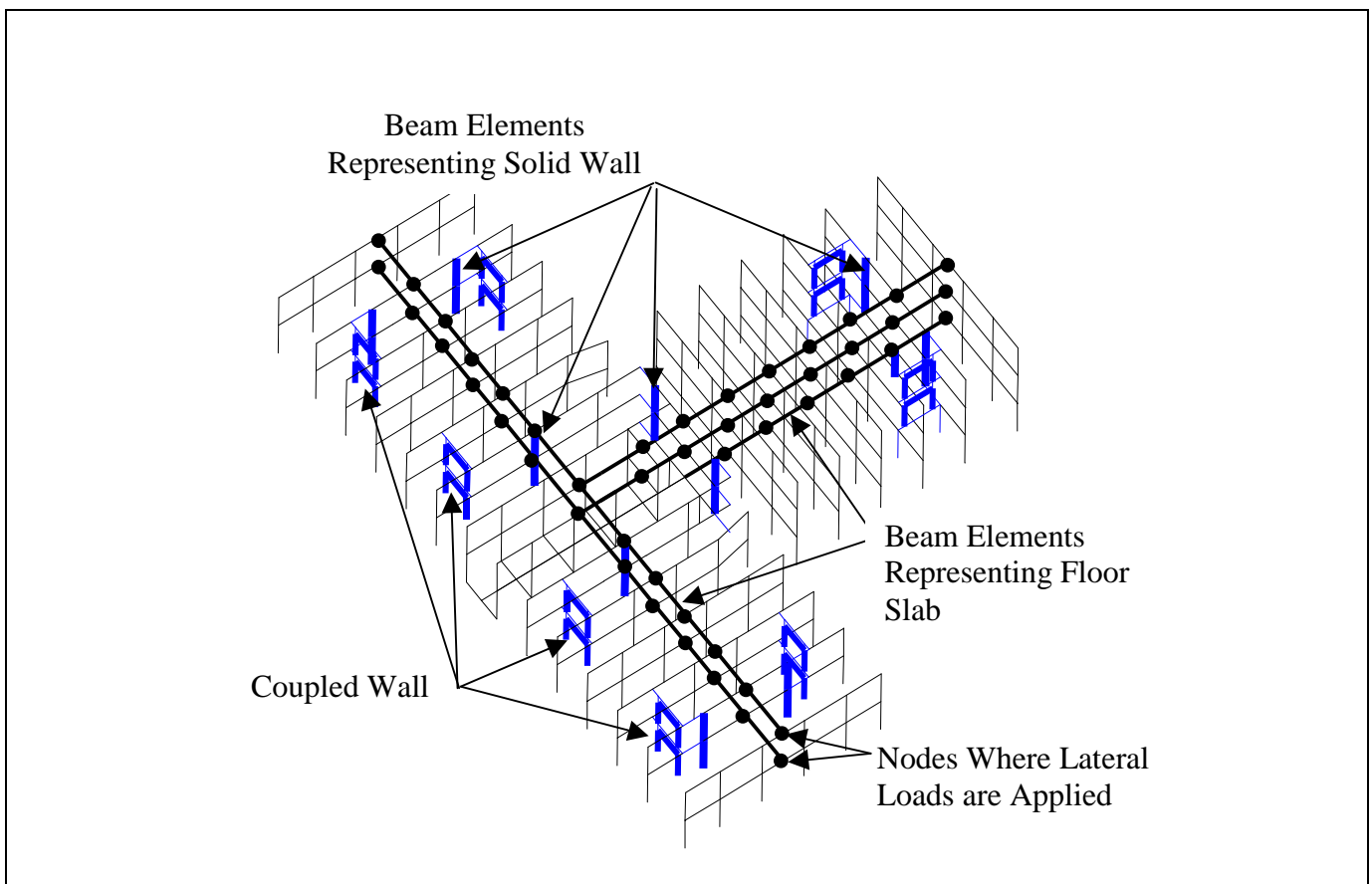


Figure 7-11 Mathematical Model of Full Building

beams are given a flexural rigidity of $0.5E_cI_g$. The base-moment columns of the structure, which support the discontinuous walls, are given a flexural rigidity of $0.7E_cI_g$. As recommended in FEMA 273, the shear rigidities of all components are set equal to gross section values.

The post-event structure is modeled with stiffness values multiplied by the λ_k factors recommended in FEMA 306. Heavily damaged coupling beams have their stiffness reduced to 20 percent ($\lambda_k = 0.2$) of the pre-event value. Moderately damaged coupling beams have their stiffness reduced to 50 percent ($\lambda_k = 0.5$) of the pre-event value. For the solid shear walls, where damage is classified between Insignificant and None, stiffness is reduced to between 80 percent to 100 percent of the pre-event stiffness depending on the amount of cracking.

The horizontal plateau of the component force/deformation curves is based on the strength of the governing behavior mode. For the pre-event structure, the strength

is based on calculations as illustrated in Section 7.2.4 of this example. For the post-event structure, the pre-event strength is multiplied by the λ_Q factors recommended in FEMA 306. Heavily damaged coupling beams have their strength reduced to 30 percent of the pre-event value. Moderately damaged coupling beams have their strength reduced to 80 percent of the pre-event value. For components where damage is classified either Insignificant or None, the strength is not reduced. Figure 7-12(b) shows the force-deformation curves for the moderately and heavily damaged coupling beams.

7.4.2.3 Foundation Rocking

Since the governing behavior mode of the solid concrete walls is identified to be foundation rocking, this behavior is incorporated into the pushover analysis. To model the rocking, the stiffness of the lower story wall elements is reduced when the shear force in those elements reaches the shear force that causes rocking. Once the wall element in the model had started to overturn in the analysis, the stiffness is adjusted so that the wall

NONLINEAR ANALYSIS USING LINEAR ANALYSIS COMPUTER PROGRAMS

Currently, there are few commercially available computer programs for direct implementation of the nonlinear analysis required for a pushover analysis. Many of the nonlinear programs available are sophisticated but can be expensive and difficult to use. For many buildings, a linear elastic analysis program can be used to assess iteratively the nonlinear behavior of the building.

There are two ways to implement a nonlinear static analysis using a linear computer program. Both methods are based on adjusting the stiffness of an element once the analysis indicates that the element has reached its yield level. One method uses the tangential stiffness of the element at the displacement level above yield; the other uses a secant stiffness. The figures below depict the difference between the two methods.

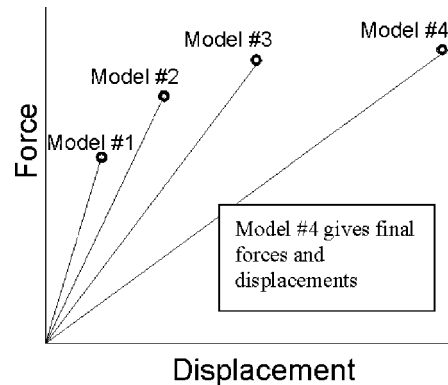


Figure ii – Secant Stiffness Method

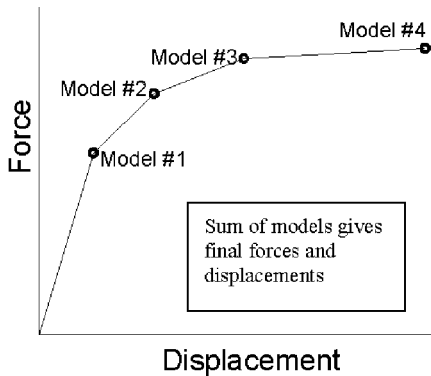


Figure i – Tangential Stiffness Method

The tangential stiffness method is described in detail in ATC 40 (ATC, 1996). Lateral forces are applied to the building and proportionally increased until an element reaches its yield level. A new model is then created in which the yielding component has its stiffness reduced to zero or a small post-yield value. An incremental load is applied to the new

model until another component reaches its yield level. The process continues until a complete mechanism has formed or until the maximum displacement level of interest has been reached. The sum of forces and deformations of each of the incremental models then represent the global behavior of the structure.

In the secant stiffness method, lateral forces are applied to the building and proportionally increased until a component reaches its yield level. A new model is then created in which the yielding element has its stiffness reduced by a value chosen to produce the correct post-yield force in the component. The new model is then rerun at the same force level, and components are checked to verify that the force in the component has not exceeded, or reduced significantly below, its yield level. If necessary, the stiffness of the yielding element may need to be adjusted so that the force in that element is approximately equal to the post-yield force level. Other elements need also be checked since they may be resisting additional load no longer resisted by the yielding element. After iterating until all elements are at approximately the correct force level, a new model is created at a larger lateral force level. The process is repeated at each force level. The behavior of the structure and each element at a given force level is represented directly by the behavior of the appropriate model, rather than combining the results of several models.

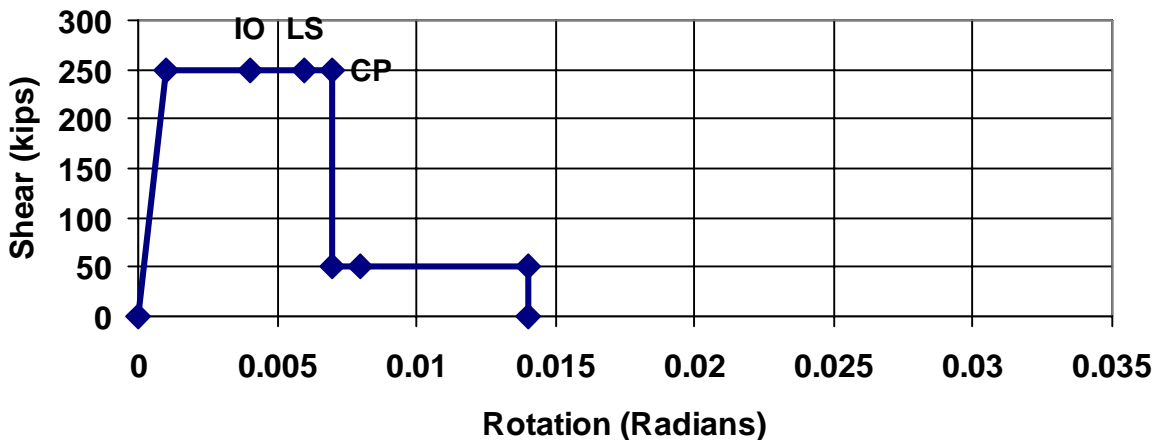
would resist about 10 to 20 percent more shear force than that calculated to cause overturning. This adjustment is made to account for the additional dead weight of the structure that the wall would pick up once it started to uplift. The amount of additional overturning resistance in the wall is based on the shear and moment capacity of the beams framing into the wall.

7.4.3 Force-Displacement Capacity (Pushover Analysis) Results

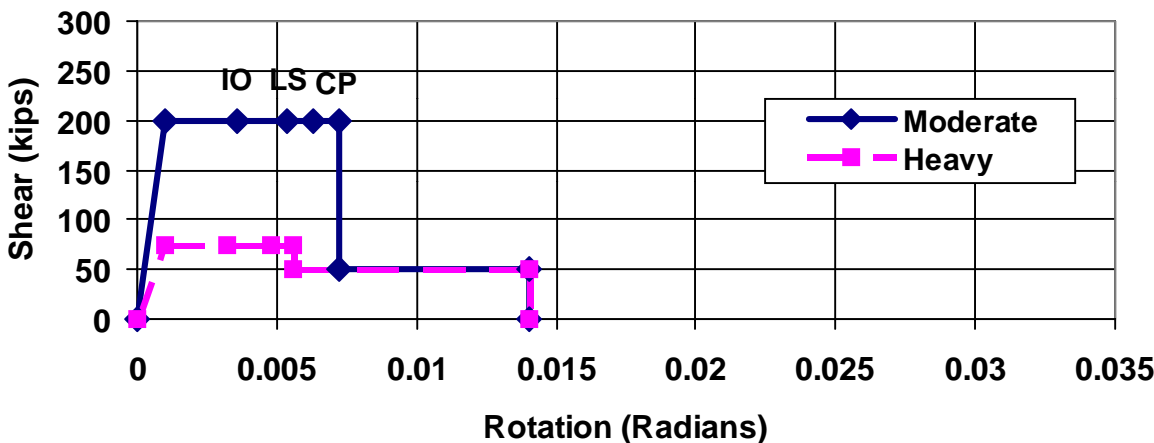
7.4.3.1 Pre-Event Structure

The results of the pushover analysis indicate the progression of displacement events to be as follows for East-West loading (See Figure 7-2 for wall locations):

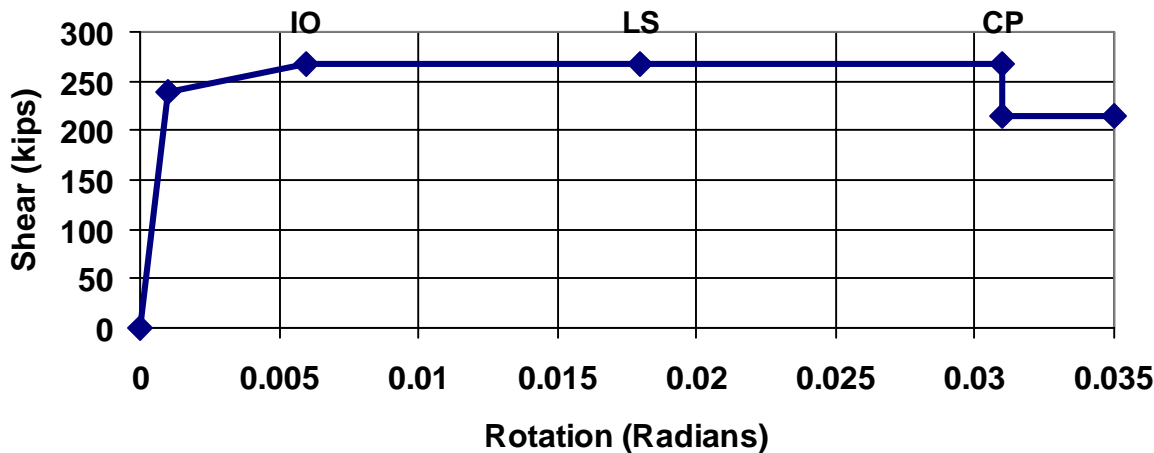
- Initially the two solid walls on lines 7 and 10 between lines C and D reach their rocking capacity.



a) Pre-event



b) Post-event



c) Replacement Coupling Beam with Diagonal Reinforcement

Figure 7-12 Component Force-Displacement Curves for Coupling Beams

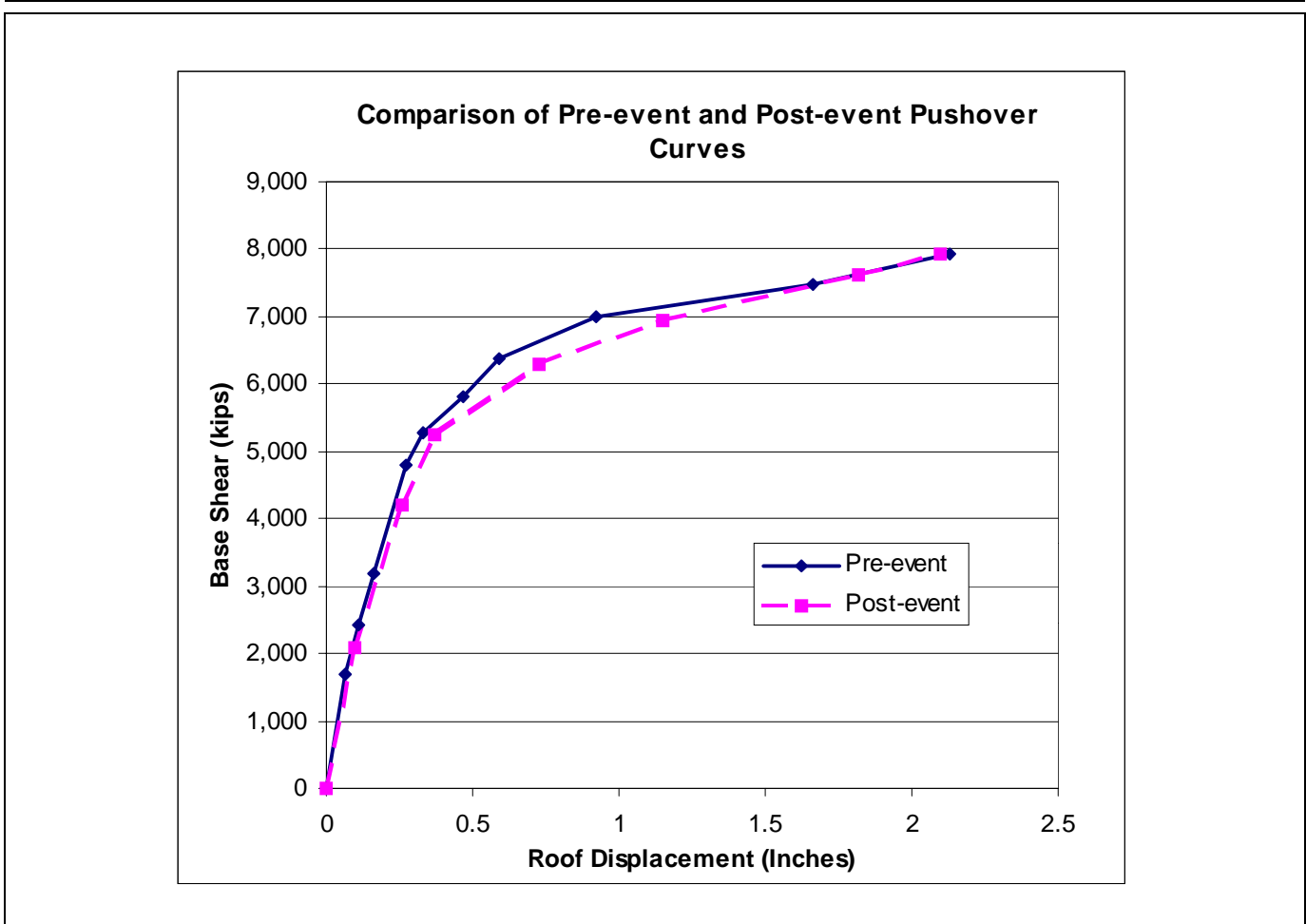


Figure 7-13 Comparison of Pre-event and Post-event Pushover Curves

- When the solid walls between lines C and D are softened, the solid walls on lines 2 and 15 between lines B and C, and between D and E at the first floor pick up additional force and reach their rocking capacity.
- As the solid walls are softened, the coupled walls on lines 7 and 10 between lines L and M resist more force. The first floor coupling beam picks up more force than the second floor coupling beam and reaches its shear capacity first.
- Additional coupling beams reach their capacity and the solid walls continue to rock as the displacement of the structure is increased.
- The approximate target roof displacement is reached after the coupling beams have exceeded their *collapse prevention* acceptability limit, requiring a reduction in their capacity.

As shown in Figure 7-13, the pushover analysis indicates that global nonlinearity begins at a base shear of approximately 5000 k. As lateral displacements increase, the base shear climbs to about 8000 k. Since 10% of the total is applied at the first floor and is transmitted directly into the foundation, the force resisted by the structure above the first floor prior to global nonlinearity is about 4500 k. Allowing for some increase in capacity to reflect rocking behavior more accurately (see Section 7.4.2.3), this agrees well with the hand-calculated capacities of the walls summarized in Tables 7-1 and 7-3. The applied load in excess of the capacity of the walls is resisted by the columns. The magnitude of the increased load is compatible with the capacity of the columns. In the analysis, the first story coupling beams are the first element to reach the immediate occupancy and life safety acceptability limits. The component deformation limit for immediate occupancy occurs when the roof displacement reaches about 0.65 inches and that for life safety is reached at

about 0.88 inch. These displacements are taken as the displacement capacity d_c , as defined in FEMA 306.

The progression of damage shown in the analysis is consistent with the observed damage.

7.4.3.2 Post-Event Condition

For the post-event structure, the progression of displacement events is essentially the same as that outlined for the pre-event structure. The results of the post-event pushover analysis are shown in Figure 7-13. In this analysis, the first story coupling beams reach the immediate occupancy acceptability limit at a roof displacement of 0.47 inches; the beams reach the life safety limit at a roof displacement of 0.66 inches. These values are used for d'_c .

Modeling of the post-event condition, Section 4.4.3.2 of FEMA 306

7.4.3.3 Comparison of Force-Displacement Capacity Curves (Pushover Curves)

The performance of the post-event building was slightly different than the pre-event performance; the overall building is softer since more deflection is obtained for the same magnitude of applied load. The reduced stiffness of the damaged components causes the global reduction of stiffness of the post-event structure. The Moderate and Heavy damage to some of the components corresponds to a reduction in their strength. At

larger displacements (greater than about 1.5 inches) the response of the pre-event and post-event structures are essentially the same.

7.4.4 Estimation of Displacement, d_e , Caused by Damaging Earthquake

The accuracy of the structural model of the building can be verified by estimating the maximum displacement, d_e , that was caused by the damaging event. This is done in two ways. If the data were available, actual ground motion records could be used to predict displacement analytically. Secondly, the pushover curve in conjunction with component capacity data could be used to estimate displacements from the observed damage.

In this case, a spectrum from recorded ground motion at a site approximately 1.5 mi. from the building was available (see Figure 7-14). *FEMA 273* (equation 3-11) uses the displacement coefficient method to estimate maximum displacement from spectral acceleration as follows:

$$d_e = C_0 C_1 C_2 C_3 S_a \frac{T_e^2}{4\pi^2} g \quad (7-1)$$

In this expression the coefficients C_0 to C_3 modify the basic relationship between spectral acceleration and dis-

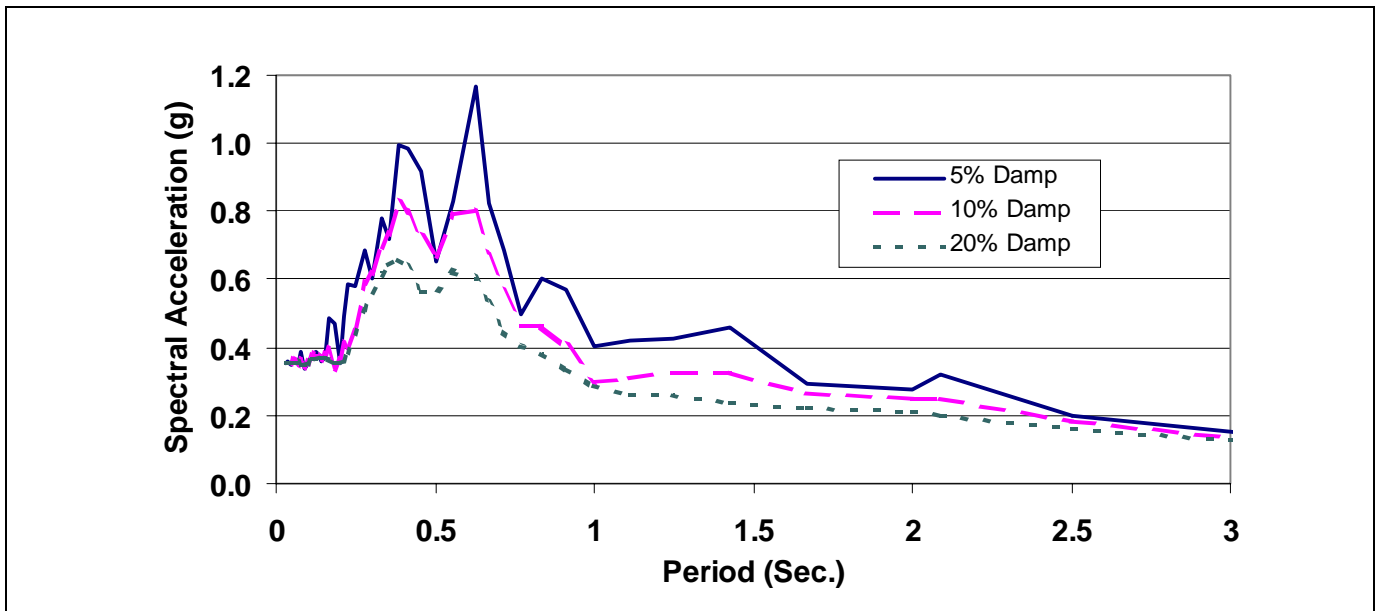


Figure 7-14 Response Spectra from Damaging Earthquake

placement for an elastic system as a function of the effective period of the structure, T_e . The effective period for the pre-event structure is approximately 0.3 sec. The spectral acceleration for this period from Figure 7-14 would be approximately 0.5 to 0.6 g producing an elastic spectral displacement between 0.4 and 0.5 in.

The coefficient C_0 converts spectral displacement to roof displacement and has an approximate value of 1.25 for two- and three-story buildings.

For short-period buildings, the maximum inelastic displacement often is greater than the elastic. *FEMA 273* provides the following expression C_1 to adjust conservatively from elastic to inelastic:

$$C_1 = \frac{\left(1.0 + (R - 1.0) \frac{T_0}{T_e}\right)}{R} \text{ where } R = \frac{S_a}{\left(\frac{V_y}{W}\right) C_0} \quad (7-2)$$

In these expressions, V_y/W is the effective base shear at yield as a portion of the building weight, or about 0.28 in this case. This would result in an R -factor of approximately 1.4 to 1.7. The point where the spectral acceleration transitions from the acceleration to velocity controlled zone occurs at a period of around 0.5 to 0.6 sec. These values would combine to result in a coefficient C_1 of around 1.2 to 1.4.

The coefficient C_2 accounts for the shape of the hysteresis curve and is equal to 1.0 in this case. The coefficient C_3 accounts for dynamic P - Δ effects and is also equal to 1.0 for this case.

Combining all of the coefficients and the elastic spectral displacement results in an estimate for the maximum displacement at the roof, d_e , of between 0.6 to 0.9 in.

From the damage observations, one of the first-floor coupling beams in the east-west direction appeared to reach its capacity, since a severe crack had developed and a transverse bar had buckled. Shear cracking had also developed in the wall piers adjacent to the coupling beams.

From the pushover analysis, at displacement demands between 0.3 inches and 0.5 inches, the coupling beams reach their capacity. The pushover analysis also indicates that the first floor coupling beam would be the first to reach its capacity, which is verified by the observations. Since only the first floor beams were heavily damaged, the displacement demand of the damaging event should not have been much greater than 0.5 in.

The difference between the analytical estimate of d_e and the estimate from the model and observed damage is not large. The difference is acceptable because the building is farther away from the epicenter than the site where the motion was recorded, and actual recorded building response is usually less than that which is predicted analytically. Based on the comparison there is no need to adjust the structural model.

7.4.5 Displacement Demand

7.4.5.1 Estimate of Target Displacement

Estimating the target displacement can be an interactive process. The nonlinear static analysis produces a force-displacement pushover curve covering the displacement range of interest. Based on the procedures of *FEMA 273*, an equivalent bilinear curve is fitted to the pushover curve and a yield point is estimated.

Using this yield point and the associated effective period, the target displacement is calculated using the coefficient method. Given the calculated target displacement, the equivalent bilinear curve can be refitted, adjusting the yield point, and giving a new target displacement. The revised target displacement is close to the original estimate so further iteration is not needed.

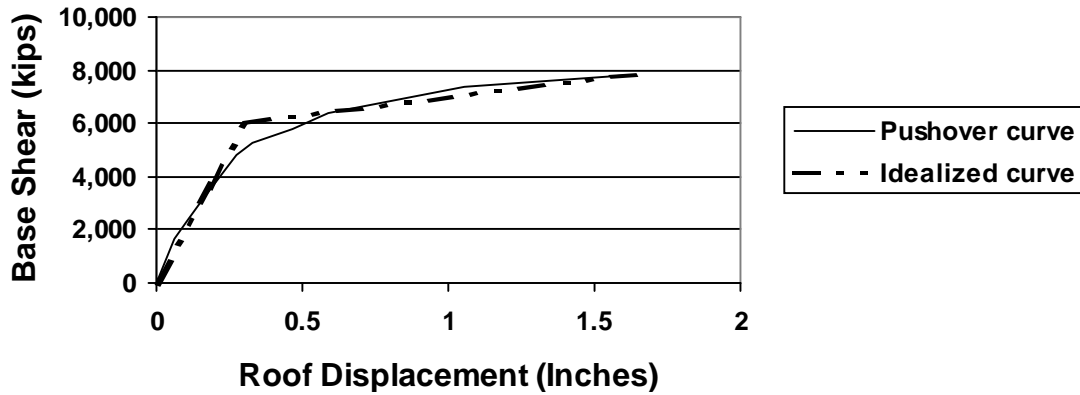
EXAMPLE CALCULATIONS FOR PRE-EVENT AND POST-EVENT DISPLACEMENT DEMANDS

Section 5.4 of *FEMA 306* describes the procedures for calculating the displacement demand for both the pre-event and the post-event structures. The pre-event and post-event pushover curves for this example are shown in Figure 7-13. For this example, the coefficient method is used to calculate the target displacements and *FEMA 306* procedures are used to determine the corresponding displacement demands.

Pre-Event Target Displacement, d_d

An idealized bi-linear capacity curve for the pre-event structure is developed to approximate the actual pushover curve. Based on this idealized curve, the yield level base shear V_y is 6000 kips and the yield level displacement D_y is 0.31 inches. The effective stiffness K_e then becomes 19,400 kips/inch.

EXAMPLE CALCULATIONS FOR PRE-EVENT AND POST-EVENT DISPLACEMENT DEMANDS (continued)



Comparison of idealized bilinear curve to pushover curve

The initial period T_i is 0.25 seconds taken from the initial structural model. The effective period is calculated to be 0.30 seconds using the ratio of the initial to the effective stiffness.

$$T_e = T_i \sqrt{\frac{K_i}{K_e}} = 0.25 \sqrt{\frac{27900}{19400}} = 0.30$$

The spectral acceleration S_a , based on the life safety earthquake response spectra at the effective period is 1.0 g.

The coefficients are:

- $C_0 = 1.25$ for a 2-to-3-story building
- $C_1 = 1.58$ using the equation for T_e in the constant acceleration region of the spectrum
- $C_2 = 1.0$
- $C_3 = 1.0$

Thus the target displacement from Equation 3-11 of FEMA 273 is:

$$d_t = 1.25 (1.58) (1.0g) (386 \text{ in/sec}^2g) (0.30)^2/4\pi^2 = 1.68 \text{ inches}$$

This value is assigned as d_d , the maximum displacement in its pre-event condition.

Post-Event Target Displacement, d'_{d1}

There are two values for the post-event displacement demand that need to be calculated. The first value, d'_{d1} uses

the pre-event effective stiffness and the post-yield stiffness for the post-event curve to calculate a target displacement. In this example, the slopes of the post-yield curves for the pre-event and post-event conditions are similar. Therefore, the target displacements will be essentially the same. The value for d'_{d1} will be taken as the pre-event demand displacement, which is 1.68 inches.

Post-Event Target Displacement, d'_{d2}

Considering the post-event pushover curve, the effective stiffness K_e , with $V_y = 5600$ and $D_y = 0.32$ is 17,500. The initial and effective periods are 0.25 seconds and 0.31 seconds.

The damping coefficient β for the post-event structure is calculated to be 0.06 based on Equation 5-3 of FEMA 306, due to the change in the post-event effective stiffness. The damping adjustments for the response spectrum (B_y and B_1), interpolating from Table 2-15 in FEMA 273, are 1.06 and 1.04 respectively. This changes the spectral acceleration for the post-event structure to 0.97.

The value for C_1 becomes 1.55, and the other coefficients are the same as for the pre-event condition. Using these values, the new target displacement is calculated as:

$$d_t = 1.71 \text{ inches}$$

This value is assigned as d'_{d2} .

The displacement demand from the damaging earthquake d_e was estimated to be 0.6 inches. Since d'_{d1} is greater than d_e , the displacement demand for the post-event structure d'_d is equal to d'_{d1} , which is 1.68 inches.

The target displacement d_d for the pre-event structure for life safety performance against the 475-year-return-period earthquake, based on the coefficient method calculations, is 1.68 inches. The displacement demand for immediate occupancy after the 100-year earthquake is 0.97 inches.

Displacement demand, Section 4.4.4 of FEMA 306

Calculations (see sidebar on previous page) indicate that displacement demand for the post-event structure is essentially the same as for the pre-event structure.

7.4.5.2 Effects of Damage on Performance

The changes in displacement capacity and displacement demand caused by the effects of damage are summarized in Table 7-7. The Performance Indices, P and P' , in Table 7-7 are the ratios of the displacement capacity, d_c or d_c' , to displacement demand, d_d or d_d' , as defined in FEMA 308. The displacement capacities calculated in Section 7.4.3 are based on the assumption that the coupling beams are primary components. FEMA 273 allows coupling beams to be treated as secondary members. Since the global capacity is controlled by the acceptability of the coupling beams, the displacement capacities are determined again assuming that the coupling beams are secondary components and the results are included in Table 7-7. The global displacement capacity, although higher for Life Safety, is still controlled by the coupling beams. The relative change in Performance Index is similar in both cases, indicating that the effects of damage are the same.

The Performance Indices for both the pre-event and post-event structures are less than one for both performance objectives, indicating that the objectives are not met. The effects of damage can be quantified by identifying restoration measures to return the Performance Index to its pre-event value, as outlined in the following sections. The actual course of action to accept, restore, or upgrade the damaged building is a separate consideration for the owner and the local building authority.

7.4.6 Analysis of Restored Structure

7.4.6.1 Proposed Performance Restoration Measures

The primary difference between the pushover models of the pre-event building and the post-event building is the performance of the coupling beams. In their post-earthquake condition, the coupling beams were considered to have less stiffness and strength than in their pre-event condition. The displacement limits were also reduced by the λ_D factor of 0.7. This resulted in the overall reduced stiffness, strength, and displacement capacity of the structure.

To restore the overall performance of the building, various schemes could be investigated, for example, the addition of new concrete walls without repairing damaged components. In this case however, the most straightforward repair appears to be the same component-by-component restoration considered in the direct method. This principally involves the repair of the damaged coupling beams. The coupling beams would be repaired as suggested by the Component Guides in FEMA 306 for the RC3H components. The moderately

Table 7-7 Performance Indices for Pre-event and Post-event Structures

| | Displacement Capacity (inches) | | Displacement Demand (Inches) | | Performance Index (Capacity/Demand) | |
|---|--------------------------------|---------------------|------------------------------|---------------------|-------------------------------------|---------------------|
| | Life Safety | Immediate Occupancy | Life Safety | Immediate Occupancy | Life Safety | Immediate Occupancy |
| Coupling beams treated as primary components | | | | | | |
| Pre-event | $d_c = 0.88$ | $d_c = 0.65$ | $d_d = 1.68$ | $d_d = 0.97$ | $P = 0.52$ | $P = 0.67$ |
| Post-event | $d_c' = 0.66$ | $d_c' = 0.47$ | $d_d' = 1.68$ | $d_d' = 0.97$ | $P' = 0.39$ | $P' = 0.48$ |
| Coupling beams treated as secondary components | | | | | | |
| Pre-event | $d_c = 1.00$ | $d_c = 0.65$ | $d_d = 1.68$ | $d_d = 0.97$ | $P = 0.60$ | $P = 0.67$ |
| Post-event | $d_c' = 0.76$ | $d_c' = 0.47$ | $d_d' = 1.68$ | $d_d' = 0.97$ | $P' = 0.45$ | $P' = 0.48$ |

damaged coupling beams are repaired by injecting the cracks with epoxy. The heavily damaged coupling beams are repaired by removing the damaged coupling beams and replacing them with new coupling beams. Each new coupling beam will be designed using the provisions of the current building code, which requires diagonal reinforcing bars be installed as the primary shear resistance. A detail of the potential repair is shown in Figure 7-8.

7.4.6.2 Analysis Results

The moderately damaged coupling beams are “repaired” in the model by revising their stiffness and strength based on the Component Damage Classification Guides. The heavily damaged coupling beams that were replaced are given stiffness values for initial, undamaged elements and displacement capacities as in FEMA 273 for flexure-governed beams with diagonal reinforcement, as shown in Figure 7-12(c). The stiffness of the moderately damaged coupling beams is restored to 80 percent of the pre-event stiffness. The strength and displacement limits are restored to the pre-event values. The strength and stiffness of the other components in

the model are unchanged from their post-event condition. The pushover analysis is then conducted using the same procedures and load patterns.

The progression of displacement events for the repaired structure is similar to that for the pre-event structure except that the replaced coupling beam does not reach its collapse prevention displacement limit. Figure 7-15 shows the pushover curve for the repaired structure. Also shown on this curve is the pre-event pushover curve. The overall behavior of the repaired structure closely matches that of the pre-earthquake structure, as it was designed to do. The ratio of displacement capacity to demand, d_c^* / d_d^* , is 0.53 for the life safety performance level and 0.66 for immediate occupancy, which are the same as those for the pre-event performance.

The displacement capacity for the repaired structure is governed by the component deformation limits of the coupling beams that were not replaced. Note that an effective upgrade measure might be to replace all coupling beams, as this would greatly increase global displacement capacity.

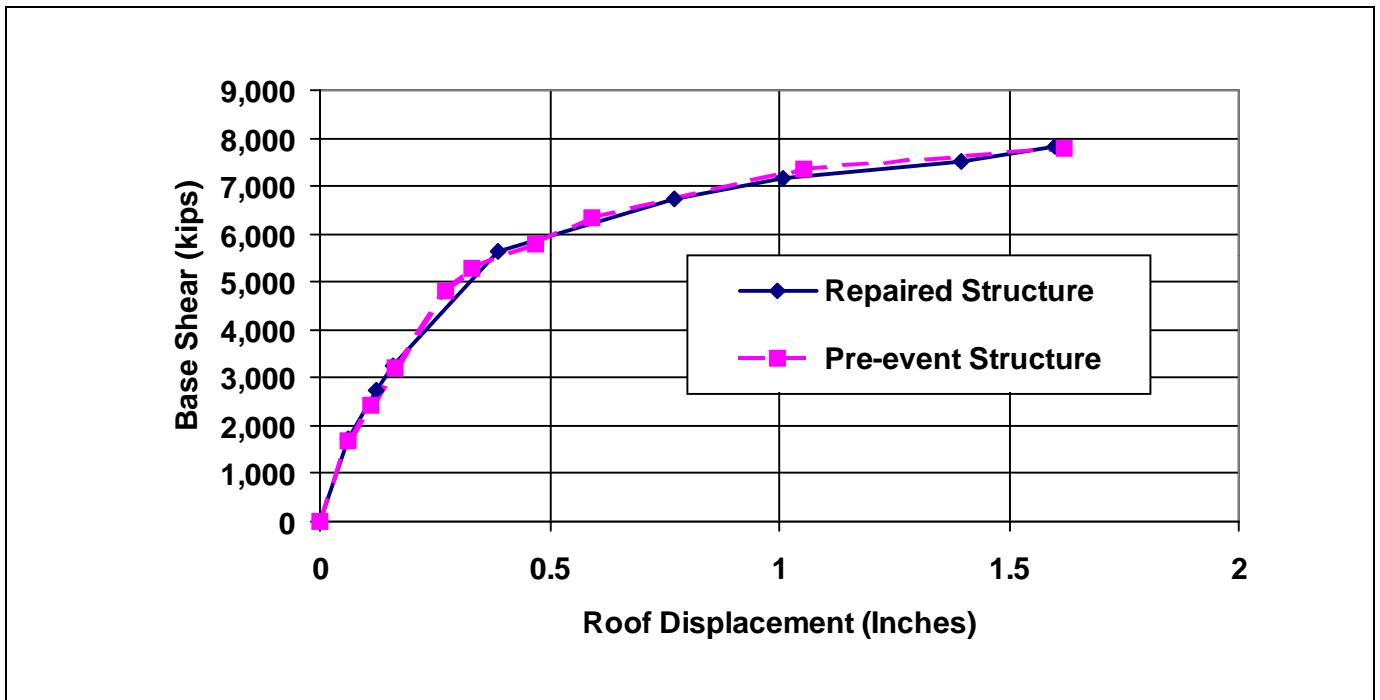


Figure 7-15 Comparison of Pre-event and Repaired Pushover Curves

7.4.7 Performance Restoration Measures

7.4.7.1 Structural Restoration Measures

Based on the relative performance analysis, replacing the three heavily damaged coupling beams and injecting the cracks in the moderately damaged coupling beams restores the performance of the structure. The volume of reinforced concrete coupling beams to be removed is estimated to be about 41 cubic feet per coupling beam. The length of shear cracks to be injected in the moderately damaged coupling beams is estimated to be 100 feet.

Hypothetical repairs for relative performance method, Section 4.5 of FEMA 306

7.4.7.2 Nonstructural Restoration Measures

The Component Guides for the type RC1B components indicate that if cracks are less than 1/8 inch, the damage can be classified as Insignificant, and therefore structural repairs are not necessary. Two of the wall components had cracks that exceeded 1/16 inch. These wall components will have all of the cracks exceeding 1/16 inch repaired by injection with epoxy. The total length of these cracks is estimated to be about 22 feet.

The wall components with visible cracks will be repaired by patching the cracks with plaster and painting the entire wall. This repair is only intended to restore the visual appearance of the wall. Restoration of other nonstructural characteristics, such as water tightness and fire protection, is not necessary.

7.4.7.3 Summary of Restoration Measures and Costs

Table 7-8 summarizes the repairs and estimated costs. Additional costs related to inspection, evaluation, management, and indirect costs may also be involved.

7.5 Discussion of Results

7.5.1 Discussion of Building Performance

The example building contains some typical features found in older concrete wall buildings, such as lightly reinforced concrete elements and discontinuous wall elements. Although the building was designed adequately according to the building code at the time, the design would not be appropriate by current building codes. Because of the improvement in seismic design provisions over the years, it is expected that the building, in its pre-event condition, would not meet the life safety performance level of FEMA 273.

The weak link in the building, as determined by analysis and confirmed with the field observations, is the shear capacity of the coupling beams. Although the analysis indicates that foundation rocking of the solid walls is probably the initial nonlinearity in the building, the rocking of the walls is not detrimental to the global behavior under the anticipated seismic demands.

In the section of the building in which the coupling beams were damaged, the coupled shear walls are discontinuous and are supported by columns at the ends of the walls. Normally, columns supporting discontinuous walls are susceptible to high compressive stresses, and consequently reduced ductility capacity, as the wall overturns. During the pushover analysis, the forces in the columns supporting the coupled walls remained within their capacity. The reason the columns were not overstressed is that the coupling beams acted as fuses for the coupled wall element. The overturning force in the columns could not be greater than the shear capacity of the coupling beams. If the strength of the replaced coupling beams is too large, the overturning force generated could cause failure of the columns below the

Table 7-8 Restoration Cost Estimate by the Relative Performance Method

| Item | Unit Cost (1997 Dollars) | Quantity | Cost (1997 Dollars) |
|---|--------------------------|------------------------|---------------------|
| Epoxy Injection | \$25.00 /lin ft | 122 ft | \$3,050. |
| Coupling Beam Removal and Replacement | \$74.00 / cu ft | 122 ft ³ | \$9,028. |
| Patch and paint walls | \$0.60 /sq ft | 10,175 ft ² | \$6,105. |
| Replace ceiling tiles | \$2.00 /sq ft | 15,000 ft ² | \$ 30,000. |
| General Conditions, Fees, Overhead & Profit (@ 30%) | | | \$ 14,455. |
| Total | | | \$ 62,638. |

wall, resulting in a partial collapse of the building. For this reason, the capacity of the repaired coupling beam was designed to be similar to that of the previous coupling beam.

One of the advantages of the relative performance analysis is the ability to assess the behavior of structure and the influence of the behavior of the individual components on the overall behavior. Strengthening a single component may not produce a significant improvement in the overall performance if the progression of failure shifts to a less desirable mode. The pushover analysis of the repaired structure needs to consider the change in overall behavior caused by the repairs.

Because of the improved performance of the first story coupling beams that were replaced, these beams no longer control the global displacement limit of the structure. The force/displacement capacity of the second story coupling beams in their repaired condition is the same as in the pre-event condition. The displacement demand at which the second story coupling beams reach their acceptability limit is very close to the limit at which the first story coupling beams in the pre-event condition reached their limit. Therefore, the overall performance of the building is not improved substantially. The information gained from these analyses can be used to assess whether an upgrade of the building to improve its performance may be cost effective.

7.5.2 Discussion of Methodology and Repair Costs

This example has illustrated some of the important aspects in the FEMA 306 approach to assessing the earthquake damage to concrete and masonry wall buildings. The example building represents an actual building that experienced a damaging earthquake.

FEMA 306 presents two methods for calculating the loss associated with earthquake damage, the direct method and the relative performance method. These methods are used to determine the loss, which is measured as the cost associated with returning the building to its pre-event performance. In this example, the cost of restoring the performance using the two methods produce the same result, principally because the repairs chosen in the relative performance method match those suggested by the direct method. In other buildings, there can be differences between the results obtained by the two methods.

The Nonlinear Static Procedure described in FEMA 273 is used in the relative performance method to assess the performance of the building in the pre-event, post-event and repaired conditions. This analysis method is relatively new and is still subject to further refinements. This procedure can be time-consuming to implement properly. As the method and the analytical tools become further developed, this method should be easier to implement.

7.6 References

- ACI Committee 201, 1994, "Guide for Making a Condition Survey of Concrete in Service," *Manual of Concrete Practice*, American Concrete Institute, Detroit, Michigan.
- CSI, 1997, *SAP2000: Integrated Structural Design & Analysis Software*, Computers and Structures Inc, Berkeley, California
- ATC, 1996, *The Seismic Evaluation and Retrofit of Concrete Buildings*, Applied Technology Council, ATC-40 Report, Redwood City, California.

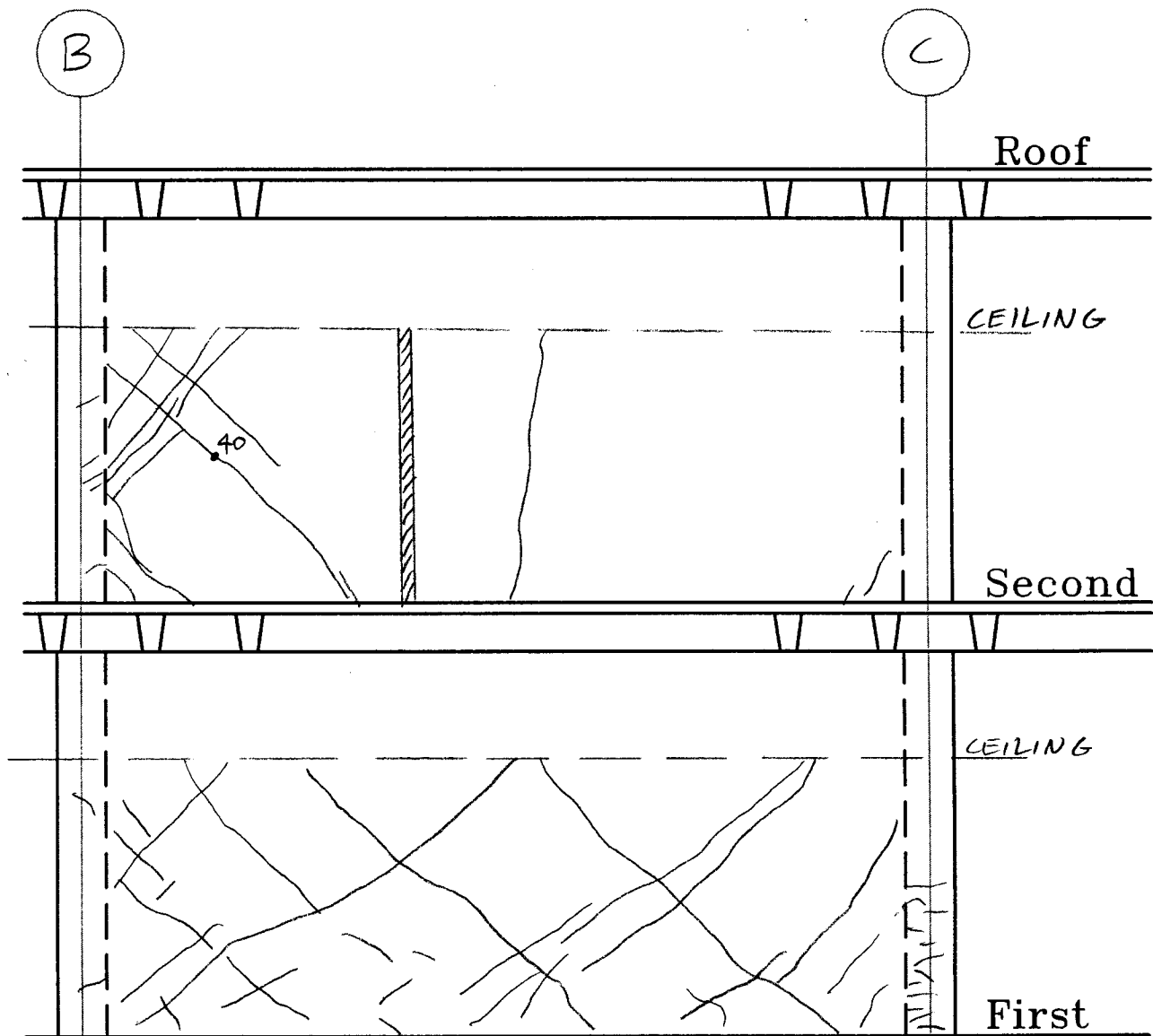
Appendix A. Component Damage Records for Building Evaluated in Example Application

Component Damage Records for Building Evaluated in Example Application

Component Damage Record D1

| | | |
|---|--------------------------------------|----------------------------|
| Building Name: Concrete Shear Wall Building | Project ID: ATC 43 Example | Prepared by: ATC |
| Location Within Building: Floor: 1 st /2 nd Column Line: 2 Component Type: | | Date: 24-Sep-97 |

Sketch and Description of Damage:



Legend:

- | | | | |
|--|-------------------------------------|--|----------------|
| | Crack | | Spall |
| | Crack Width in Mils (0.001 Inch) | | Not Accessible |
| | Crack Previously Filled with Epoxy | | Partition |
| | Crack at Pre-existing Surface Patch | | |

Component Damage Records for Building Evaluated in Example Application

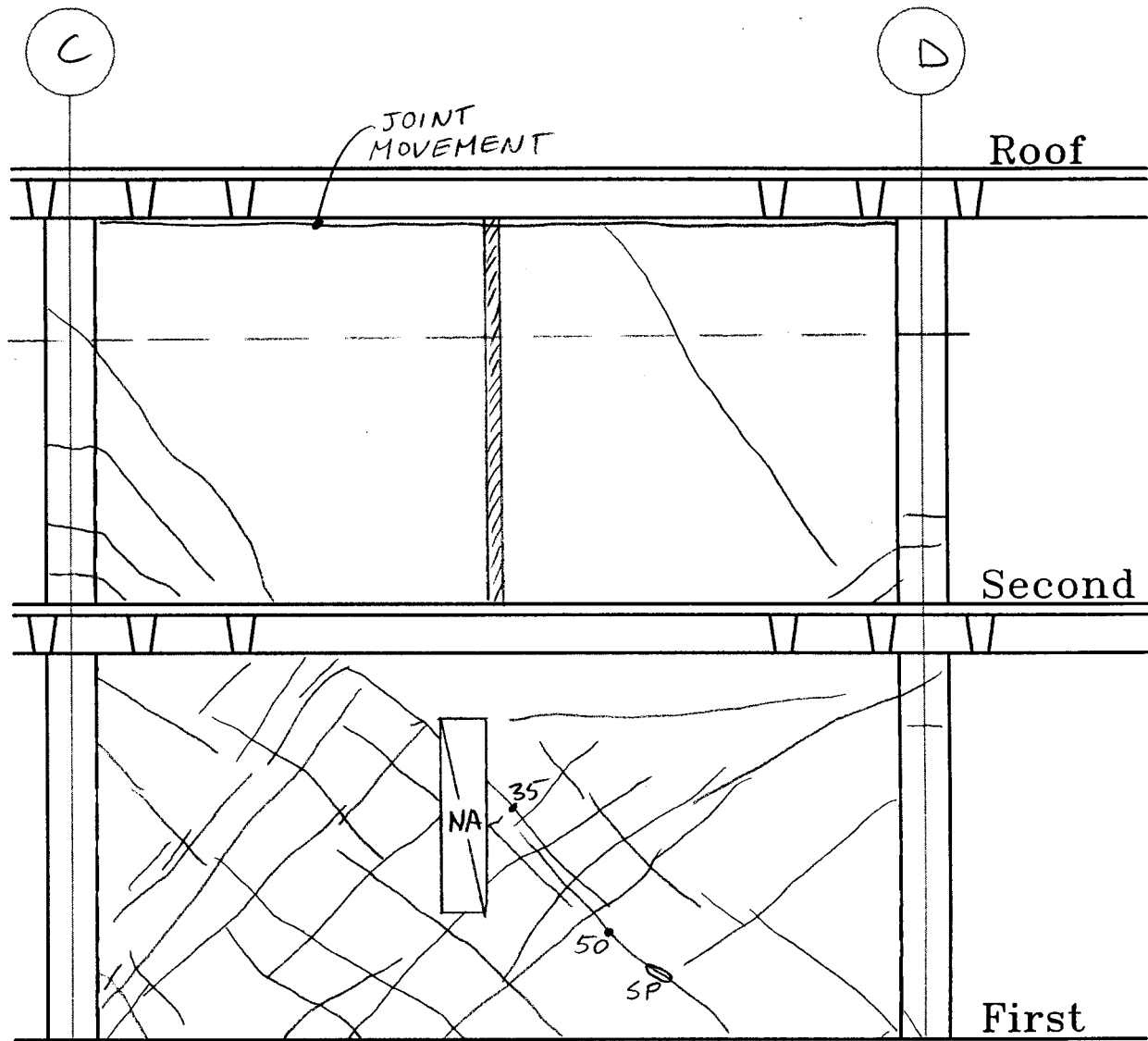
| Component Damage Record D2 | | | |
|---|--------------------------------------|----------------------------|----------------|
| Building Name: Concrete Shear Wall Building | Project ID: ATC 43 Example | Prepared by: ATC | |
| Location Within Building: Floor: 1 st /2 nd Column Line: 2 Component Type: | | Date: 24-Sep-97 | |
| Sketch and Description of Damage: | | | |
| | | | |
| Legend: | | | |
| | Crack | | Spall |
| | Crack Width in Mils (0.001 Inch) | | Not Accessible |
| | Crack Previously Filled with Epoxy | | Partition |
| | Crack at Pre-existing Surface Patch | | |

Component Damage Records for Building Evaluated in Example Application

Component Damage Record D3

| | | | |
|---|--|--------------------------------------|----------------------------|
| Building Name: Concrete Shear Wall Building | | Project ID: ATC 43 Example | Prepared by: ATC |
| Location Within Building: Floor: 1 st /2 nd Column Line: 7 Component Type: | | | Date: 24-Sep-97 |

Sketch and Description of Damage:



Legend:

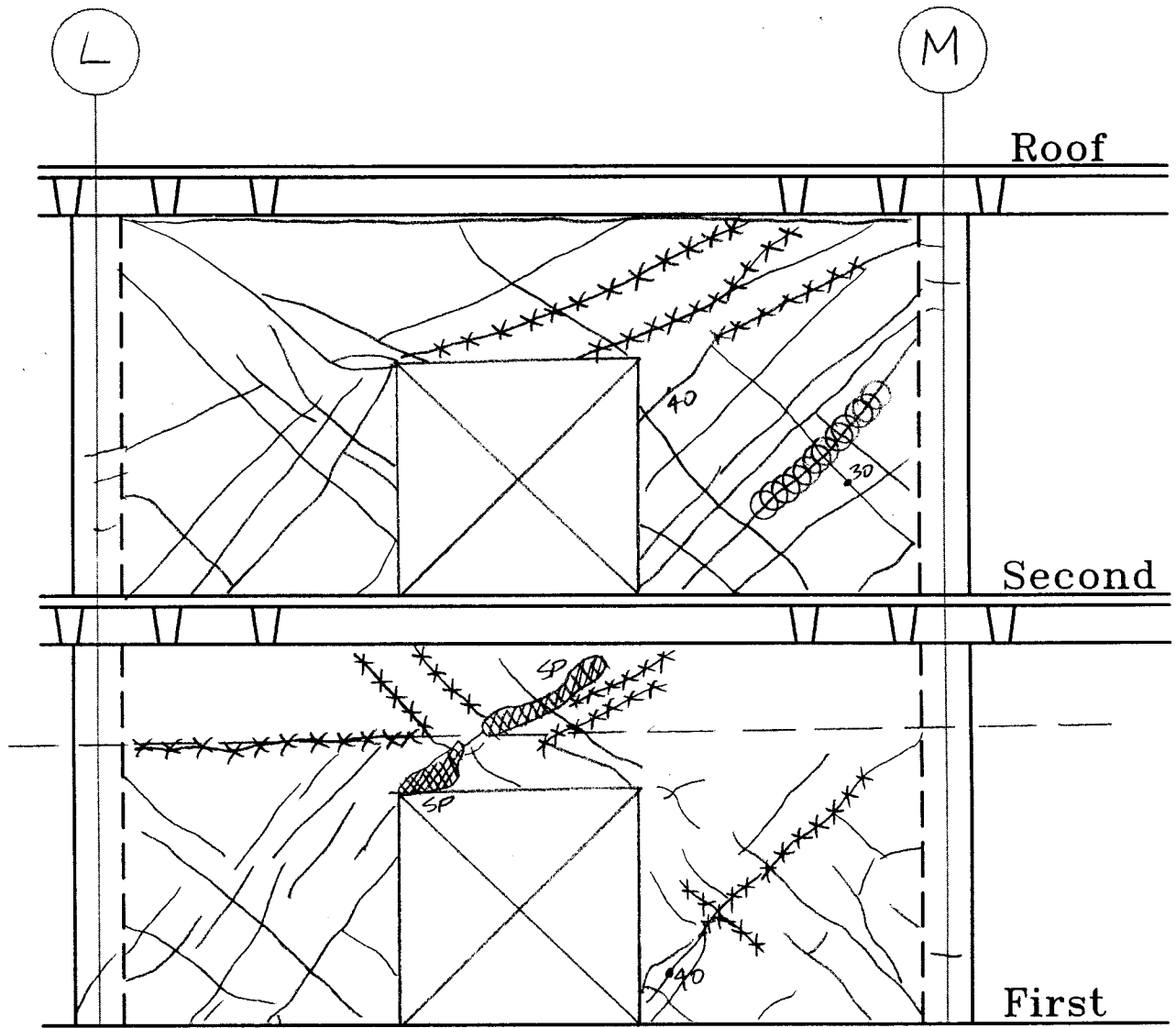
- | | | | |
|--|-------------------------------------|--|----------------|
| | Crack | | Spall |
| | Crack Width in Mils (0.001 Inch) | | Not Accessible |
| | Crack Previously Filled with Epoxy | | Partition |
| | Crack at Pre-existing Surface Patch | | |

Component Damage Records for Building Evaluated in Example Application

Component Damage Record D4

| | | |
|---|--------------------------------------|----------------------------|
| Building Name: Concrete Shear Wall Building | Project ID: ATC 43 Example | Prepared by: ATC |
| Location Within Building: Floor: 1 st /2 nd Column Line: 7 Component Type: | | Date: 24-Sep-97 |

Sketch and Description of Damage:



Legend:

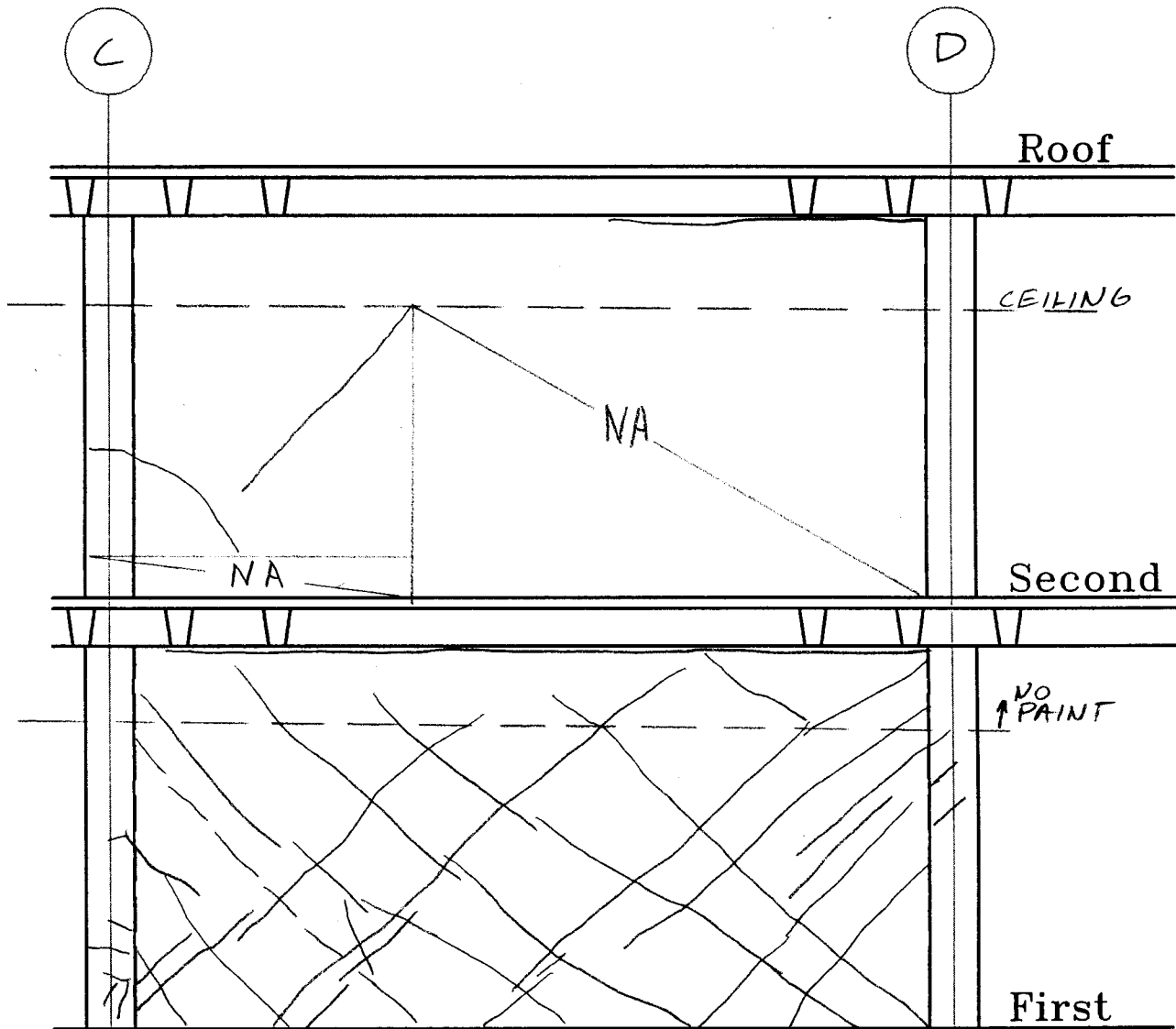
| | | | |
|--|-------------------------------------|--|----------------|
| | Crack | | Spall |
| | Crack Width in Mils (0.001 Inch) | | Not Accessible |
| | Crack Previously Filled with Epoxy | | Partition |
| | Crack at Pre-existing Surface Patch | | |

Component Damage Records for Building Evaluated in Example Application

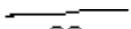
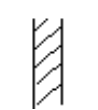
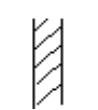
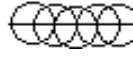
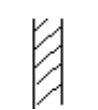
Component Damage Record D5

| | | | |
|--|--|--------------------------------------|----------------------------|
| Building Name: Concrete Shear Wall Building | | Project ID: ATC 43 Example | Prepared by: ATC |
| Location Within Building: Floor: 1 st /2 nd Column Line: 10 Component Type: | | Date: 24-Sep-97 | |

Sketch and Description of Damage:



Legend:

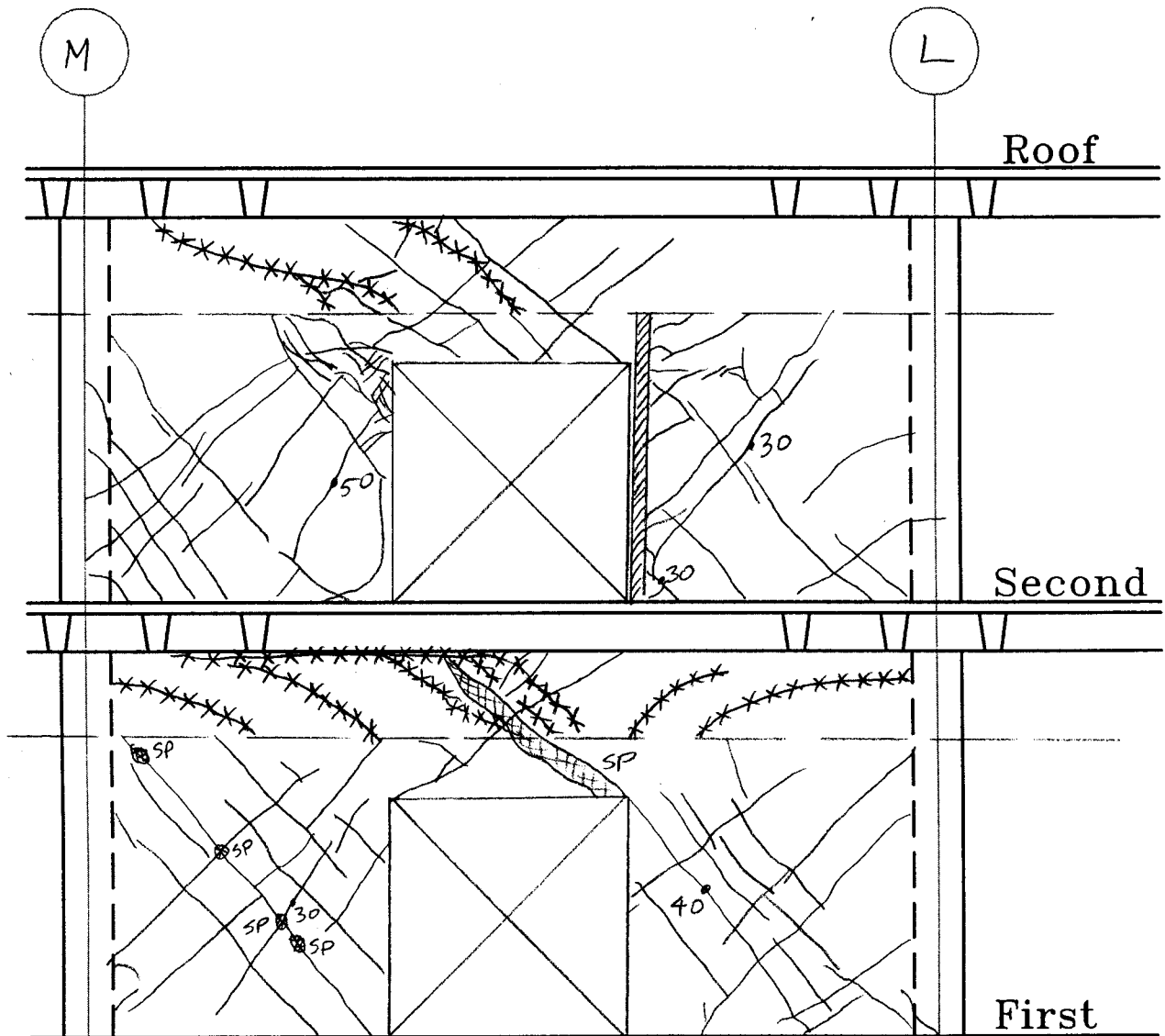
- | | | | | | |
|---|-------------------------------------|---|-------------------------------------|---|----------------|
|  | Crack |  | Crack Width in Mills (0.001 Inch) |  | Spall |
|  | Crack Previously Filled with Epoxy |  | Crack at Pre-existing Surface Patch |  | Not Accessible |
|  | Crack at Pre-existing Surface Patch | | |  | Partition |

Component Damage Records for Building Evaluated in Example Application

Component Damage Record D6

| | | |
|--|--------------------------------------|----------------------------|
| Building Name: Concrete Shear Wall Building | Project ID: ATC 43 Example | Prepared by: ATC |
| Location Within Building: Floor: 1 st /2 nd Column Line: 10 Component Type: | | Date: 24-Sep-97 |

Sketch and Description of Damage:



Legend:

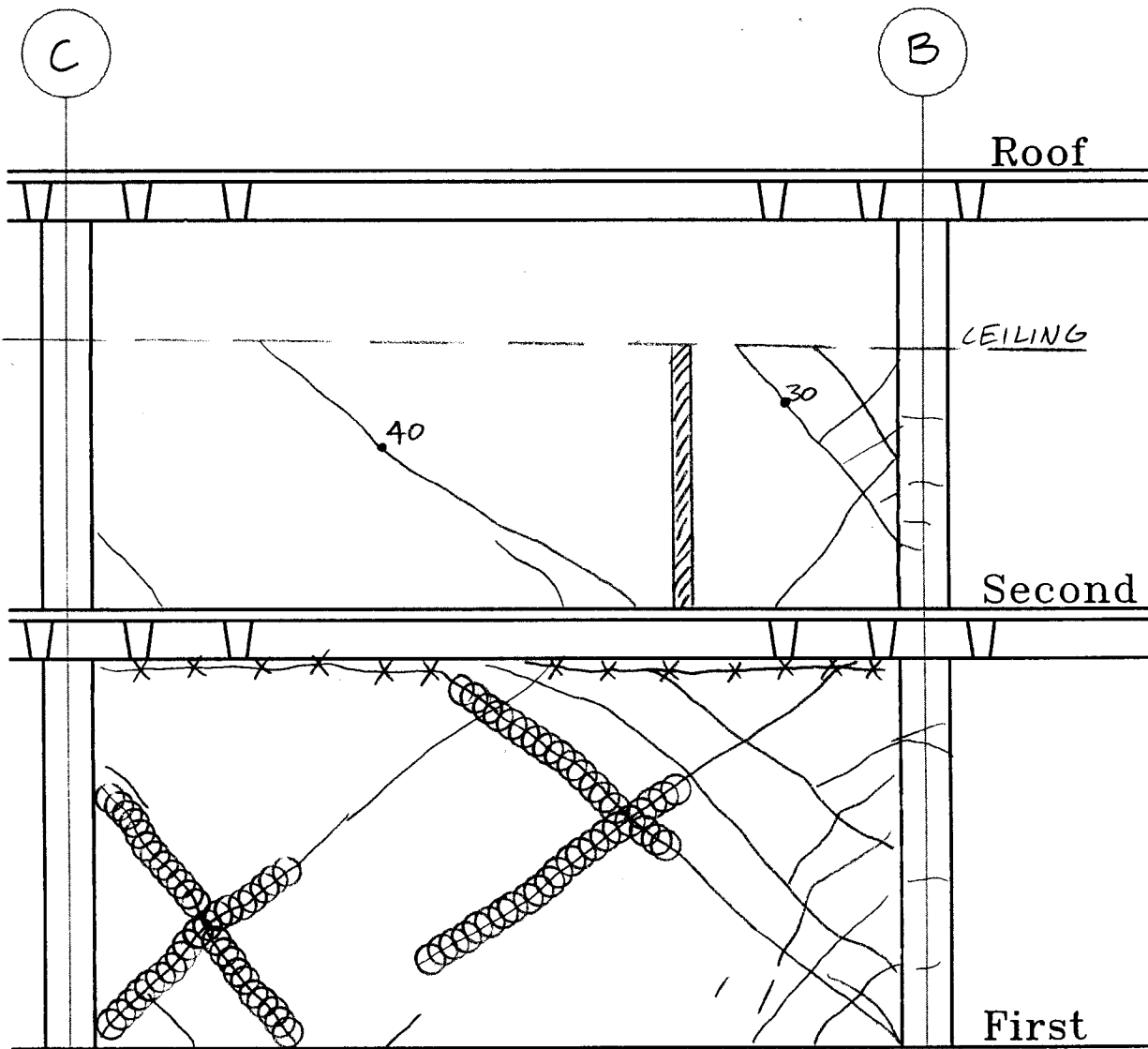
| | | | |
|--|-------------------------------------|--|----------------|
| | Crack | | Not Accessible |
| | Crack Width in Mils (0.001 Inch) | | Spall |
| | Crack Previously Filled with Epoxy | | Partition |
| | Crack at Pre-existing Surface Patch | | |

Component Damage Records for Building Evaluated in Example Application

Component Damage Record D7

| | | |
|--|--------------------------------------|----------------------------|
| Building Name: Concrete Shear Wall Building | Project ID: ATC 43 Example | Prepared by: ATC |
| Location Within Building: Floor: 1 st /2 nd Column Line: 15 Component Type: | | Date: 24-Sep-97 |

Sketch and Description of Damage:



Legend:

| | | | |
|--|-------------------------------------|--|----------------|
| | Crack | | Spall |
| | Crack Width in Mils (0.001 Inch) | | Not Accessible |
| | Crack Previously Filled with Epoxy | | Partition |
| | Crack at Pre-existing Surface Patch | | |

Component Damage Records for Building Evaluated in Example Application

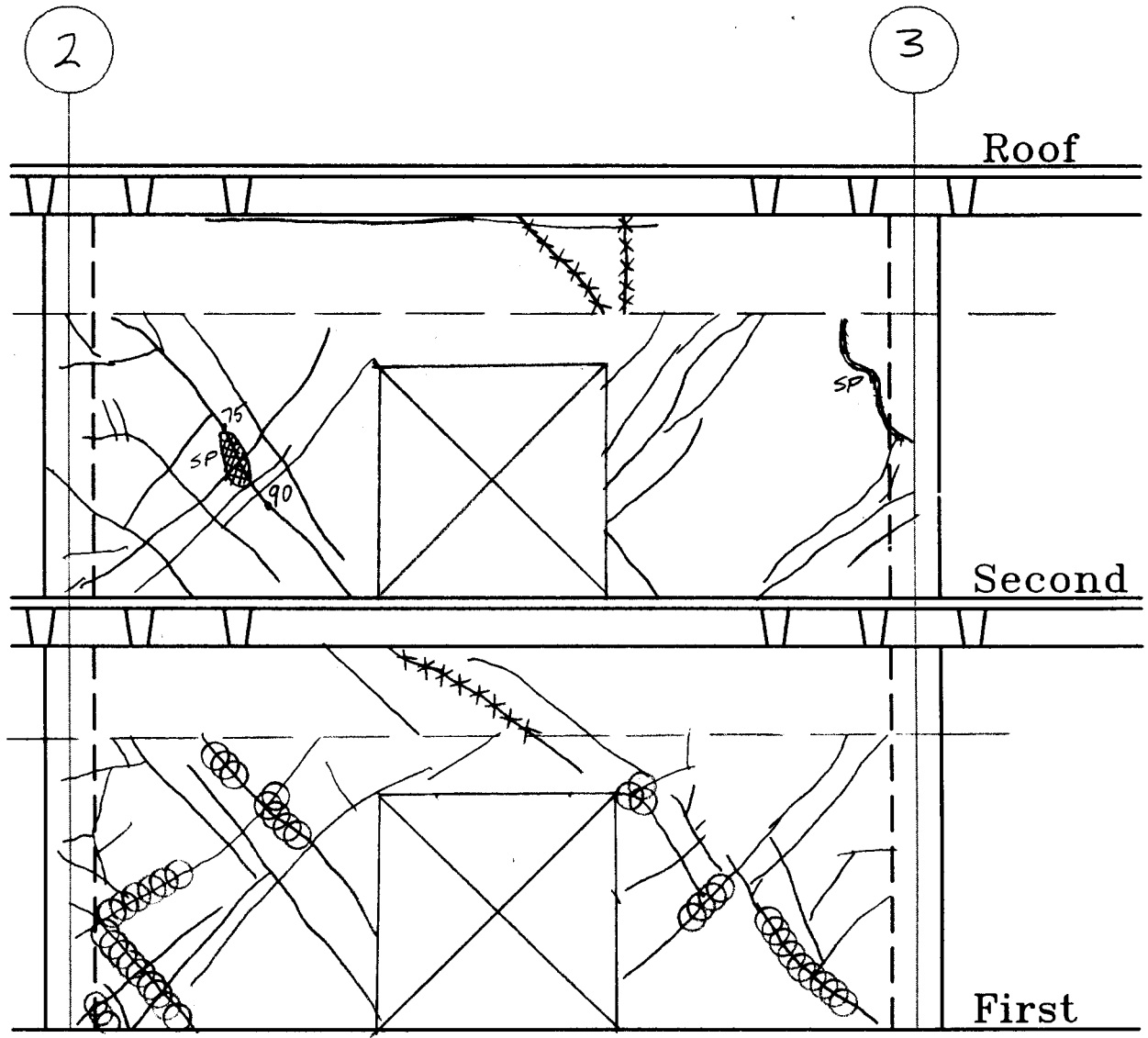
| Component Damage Record D8 | | | |
|--|--------------------------------------|----------------------------|----------------|
| Building Name: Concrete Shear Wall Building | Project ID: ATC 43 Example | Prepared by: ATC | |
| Location Within Building: Floor: 1 st /2 nd Column Line: 15 Component Type: | | Date: 24-Sep-97 | |
| Sketch and Description of Damage: | | | |
| | | | |
| Legend: | | | |
| | Crack | | Spall |
| | Crack Width in Mils (0.001 Inch) | | Not Accessible |
| | Crack Previously Filled with Epoxy | | Partition |
| | Crack at Pre-existing Surface Patch | | |

Component Damage Records for Building Evaluated in Example Application

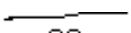
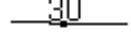
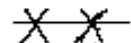
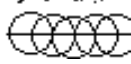
Component Damage Record D9

| | | | |
|---|--|--------------------------------------|----------------------------|
| Building Name: Concrete Shear Wall Building | | Project ID: ATC 43 Example | Prepared by: ATC |
| Location Within Building: Floor: 1 st /2 nd Column Line: B Component Type: | | | Date: 24-Sep-97 |

Sketch and Description of Damage:



Legend:

- | | | | |
|---|-------------------------------------|---|----------------|
|  | Crack |  | Spall |
|  | Crack Width in Mills (0.001 Inch) |  | Not Accessible |
|  | Crack Previously Filled with Epoxy |  | Partition |
|  | Crack at Pre-existing Surface Patch | | |

Component Damage Records for Building Evaluated in Example Application

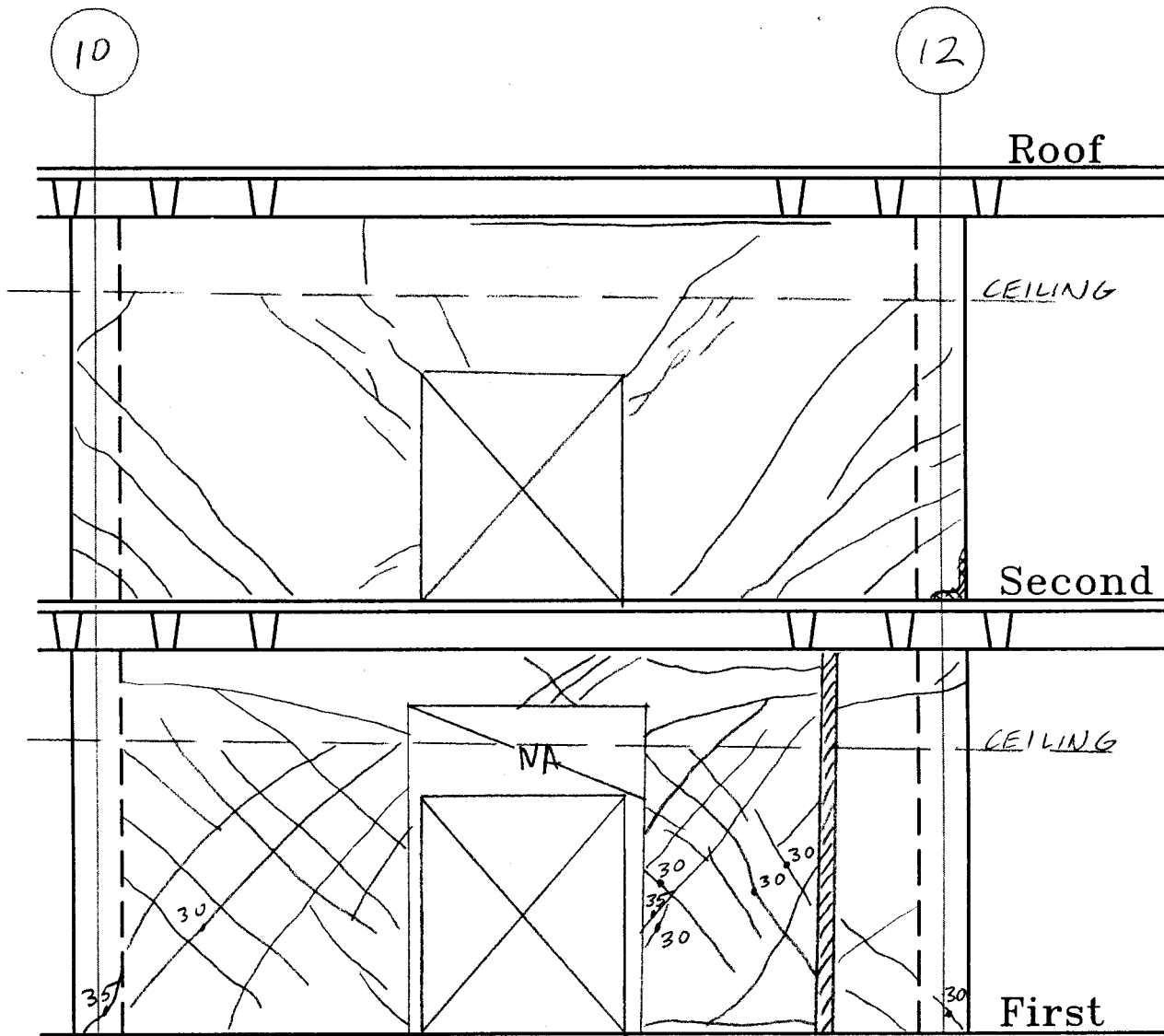
| Component Damage Record D10 | | | |
|---|--------------------------------------|----------------------------|----------------|
| Building Name: Concrete Shear Wall Building | Project ID: ATC 43 Example | Prepared by: ATC | |
| Location Within Building: Floor: 1 st /2 nd Column Line: B Component Type: | | Date: 24-Sep-97 | |
| Sketch and Description of Damage: | | | |
| | | | |
| Legend: | | | |
| | Crack | | Spall |
| | Crack Width in Mils (0.001 Inch) | | Not Accessible |
| | Crack Previously Filled with Epoxy | | Partition |
| | Crack at Pre-existing Surface Patch | | |

Component Damage Records for Building Evaluated in Example Application

Component Damage Record D11

| | | |
|---|--------------------------------------|----------------------------|
| Building Name: Concrete Shear Wall Building | Project ID: ATC 43 Example | Prepared by: ATC |
| Location Within Building: Floor: 1 st /2 nd Column Line: B Component Type: | | Date: 24-Sep-97 |

Sketch and Description of Damage:



Legend:

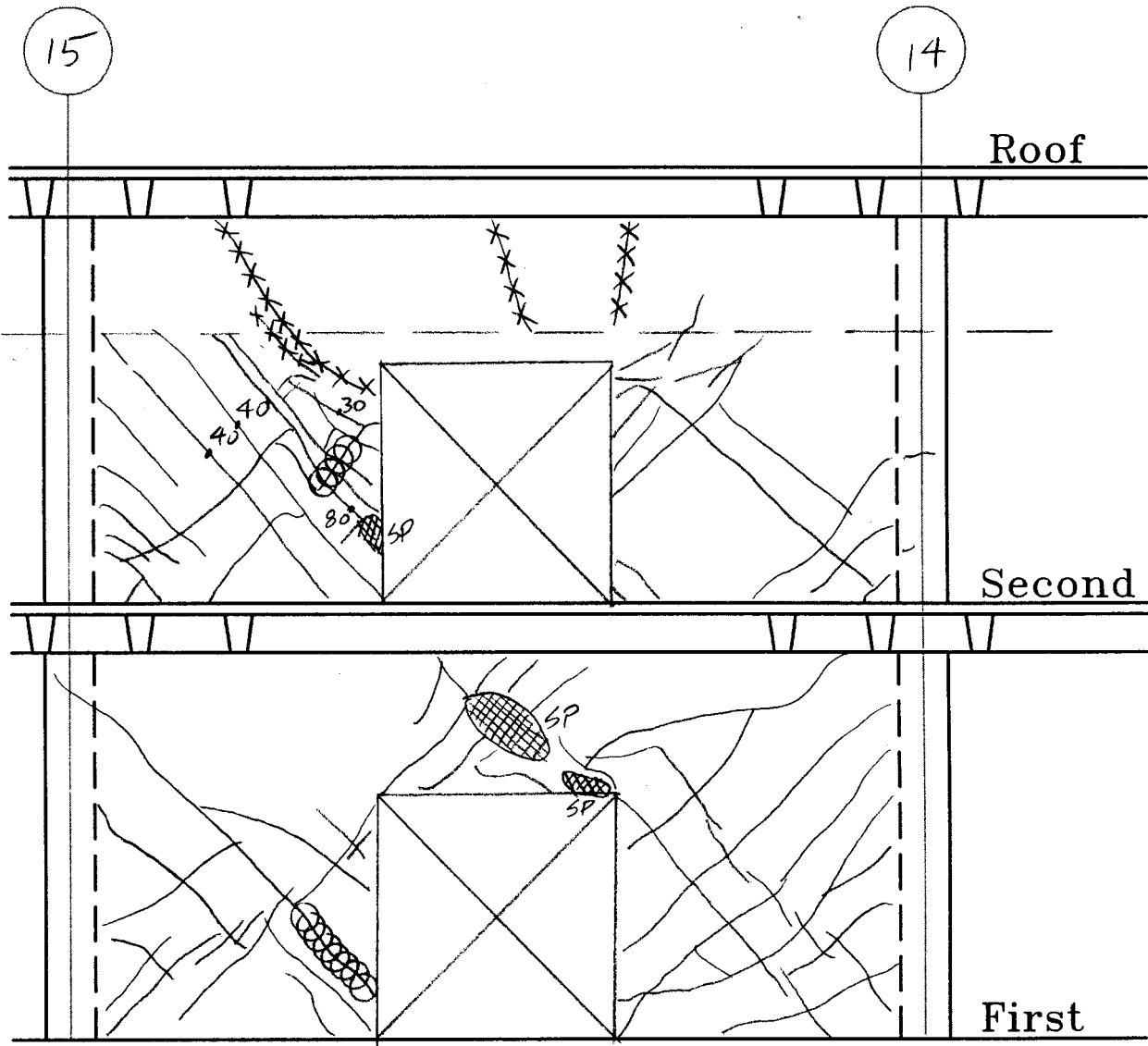
- | | | | |
|--|-------------------------------------|--|----------------|
| | Crack | | Spall |
| | Crack Width in Mils (0.001 Inch) | | Not Accessible |
| | Crack Previously Filled with Epoxy | | Partition |
| | Crack at Pre-existing Surface Patch | | |

Component Damage Records for Building Evaluated in Example Application

Component Damage Record D12

| | | |
|---|--------------------------------------|----------------------------|
| Building Name: Concrete Shear Wall Building | Project ID: ATC 43 Example | Prepared by: ATC |
| Location Within Building: Floor: 1 st /2 nd Column Line: B Component Type: | | Date: 24-Sep-97 |

Sketch and Description of Damage:



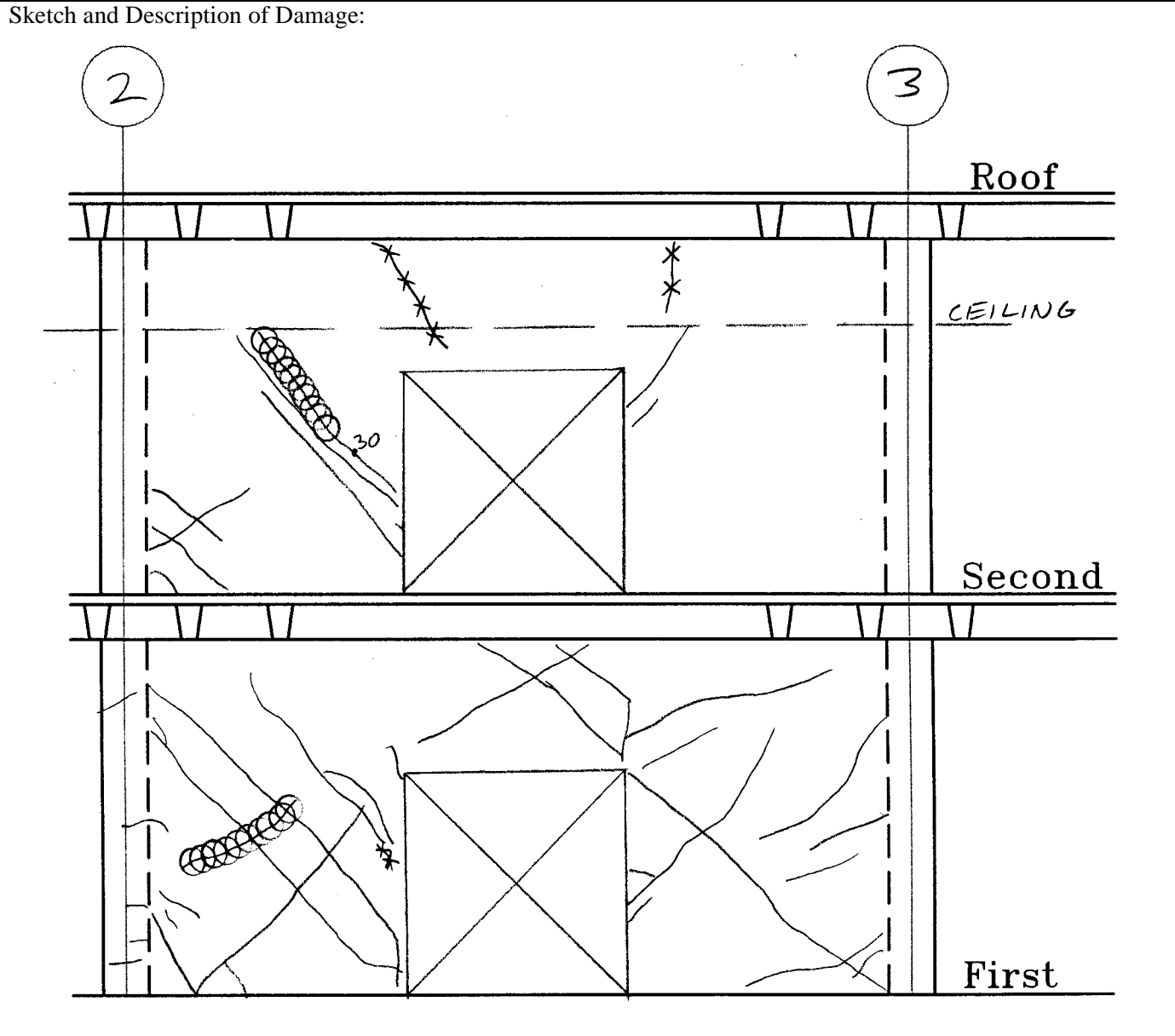
Legend:

| | | | |
|--|-------------------------------------|--|----------------|
| | Crack | | Spall |
| | Crack Width in Mils (0.001 Inch) | | Not Accessible |
| | Crack Previously Filled with Epoxy | | Partition |
| | Crack at Pre-existing Surface Patch | | |

Component Damage Records for Building Evaluated in Example Application

Component Damage Record D13

| | | |
|---|--------------------------------------|----------------------------|
| Building Name: Concrete Shear Wall Building | Project ID: ATC 43 Example | Prepared by: ATC |
| Location Within Building: Floor: 1 st /2 nd Column Line: E Component Type: | | Date: 24-Sep-97 |



Legend:

| | | | |
|--|-------------------------------------|--|----------------|
| | Crack | | Spall |
| | Crack Width in Mils (0.001 Inch) | | Not Accessible |
| | Crack Previously Filled with Epoxy | | Partition |
| | Crack at Pre-existing Surface Patch | | |

Component Damage Records for Building Evaluated in Example Application

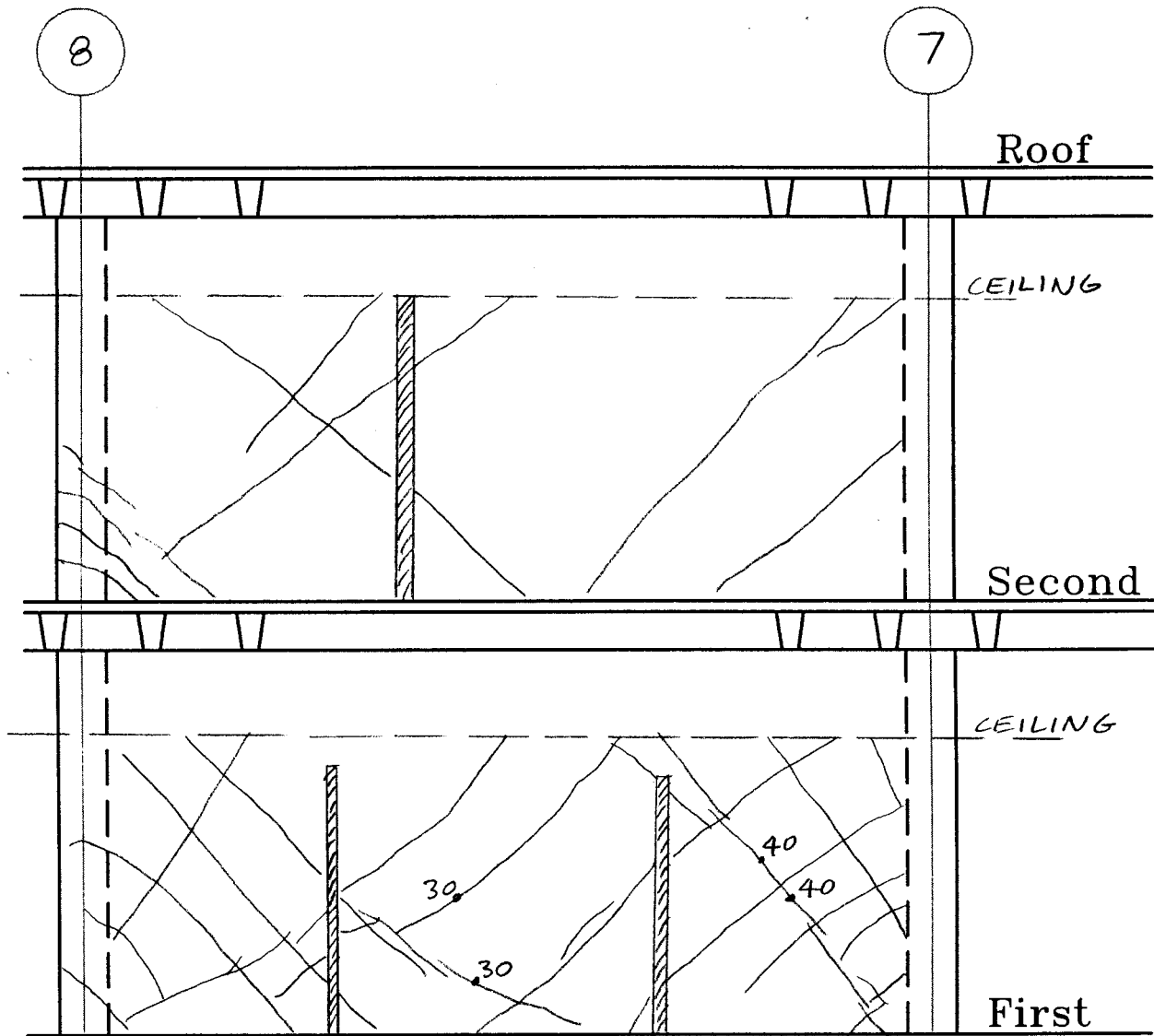
| Component Damage Record D14 | | | |
|---|--------------------------------------|----------------------------|----------------|
| Building Name: Concrete Shear Wall Building | Project ID: ATC 43 Example | Prepared by: ATC | |
| Location Within Building: Floor: 1 st /2 nd Column Line: E Component Type: | | Date: 24-Sep-97 | |
| Sketch and Description of Damage: | | | |
| | | | |
| Legend: | | | |
| | Crack | | Spall |
| | Crack Width in Mils (0.001 Inch) | | Not Accessible |
| | Crack Previously Filled with Epoxy | | Partition |
| | Crack at Pre-existing Surface Patch | | |

Component Damage Records for Building Evaluated in Example Application

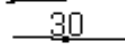
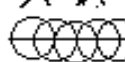
Component Damage Record D15

| | | |
|---|--------------------------------------|----------------------------|
| Building Name: Concrete Shear Wall Building | Project ID: ATC 43 Example | Prepared by: ATC |
| Location Within Building: Floor: 1 st /2 nd Column Line: G Component Type: | | Date: 24-Sep-97 |

Sketch and Description of Damage:



Legend:

- | | | | |
|---|-------------------------------------|---|----------------|
|  | Crack |  | Spall |
|  | Crack Width in Mils (0.001 Inch) |  | Not Accessible |
|  | Crack Previously Filled with Epoxy |  | Partition |
|  | Crack at Pre-existing Surface Patch | | |

Component Damage Records for Building Evaluated in Example Application

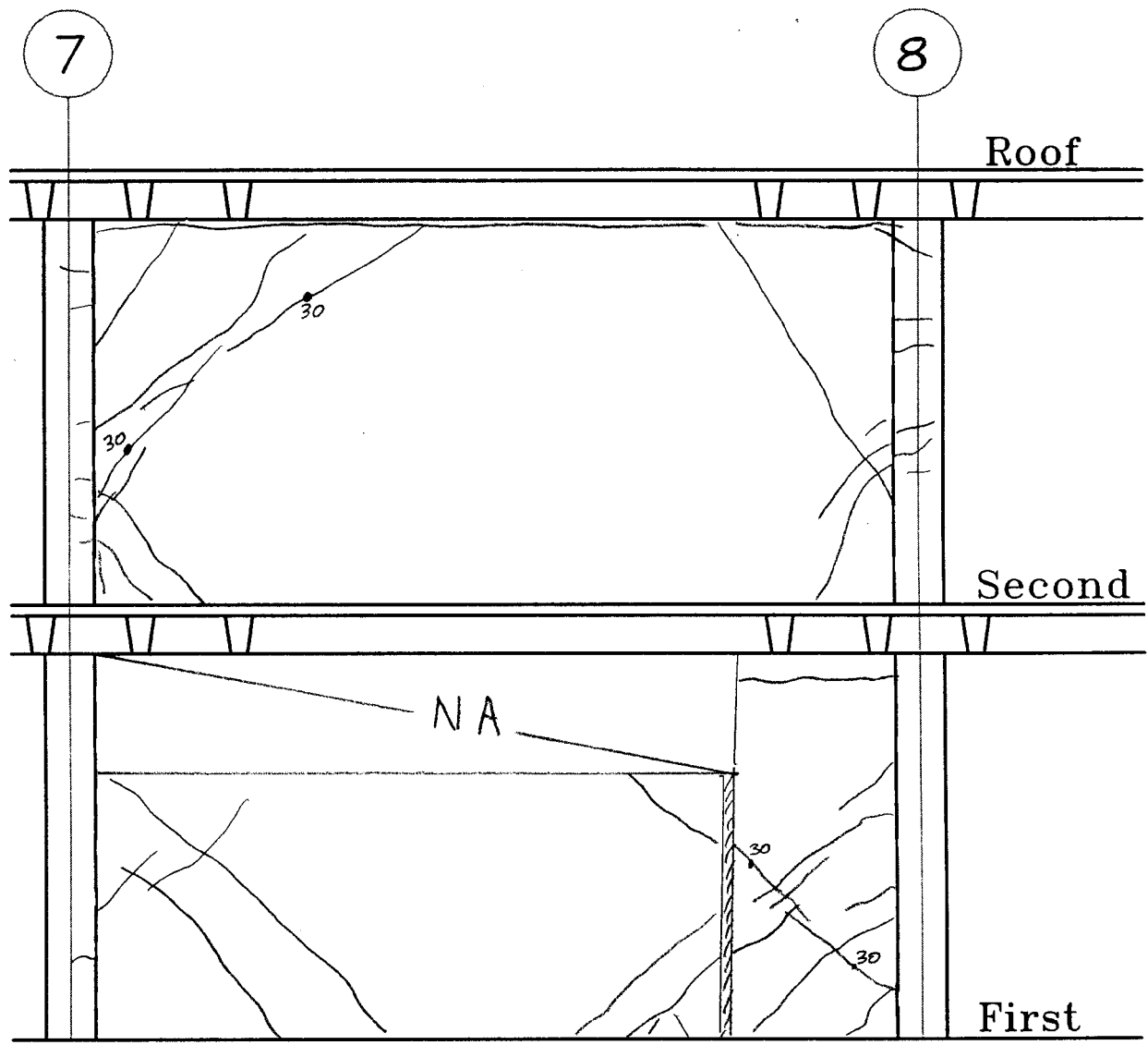
| Component Damage Record D16 | | | |
|---|--------------------------------------|----------------------------|----------------|
| Building Name: Concrete Shear Wall Building | Project ID: ATC 43 Example | Prepared by: ATC | |
| Location Within Building: Floor: 1 st /2 nd Column Line: G Component Type: | | Date: 24-Sep-97 | |
| Sketch and Description of Damage: | | | |
| | | | |
| Legend: | | | |
| | Crack | | Spall |
| | Crack Width in Mils (0.001 Inch) | | Not Accessible |
| | Crack Previously Filled with Epoxy | | Partition |
| | Crack at Pre-existing Surface Patch | | |

Component Damage Records for Building Evaluated in Example Application

Component Damage Record D17

| | | |
|---|--------------------------------------|----------------------------|
| Building Name: Concrete Shear Wall Building | Project ID: ATC 43 Example | Prepared by: ATC |
| Location Within Building: Floor: 1 st /2 nd Column Line: M Component Type: | | Date: 24-Sep-97 |

Sketch and Description of Damage:



Legend:

- | | | | |
|--|-------------------------------------|--|----------------|
| | Crack | | Spall |
| | Crack Width in Mils (0.001 Inch) | | Not Accessible |
| | Crack Previously Filled with Epoxy | | Partition |
| | Crack at Pre-existing Surface Patch | | |

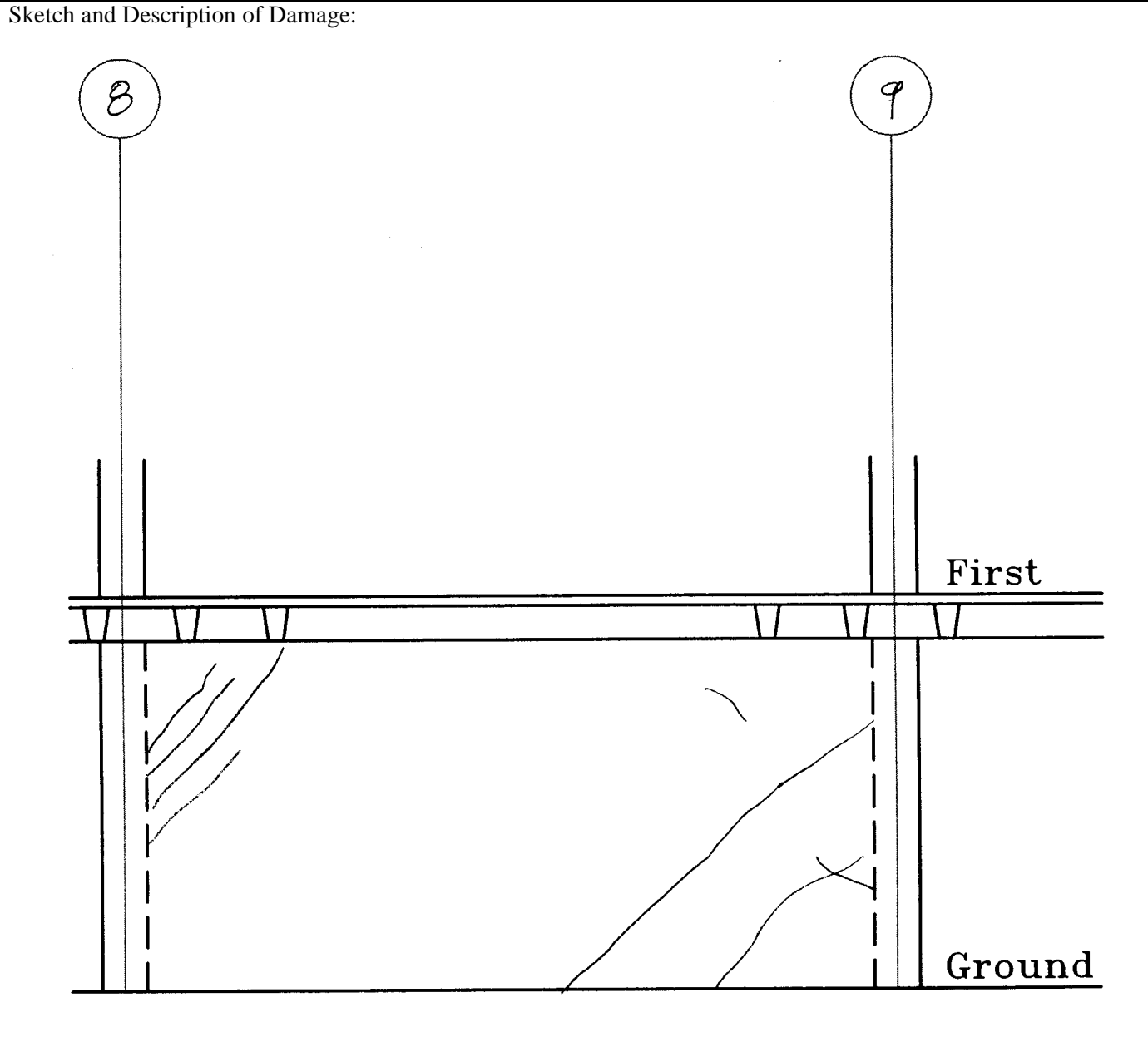
Component Damage Records for Building Evaluated in Example Application

| Component Damage Record D18 | | | |
|---|--------------------------------------|----------------------------|----------------|
| Building Name: Concrete Shear Wall Building | Project ID: ATC 43 Example | Prepared by: ATC | |
| Location Within Building: Floor: 1 st /2 nd Column Line: M Component Type: | | Date: 24-Sep-97 | |
| Sketch and Description of Damage: | | | |
| | | | |
| Legend: | | | |
| | Crack | | Spall |
| | Crack Width in Mills (0.001 Inch) | | Not Accessible |
| | Crack Previously Filled with Epoxy | | Partition |
| | Crack at Pre-existing Surface Patch | | |

Component Damage Records for Building Evaluated in Example Application

Component Damage Record D19

| | | |
|---|--------------------------------------|----------------------------|
| Building Name: Concrete Shear Wall Building | Project ID: ATC 43 Example | Prepared by: ATC |
| Location Within Building: Floor: 1 st /2 nd Column Line: M Component Type: | | Date: 24-Sep-97 |



Legend:

| | | | |
|--|-------------------------------------|--|----------------|
| | Crack | | Spall |
| | Crack Width in Mils (0.001 Inch) | | Not Accessible |
| | Crack Previously Filled with Epoxy | | Partition |
| | Crack at Pre-existing Surface Patch | | |

ATC-43 Project Participants

ATC MANAGEMENT

Mr. Christopher Rojahn,
Principal Investigator
Applied Technology Council
555 Twin Dolphin Drive, Suite 550
Redwood City, CA 94065

Mr. Craig Comartin,
Co-PI and Project Director
7683 Andrea Avenue
Stockton, CA 95207

Technical Management Committee

Prof. Dan Abrams
University of Illinois
1245 Newmark Civil Eng'g. Lab., MC 250
205 North Mathews Avenue
Urbana, IL 61801-2397

Mr. Andrew T. Merovich
A.T. Merovich & Associates, Inc.
1163 Francisco Blvd., Second Floor
San Rafael, CA 94901

Mr. James Hill
James A. Hill & Associates, Inc.
1349 East 28th Street
Signal Hill, CA 90806

Prof. Jack Moehle
Earthquake Engineering Research Center
University of California at Berkeley
1301 South 46th Street
Richmond, CA 94804

FEMA/PARR Representatives

Mr. Timothy McCormick
PaRR Task Manager
Dewberry & Davis
8401 Arlington Boulevard
Fairfax, VA 22031-4666

Prof. Robert Hanson
FEMA Technical Monitor
74 North Pasadena Avenue, CA-1009-DR
Parsons Bldg., West Annex, Room 308
Pasadena, CA 91103

Mr. Mark Doroudian
PaRR Representative
42 Silkwood
Aliso Viejo, CA 92656

Materials Working Group

Dr. Joe Maffei, Group Leader
Consulting Structural Engineer
148 Hermosa Avenue
Oakland California

Mr. Brian Kehoe, Lead Consultant
Wiss, Janney, Elstner Associates, Inc.
2200 Powell Street, Suite 925
Emeryville, CA 94608

Dr. Greg Kingsley
KL&A of Colorado
805 14th Street
Golden, CO 80401

Mr. Bret Lizundia
Rutherford & Chekene
303 Second Street, Suite 800 North
San Francisco, CA 94107

Prof. John Mander
SUNY at Buffalo
Department of Civil Engineering
212 Ketter Hall
Buffalo, NY 14260

Analysis Working Group

Prof. Mark Aschheim, Group Leader
University of Illinois at Urbana
2118 Newmark CE Lab
205 North Mathews, MC 250
Urbana, IL 61801

Prof. Mete Sozen, Senior Consultant
Purdue University, School of Engineering
1284 Civil Engineering Building
West Lafayette, IN 47907-1284

Project Review Panel

Mr. Gregg J. Borchelt
Brick Institute of America
11490 Commerce Park Drive, #300
Reston, VA 20191

Dr. Gene Corley
Construction Technology Labs
5420 Old Orchard Road
Skokie, IL 60077-1030

Mr. Edwin Huston
Smith & Huston
Plaza 600 Building, 6th & Stewart, #620
Seattle, WA 98101

Prof. Richard E. Klingner
University of Texas
Civil Engineering Department
Cockbell Building, Room 4-2
Austin, TX 78705

Mr. Vilas Mujumdar
Office of Regulation Services
Division of State Architect
General Services
1300 I Street, Suite 800
Sacramento, CA 95814

Dr. Hassan A. Sassi
Governors Office of Emergency Services
74 North Pasadena Avenue
Pasadena, CA 91103

Mr. Carl Schulze
Libby Engineers
4452 Glacier Avenue
San Diego, CA 92120

Mr. Daniel Shapiro
SOH & Associates
550 Kearny Street, Suite 200
San Francisco, CA 94108

ATC-43 Project Participants

Prof. James K. Wight
University of Michigan
Department of Civil Engineering
2368 G G Brown
Ann Arbor, MI 48109-2125

Mr. Eugene Zeller
Long Beach Department of Building & Safety
333 W. Ocean Boulevard, Fourth Floor
Long Beach, CA 90802

Applied Technology Council Projects And Report Information

One of the primary purposes of Applied Technology Council is to develop resource documents that translate and summarize useful information to practicing engineers. This includes the development of guidelines and manuals, as well as the development of research recommendations for specific areas determined by the profession. ATC is not a code development organization, although several of the ATC project reports serve as resource documents for the development of codes, standards and specifications.

Applied Technology Council conducts projects that meet the following criteria:

1. The primary audience or benefactor is the design practitioner in structural engineering.
2. A cross section or consensus of engineering opinion is required to be obtained and presented by a neutral source.
3. The project fosters the advancement of structural engineering practice.

A brief description of several major completed projects and reports is given in the following section. Funding for projects is obtained from government agencies and tax-deductible contributions from the private sector.

ATC-1: This project resulted in five papers that were published as part of *Building Practices for Disaster Mitigation, Building Science Series 46*, proceedings of a workshop sponsored by the National Science Foundation (NSF) and the National Bureau of Standards (NBS). Available through the National Technical Information Service (NTIS), 5285 Port Royal Road, Springfield, VA 22151, as NTIS report No. COM-73-50188.

ATC-2: The report, *An Evaluation of a Response Spectrum Approach to Seismic Design of Buildings*, was funded by NSF and NBS and was conducted as part of the Cooperative Federal Program in Building Practices for Disaster Mitigation. Available through the ATC office. (Published 1974, 270 Pages)

ABSTRACT: This study evaluated the applicability and cost of the response spectrum approach to seis-

mic analysis and design that was proposed by various segments of the engineering profession. Specific building designs, design procedures and parameter values were evaluated for future application. Eleven existing buildings of varying dimensions were redesigned according to the procedures.

ATC-3: The report, *Tentative Provisions for the Development of Seismic Regulations for Buildings (ATC-3-06)*, was funded by NSF and NBS. The second printing of this report, which includes proposed amendments, is available through the ATC office. (Published 1978, amended 1982, 505 pages plus proposed amendments)

ABSTRACT: The tentative provisions in this document represent the results of a concerted effort by a multi-disciplinary team of 85 nationally recognized experts in earthquake engineering. The provisions serve as the basis for the seismic provisions of the 1988 *Uniform Building Code* and the 1988 and subsequent issues of the *NEHRP Recommended Provisions for the Development of Seismic Regulation for New Buildings*. The second printing of this document contains proposed amendments prepared by a joint committee of the Building Seismic Safety Council (BSSC) and the NBS.

ATC-3-2: The project, *Comparative Test Designs of Buildings Using ATC-3-06 Tentative Provisions*, was funded by NSF. The project consisted of a study to develop and plan a program for making comparative test designs of the ATC-3-06 Tentative Provisions. The project report was written to be used by the Building Seismic Safety Council in its refinement of the ATC-3-06 Tentative Provisions.

ATC-3-4: The report, *Redesign of Three Multistory Buildings: A Comparison Using ATC-3-06 and 1982 Uniform Building Code Design Provisions*, was published under a grant from NSF. Available through the ATC office. (Published 1984, 112 pages)

ABSTRACT: This report evaluates the cost and technical impact of using the 1978 ATC-3-06 report, *Tentative Provisions for the Development of Seismic Regulations for Buildings*, as amended by a joint

committee of the Building Seismic Safety Council and the National Bureau of Standards in 1982. The evaluations are based on studies of three existing California buildings redesigned in accordance with the ATC-3-06 Tentative Provisions and the 1982 *Uniform Building Code*. Included in the report are recommendations to code implementing bodies.

ATC-3-5: This project, Assistance for First Phase of ATC-3-06 Trial Design Program Being Conducted by the Building Seismic Safety Council, was funded by the Building Seismic Safety Council to provide the services of the ATC Senior Consultant and other ATC personnel to assist the BSSC in the conduct of the first phase of its Trial Design Program. The first phase provided for trial designs conducted for buildings in Los Angeles, Seattle, Phoenix, and Memphis.

ATC-3-6: This project, Assistance for Second Phase of ATC-3-06 Trial Design Program Being Conducted by the Building Seismic Safety Council, was funded by the Building Seismic Safety Council to provide the services of the ATC Senior Consultant and other ATC personnel to assist the BSSC in the conduct of the second phase of its Trial Design Program. The second phase provided for trial designs conducted for buildings in New York, Chicago, St. Louis, Charleston, and Fort Worth.

ATC-4: The report, *A Methodology for Seismic Design and Construction of Single-Family Dwellings*, was published under a contract with the Department of Housing and Urban Development (HUD). Available through the ATC office. (Published 1976, 576 pages)

ABSTRACT: This report presents the results of an in-depth effort to develop design and construction details for single-family residences that minimize the potential economic loss and life-loss risk associated with earthquakes. The report: (1) discusses the ways structures behave when subjected to seismic forces, (2) sets forth suggested design criteria for conventional layouts of dwellings constructed with conventional materials, (3) presents construction details that do not require the designer to perform analytical calculations, (4) suggests procedures for efficient plan-checking, and (5) presents recommendations including details and schedules for use in the field by construction personnel and building inspectors.

ATC-4-1: The report, *The Home Builders Guide for Earthquake Design*, was published under a contract with HUD. Available through the ATC office. (Published 1980, 57 pages)

ABSTRACT: This report is an abridged version of the ATC-4 report. The concise, easily understood text of the Guide is supplemented with illustrations and 46 construction details. The details are provided to ensure that houses contain structural features that are properly positioned, dimensioned and constructed to resist earthquake forces. A brief description is included on how earthquake forces impact on houses and some precautionary constraints are given with respect to site selection and architectural designs.

ATC-5: The report, *Guidelines for Seismic Design and Construction of Single-Story Masonry Dwellings in Seismic Zone 2*, was developed under a contract with HUD. Available through the ATC office. (Published 1986, 38 pages)

ABSTRACT: The report offers a concise methodology for the earthquake design and construction of single-story masonry dwellings in Seismic Zone 2 of the United States, as defined by the 1973 *Uniform Building Code*. The Guidelines are based in part on shaking table tests of masonry construction conducted at the University of California at Berkeley Earthquake Engineering Research Center. The report is written in simple language and includes basic house plans, wall evaluations, detail drawings, and material specifications.

ATC-6: The report, *Seismic Design Guidelines for Highway Bridges*, was published under a contract with the Federal Highway Administration (FHWA). Available through the ATC office. (Published 1981, 210 pages)

ABSTRACT: The Guidelines are the recommendations of a team of sixteen nationally recognized experts that included consulting engineers, academics, state and federal agency representatives from throughout the United States. The Guidelines embody several new concepts that were significant departures from then existing design provisions. Included in the Guidelines are an extensive commentary, an example demonstrating the use of the

Guidelines, and summary reports on 21 bridges redesigned in accordance with the Guidelines.

The guidelines have been adopted by the American Association of Highway and Transportation Officials as a guide specification.

ATC-6-1: The report, *Proceedings of a Workshop on Earthquake Resistance of Highway Bridges*, was published under a grant from NSF. Available through the ATC office. (Published 1979, 625 pages)

ABSTRACT: The report includes 23 state-of-the-art and state-of-practice papers on earthquake resistance of highway bridges. Seven of the twenty-three papers were authored by participants from Japan, New Zealand and Portugal. The Proceedings also contain recommendations for future research that were developed by the 45 workshop participants.

ATC-6-2: The report, *Seismic Retrofitting Guidelines for Highway Bridges*, was published under a contract with FHWA. Available through the ATC office. (Published 1983, 220 pages)

ABSTRACT: The Guidelines are the recommendations of a team of thirteen nationally recognized experts that included consulting engineers, academics, state highway engineers, and federal agency representatives. The Guidelines, applicable for use in all parts of the United States, include a preliminary screening procedure, methods for evaluating an existing bridge in detail, and potential retrofitting measures for the most common seismic deficiencies. Also included are special design requirements for various retrofitting measures.

ATC-7: The report, *Guidelines for the Design of Horizontal Wood Diaphragms*, was published under a grant from NSF. Available through the ATC office. (Published 1981, 190 pages)

ABSTRACT: Guidelines are presented for designing roof and floor systems so these can function as horizontal diaphragms in a lateral force resisting system. Analytical procedures, connection details and design examples are included in the Guidelines.

ATC-7-1: The report, *Proceedings of a Workshop of Design of Horizontal Wood Diaphragms*, was

published under a grant from NSF. Available through the ATC office. (Published 1980, 302 pages)

ABSTRACT: The report includes seven papers on state-of-the-practice and two papers on recent research. Also included are recommendations for future research that were developed by the 35 workshop participants.

ATC-8: This report, *Proceedings of a Workshop on the Design of Prefabricated Concrete Buildings for Earthquake Loads*, was funded by NSF. Available through the ATC office. (Published 1981, 400 pages)

ABSTRACT: The report includes eighteen state-of-the-art papers and six summary papers. Also included are recommendations for future research that were developed by the 43 workshop participants.

ATC-9: The report, *An Evaluation of the Imperial County Services Building Earthquake Response and Associated Damage*, was published under a grant from NSF. Available through the ATC office. (Published 1984, 231 pages)

ABSTRACT: The report presents the results of an in-depth evaluation of the Imperial County Services Building, a 6-story reinforced concrete frame and shear wall building severely damaged by the October 15, 1979 Imperial Valley, California, earthquake. The report contains a review and evaluation of earthquake damage to the building; a review and evaluation of the seismic design; a comparison of the requirements of various building codes as they relate to the building; and conclusions and recommendations pertaining to future building code provisions and future research needs.

ATC-10: This report, *An Investigation of the Correlation Between Earthquake Ground Motion and Building Performance*, was funded by the U.S. Geological Survey (USGS). Available through the ATC office. (Published 1982, 114 pages)

ABSTRACT: The report contains an in-depth analytical evaluation of the ultimate or limit capacity of selected representative building framing types, a discussion of the factors affecting the seismic performance of buildings, and a sum-

mary and comparison of seismic design and seismic risk parameters currently in widespread use.

ATC-10-1: This report, *Critical Aspects of Earthquake Ground Motion and Building Damage Potential*, was co-funded by the USGS and the NSF. Available through the ATC office. (Published 1984, 259 pages)

ABSTRACT: This document contains 19 state-of-the-art papers on ground motion, structural response, and structural design issues presented by prominent engineers and earth scientists in an ATC seminar. The main theme of the papers is to identify the critical aspects of ground motion and building performance that currently are not being considered in building design. The report also contains conclusions and recommendations of working groups convened after the Seminar.

ATC-11: The report, *Seismic Resistance of Reinforced Concrete Shear Walls and Frame Joints: Implications of Recent Research for Design Engineers*, was published under a grant from NSF. Available through the ATC office. (Published 1983, 184 pages)

ABSTRACT: This document presents the results of an in-depth review and synthesis of research reports pertaining to cyclic loading of reinforced concrete shear walls and cyclic loading of joint reinforced concrete frames. More than 125 research reports published since 1971 are reviewed and evaluated in this report. The preparation of the report included a consensus process involving numerous experienced design professionals from throughout the United States. The report contains reviews of current and past design practices, summaries of research developments, and in-depth discussions of design implications of recent research results.

ATC-12: This report, *Comparison of United States and New Zealand Seismic Design Practices for Highway Bridges*, was published under a grant from NSF. Available through the ATC office. (Published 1982, 270 pages)

ABSTRACT: The report contains summaries of all aspects and innovative design procedures used in New Zealand as well as comparison of United States and New Zealand design practice. Also included are research recommendations developed

at a 3-day workshop in New Zealand attended by 16 U.S. and 35 New Zealand bridge design engineers and researchers.

ATC-12-1: This report, *Proceedings of Second Joint U.S.-New Zealand Workshop on Seismic Resistance of Highway Bridges*, was published under a grant from NSF. Available through the ATC office. (Published 1986, 272 pages)

ABSTRACT: This report contains written versions of the papers presented at this 1985 Workshop as well as a list and prioritization of workshop recommendations. Included are summaries of research projects being conducted in both countries as well as state-of-the-practice papers on various aspects of design practice. Topics discussed include bridge design philosophy and loadings; design of columns, footings, piles, abutments and retaining structures; geotechnical aspects of foundation design; seismic analysis techniques; seismic retrofitting; case studies using base isolation; strong-motion data acquisition and interpretation; and testing of bridge components and bridge systems.

ATC-13: The report, *Earthquake Damage Evaluation Data for California*, was developed under a contract with the Federal Emergency Management Agency (FEMA). Available through the ATC office. (Published 1985, 492 pages)

ABSTRACT: This report presents expert-opinion earthquake damage and loss estimates for industrial, commercial, residential, utility and transportation facilities in California. Included are damage probability matrices for 78 classes of structures and estimates of time required to restore damaged facilities to pre-earthquake usability. The report also describes the inventory information essential for estimating economic losses and the methodology used to develop loss estimates on a regional basis.

ATC-14: The report, *Evaluating the Seismic Resistance of Existing Buildings*, was developed under a grant from the NSF. Available through the ATC office. (Published 1987, 370 pages)

ABSTRACT: This report, written for practicing structural engineers, describes a methodology for performing preliminary and detailed building seis-

mic evaluations. The report contains a state-of-practice review; seismic loading criteria; data collection procedures; a detailed description of the building classification system; preliminary and detailed analysis procedures; and example case studies, including nonstructural considerations.

ATC-15: The report, *Comparison of Seismic Design Practices in the United States and Japan*, was published under a grant from NSF. Available through the ATC office. (Published 1984, 317 pages)

ABSTRACT: The report contains detailed technical papers describing design practices in the United States and Japan as well as recommendations emanating from a joint U.S.-Japan workshop held in Hawaii in March, 1984. Included are detailed descriptions of new seismic design methods for buildings in Japan and case studies of the design of specific buildings (in both countries). The report also contains an overview of the history and objectives of the Japan Structural Consultants Association.

ATC-15-1: The report, *Proceedings of Second U.S.-Japan Workshop on Improvement of Building Seismic Design and Construction Practices*, was published under a grant from NSF. Available through the ATC office. (Published 1987, 412 pages)

ABSTRACT: This report contains 23 technical papers presented at this San Francisco workshop in August, 1986, by practitioners and researchers from the U.S. and Japan. Included are state-of-the-practice papers and case studies of actual building designs and information on regulatory, contractual, and licensing issues.

ATC-15-2: The report, *Proceedings of Third U.S.-Japan Workshop on Improvement of Building Structural Design and Construction Practices*, was published jointly by ATC and the Japan Structural Consultants Association. Available through the ATC office. (Published 1989, 358 pages)

ABSTRACT: This report contains 21 technical papers presented at this Tokyo, Japan, workshop in July, 1988, by practitioners and researchers from the U.S., Japan, China, and New Zealand. Included are state-of-the-practice papers on various topics,

including braced steel frame buildings, beam-column joints in reinforced concrete buildings, summaries of comparative U. S. and Japanese design, and base isolation and passive energy dissipation devices.

ATC-15-3: The report, *Proceedings of Fourth U.S.-Japan Workshop on Improvement of Building Structural Design and Construction Practices*, was published jointly by ATC and the Japan Structural Consultants Association. Available through the ATC office. (Published 1992, 484 pages)

ABSTRACT: This report contains 22 technical papers presented at this Kailua-Kona, Hawaii, workshop in August, 1990, by practitioners and researchers from the United States, Japan, and Peru. Included are papers on postearthquake building damage assessment; acceptable earth-quake damage; repair and retrofit of earthquake damaged buildings; base-isolated buildings, including Architectural Institute of Japan recommendations for design; active damping systems; wind-resistant design; and summaries of working group conclusions and recommendations.

ATC-15-4: The report, *Proceedings of Fifth U.S.-Japan Workshop on Improvement of Building Structural Design and Construction Practices*, was published jointly by ATC and the Japan Structural Consultants Association. Available through the ATC office. (Published 1994, 360 pages)

ABSTRACT: This report contains 20 technical papers presented at this San Diego, California workshop in September, 1992. Included are papers on performance goals/acceptable damage in seismic design; seismic design procedures and case studies; construction influences on design; seismic isolation and passive energy dissipation; design of irregular structures; seismic evaluation, repair and upgrading; quality control for design and construction; and summaries of working group discussions and recommendations.

ATC-16: This project, Development of a 5-Year Plan for Reducing the Earthquake Hazards Posed by Existing Nonfederal Buildings, was funded by FEMA and was conducted by a joint venture of ATC, the Building Seismic Safety Council and the Earthquake Engineering

Research Institute. The project involved a workshop in Phoenix, Arizona, where approximately 50 earthquake specialists met to identify the major tasks and goals for reducing the earthquake hazards posed by existing non-federal buildings nationwide. The plan was developed on the basis of nine issue papers presented at the workshop and workshop working group discussions. The Workshop Proceedings and Five-Year Plan are available through the Federal Emergency Management Agency, 500 "C" Street, S.W., Washington, DC 20472.

ATC-17: This report, *Proceedings of a Seminar and Workshop on Base Isolation and Passive Energy Dissipation*, was published under a grant from NSF. Available through the ATC office. (Published 1986, 478 pages)

ABSTRACT: The report contains 42 papers describing the state-of-the-art and state-of-the-practice in base-isolation and passive energy-dissipation technology. Included are papers describing case studies in the United States, applications and developments worldwide, recent innovations in technology development, and structural and ground motion issues. Also included is a proposed 5-year research agenda that addresses the following specific issues: (1) strong ground motion; (2) design criteria; (3) materials, quality control, and long-term reliability; (4) life cycle cost methodology; and (5) system response.

ATC-17-1: This report, *Proceedings of a Seminar on Seismic Isolation, Passive Energy Dissipation and Active Control*, was published under a grant from NSF. Available through the ATC office. (Published 1993, 841 pages)

ABSTRACT: The 2-volume report documents 70 technical papers presented during a two-day seminar in San Francisco in early 1993. Included are invited theme papers and competitively selected papers on issues related to seismic isolation systems, passive energy dissipation systems, active control systems and hybrid systems.

ATC-18: The report, *Seismic Design Criteria for Bridges and Other Highway Structures: Current and Future*, was published under a contract from the Multi-disciplinary Center for Earthquake Engineering Research (formerly NCEER), with funding from the

Federal Highway Administration. Available through the ATC office. (Published 1997, 152 pages)

ABSTRACT: This report documents the findings of a 4-year project to review and assess current seismic design criteria for new highway construction. The report addresses performance criteria, importance classification, definitions of seismic hazard for areas where damaging earthquakes have longer return periods, design ground motion, duration effects, site effects, structural response modification factors, ductility demand, design procedures, foundation and abutment modeling, soil-structure interaction, seat widths, joint details and detailing reinforced concrete for limited ductility in areas with low-to-moderate seismic activity. The report also provides lengthy discussion on future directions for code development and recommended research and development topics.

ATC-19: The report, *Structural Response Modification Factors* was funded by NSF and NCEER. Available through the ATC office. (Published 1995, 70 pages)

ABSTRACT: This report addresses structural response modification factors (R factors), which are used to reduce the seismic forces associated with elastic response to obtain design forces. The report documents the basis for current R values, how R factors are used for seismic design in other countries, a rational means for decomposing R into key components, a framework (and methods) for evaluating the key components of R, and the research necessary to improve the reliability of engineered construction designed using R factors.

ATC-20: The report, *Procedures for Postearthquake Safety Evaluation of Buildings*, was developed under a contract from the California Office of Emergency Services (OES), California Office of Statewide Health Planning and Development (OSHPD) and FEMA. Available through the ATC office (Published 1989, 152 pages)

ABSTRACT: This report provides procedures and guidelines for making on-the-spot evaluations and decisions regarding continued use and occupancy of earthquake damaged buildings. Written specifically for volunteer structural engineers and building inspectors, the report includes rapid and detailed

evaluation procedures for inspecting buildings and posting them as “inspected” (apparently safe), “limited entry” or “unsafe”. Also included are special procedures for evaluation of essential buildings (e.g., hospitals), and evaluation procedures for non-structural elements, and geotechnical hazards.

ATC-20-1: The report, *Field Manual: Postearthquake Safety Evaluation of Buildings*, was developed under a contract from OES and OSHPD. Available through the ATC office (Published 1989, 114 pages)

ABSTRACT: This report, a companion Field Manual for the ATC-20 report, summarizes the postearthquake safety evaluation procedures in brief concise format designed for ease of use in the field.

ATC-20-2: The report, *Addendum to the ATC-20 Postearthquake Building Safety Procedures* was published under a grant from the NSF and funded by the USGS. Available through the ATC office. (Published 1995, 94 pages)

ABSTRACT: This report provides updated assessment forms, placards, and procedures that are based on an in-depth review and evaluation of the widespread application of the ATC-20 procedures following five earthquakes occurring since the initial release of the ATC-20 report in 1989.

ATC-20-3: The report, *Case Studies in Rapid Postearthquake Safety Evaluation of Buildings*, was funded by ATC and R. P. Gallagher Associates. Available through the ATC office. (Published 1996, 295 pages)

ABSTRACT: This report contains 53 case studies using the ATC-20 Rapid Evaluation procedure. Each case study is illustrated with photos and describes how a building was inspected and evaluated for life safety, and includes a completed safety assessment form and placard. The report is intended to be used as a training and reference manual for building officials, building inspectors, civil and structural engineers, architects, disaster workers, and others who may be asked to perform safety evaluations after an earthquake.

ATC-20-T: The report, *Postearthquake Safety Evaluation of Buildings Training Manual* was developed under

a contract with FEMA. Available through the ATC office. (Published 1993, 177 pages; 160 slides)

ABSTRACT: This training manual is intended to facilitate the presentation of the contents of the ATC-20 and ATC-20-1. The training materials consist of 160 slides of photographs, schematic drawings and textual information and a companion training presentation narrative coordinated with the slides. Topics covered include: posting system; evaluation procedures; structural basics; wood frame, masonry, concrete, and steel frame structures; nonstructural elements; geotechnical hazards; hazardous materials; and field safety.

ATC-21: The report, *Rapid Visual Screening of Buildings for Potential Seismic Hazards: A Handbook*, was developed under a contract from FEMA. Available through the ATC office. (Published 1988, 185 pages)

ABSTRACT: This report describes a rapid visual screening procedure for identifying those buildings that might pose serious risk of loss of life and injury, or of severe curtailment of community services, in case of a damaging earthquake. The screening procedure utilizes a methodology based on a "sidewalk survey" approach that involves identification of the primary structural load resisting system and building materials, and assignment of a basic structural hazards score and performance modification factors based on observed building characteristics. Application of the methodology identifies those buildings that are potentially hazardous and should be analyzed in more detail by a professional engineer experienced in seismic design.

ATC-21-1: The report, *Rapid Visual Screening of Buildings for Potential Seismic Hazards: Supporting Documentation*, was developed under a contract from FEMA. Available through the ATC office. (Published 1988, 137 pages)

ABSTRACT: Included in this report are (1) a review and evaluation of existing procedures; (2) a listing of attributes considered ideal for a rapid visual screening procedure; and (3) a technical discussion of the recommended rapid visual screening procedure that is documented in the ATC-21 report.

ATC-21-2: The report, *Earthquake Damaged Buildings: An Overview of Heavy Debris and Victim Extrication*, was developed under a contract from FEMA. (Published 1988, 95 pages)

ABSTRACT: Included in this report, a companion volume to the ATC-21 and ATC-21-1 reports, is state-of-the-art information on (1) the identification of those buildings that might collapse and trap victims in debris or generate debris of such a size that its handling would require special or heavy lifting equipment; (2) guidance in identifying these types of buildings, on the basis of their major exterior features, and (3) the types and life capacities of equipment required to remove the heavy portion of the debris that might result from the collapse of such buildings.

ATC-21-T: The report, *Rapid Visual Screening of Buildings for Potential Seismic Hazards Training Manual* was developed under a contract with FEMA. Available through the ATC office. (Published 1996, 135 pages; 120 slides)

ABSTRACT: This training manual is intended to facilitate the presentation of the contents of the ATC-21 report. The training materials consist of 120 slides and a companion training presentation narrative coordinated with the slides. Topics covered include: description of procedure, building behavior, building types, building scores, occupancy and falling hazards, and implementation.

ATC-22: The report, *A Handbook for Seismic Evaluation of Existing Buildings (Preliminary)*, was developed under a contract from FEMA. Available through the ATC office. (Originally published in 1989; revised by BSSC and published as the *NEHRP Handbook for Seismic Evaluation of Existing Buildings* in 1992, 211 pages)

ABSTRACT: This handbook provides a methodology for seismic evaluation of existing buildings of different types and occupancies in areas of different seismicity throughout the United States. The methodology, which has been field tested in several programs nationwide, utilizes the information and procedures developed for and documented in the ATC-14 report. The handbook includes checklists, diagrams, and sketches designed to assist the user.

ATC-22-1: The report, *Seismic Evaluation of Existing Buildings: Supporting Documentation*, was developed under a contract from FEMA. (Published 1989, 160 pages)

ABSTRACT: Included in this report, a companion volume to the ATC-22 report, are (1) a review and evaluation of existing buildings seismic evaluation methodologies; (2) results from field tests of the ATC-14 methodology; and (3) summaries of evaluations of ATC-14 conducted by the National Center for Earthquake Engineering Research (State University of New York at Buffalo) and the City of San Francisco.

ATC-23A: The report, *General Acute Care Hospital Earthquake Survivability Inventory for California, Part A: Survey Description, Summary of Results, Data Analysis and Interpretation*, was developed under a contract from the Office of Statewide Health Planning and Development (OSHPD), State of California. Available through the ATC office. (Published 1991, 58 pages)

ABSTRACT: This report summarizes results from a seismic survey of 490 California acute care hospitals. Included are a description of the survey procedures and data collected, a summary of the data, and an illustrative discussion of data analysis and interpretation that has been provided to demonstrate potential applications of the ATC-23 database.

ATC-23B: The report, *General Acute Care Hospital Earthquake Survivability Inventory for California, Part B: Raw Data*, is a companion document to the ATC-23A Report and was developed under the above-mentioned contract from OSHPD. Available through the ATC office. (Published 1991, 377 pages)

ABSTRACT: Included in this report are tabulations of raw general site and building data for 490 acute care hospitals in California.

ATC-24: The report, *Guidelines for Seismic Testing of Components of Steel Structures*, was jointly funded by the American Iron and Steel Institute (AISI), American Institute of Steel Construction (AISC), National Center for Earthquake Engineering Research (NCEER), and NSF. Available through the ATC office. (Published 1992, 57 pages)

ABSTRACT: This report provides guidance for most cyclic experiments on components of steel structures for the purpose of consistency in experimental procedures. The report contains recommendations and companion commentary pertaining to loading histories, presentation of test results, and other aspects of experimentation. The recommendations are written specifically for experiments with slow cyclic load application.

ATC-25: The report, *Seismic Vulnerability and Impact of Disruption of Lifelines in the Conterminous United States*, was developed under a contract from FEMA. Available through the ATC office. (Published 1991, 440 pages)

ABSTRACT: Documented in this report is a national overview of lifeline seismic vulnerability and impact of disruption. Lifelines considered include electric systems, water systems, transportation systems, gas and liquid fuel supply systems, and emergency service facilities (hospitals, fire and police stations). Vulnerability estimates and impacts developed are presented in terms of estimated first approximation direct damage losses and indirect economic losses.

ATC-25-1: The report, *A Model Methodology for Assessment of Seismic Vulnerability and Impact of Disruption of Water Supply Systems*, was developed under a contract from FEMA. Available through the ATC office. (Published 1992, 147 pages)

ABSTRACT: This report contains a practical methodology for the detailed assessment of seismic vulnerability and impact of disruption of water supply systems. The methodology has been designed for use by water system operators. Application of the methodology enables the user to develop estimates of direct damage to system components and the time required to restore damaged facilities to pre-earthquake usability. Suggested measures for mitigation of seismic hazards are also provided.

ATC-28: The report, *Development of Recommended Guidelines for Seismic Strengthening of Existing Buildings, Phase I: Issues Identification and Resolution*, was developed under a contract with FEMA. Available through the ATC office. (Published 1992, 150 pages)

ABSTRACT: This report identifies and provides resolutions for issues that will affect the development of guidelines for the seismic strengthening of existing buildings. Issues addressed include: implementation and format, coordination with other efforts, legal and political, social, economic, historic buildings, research and technology, seismicity and mapping, engineering philosophy and goals, issues related to the development of specific provisions, and nonstructural element issues.

ATC-29: The report, *Proceedings of a Seminar and Workshop on Seismic Design and Performance of Equipment and Nonstructural Elements in Buildings and Industrial Structures*, was developed under a grant from NCEER and NSF. Available through the ATC office. (Published 1992, 470 pages)

ABSTRACT: These Proceedings contain 35 papers describing state-of-the-art technical information pertaining to the seismic design and performance of equipment and nonstructural elements in buildings and industrial structures. The papers were presented at a seminar in Irvine, California in 1990. Included are papers describing current practice, codes and regulations; earthquake performance; analytical and experimental investigations; development of new seismic qualification methods; and research, practice, and code development needs for specific elements and systems. The report also includes a summary of a proposed 5-year research agenda for NCEER.

ATC-29-1: The report, *Proceedings Of Seminar On Seismic Design, Retrofit, And Performance Of Nonstructural Components*, was developed under a grant from NCEER and NSF. Available through the ATC office. (Published 1998, 518 pages)

ABSTRACT: These Proceedings contain 38 papers presenting current research, practice, and informed thinking pertinent to seismic design, retrofit, and performance of nonstructural components. The papers were presented at a seminar in San Francisco, California, in 1998. Included are papers describing observed performance in recent earthquakes; seismic design codes, standards, and procedures for commercial and institutional buildings; seismic design issues relating to industrial and hazardous material facilities; design, analysis, and test-

ing; and seismic evaluation and rehabilitation of conventional and essential facilities, including hospitals.

ATC-30: The report, *Proceedings of Workshop for Utilization of Research on Engineering and Socioeconomic Aspects of 1985 Chile and Mexico Earthquakes*, was developed under a grant from the NSF. Available through the ATC office. (Published 1991, 113 pages)

ABSTRACT: This report documents the findings of a 1990 technology transfer workshop in San Diego, California, co-sponsored by ATC and the Earthquake Engineering Research Institute. Included in the report are invited papers and working group recommendations on geotechnical issues, structural response issues, architectural and urban design considerations, emergency response planning, search and rescue, and reconstruction policy issues.

ATC-31: The report, *Evaluation of the Performance of Seismically Retrofitted Buildings*, was developed under a contract from the National Institute of Standards and Technology (NIST, formerly NBS) and funded by the USGS. Available through the ATC office. (Published 1992, 75 pages)

ABSTRACT: This report summarizes the results from an investigation of the effectiveness of 229 seismically retrofitted buildings, primarily unreinforced masonry and concrete tilt-up buildings. All buildings were located in the areas affected by the 1987 Whittier Narrows, California, and 1989 Loma Prieta, California, earthquakes.

ATC-32: The report, *Improved Seismic Design Criteria for California Bridges: Provisional Recommendations*, was funded by the California Department of Transportation (Caltrans). Available through the ATC office. (Published 1996, 215 Pages)

ABSTRACT: This report provides recommended revisions to the current *Caltrans Bridge Design Specifications* (BDS) pertaining to seismic loading, structural response analysis, and component design. Special attention is given to design issues related to reinforced concrete components, steel components, foundations, and conventional bearings. The recommendations are based on recent research in the field of bridge seismic design and the performance

of Caltrans-designed bridges in the 1989 Loma Prieta and other recent California earthquakes.

ATC-34: The report, *A Critical Review of Current Approaches to Earthquake Resistant Design*, was developed under a grant from NCEER and NSF. Available through the ATC office. (Published, 1995, 94 pages)

ABSTRACT. This report documents the history of U. S. codes and standards of practice, focusing primarily on the strengths and deficiencies of current code approaches. Issues addressed include: seismic hazard analysis, earthquake collateral hazards, performance objectives, redundancy and configuration, response modification factors (*R* factors), simplified analysis procedures, modeling of structural components, foundation design, nonstructural component design, and risk and reliability. The report also identifies goals that a new seismic code should achieve.

ATC-35: This report, *Enhancing the Transfer of U.S. Geological Survey Research Results into Engineering Practice* was developed under a contract with the USGS. Available through the ATC office. (Published 1996, 120 pages)

ABSTRACT: The report provides a program of recommended "technology transfer" activities for the USGS; included are recommendations pertaining to management actions, communications with practicing engineers, and research activities to enhance development and transfer of information that is vital to engineering practice.

ATC-35-1: The report, *Proceedings of Seminar on New Developments in Earthquake Ground Motion Estimation and Implications for Engineering Design Practice*, was developed under a cooperative agreement with USGS. Available through the ATC office. (Published 1994, 478 pages)

ABSTRACT: These Proceedings contain 22 technical papers describing state-of-the-art information on regional earthquake risk (focused on five specific regions--California, Pacific Northwest, Central United States, and northeastern North America); new techniques for estimating strong ground motions as a function of earthquake source, travel path, and site parameters; and new developments

Applied Technology Council Projects And Report Information

specifically applicable to geotechnical engineering and the seismic design of buildings and bridges.

ATC-37: The report, *Review of Seismic Research Results on Existing Buildings*, was developed in conjunction with the Structural Engineers Association of California and California Universities for Research in Earthquake Engineering under a contract from the California Seismic Safety Commission (SSC). Available through the Seismic Safety Commission as Report SSC 94-03. (Published, 1994, 492 pages)

ABSTRACT. This report describes the state of knowledge of the earthquake performance of nonductile concrete frame, shear wall, and infilled buildings. Included are summaries of 90 recent research efforts with key results and conclusions in a simple, easy-to-access format written for practicing design professionals.

ATC-40: The report, *Seismic Evaluation and Retrofit of Concrete Buildings*, was developed under a contract from the California Seismic Safety Commission. Available through the ATC office. (Published, 1996, 612 pages)

ABSTRACT. This 2-volume report provides a state-of-the-art methodology for the seismic evaluation and retrofit of concrete buildings. Specific guidance is provided on the following topics: performance objectives; seismic hazard; determination of deficiencies; retrofit strategies; quality assurance procedures; nonlinear static analysis procedures; modeling rules; foundation effects; response limits; and nonstructural components. In 1997 this report received the West-

ern States Seismic Policy Council "Overall Excellence and New Technology Award."

ATC-44: The report, *Hurricane Fran, South Carolina, September 5, 1996: Reconnaissance Report*, is available through the ATC office. (Published 1997, 36 pages.)

ABSTRACT: This report represents ATC's expanded mandate into structural engineering problems arising from wind storms and coastal flooding. It contains information on the causative hurricane; coastal impacts, including storm surge, waves, structural forces and erosion; building codes; observations and interpretations of damage; and lifeline performance. Conclusions address man-made beach nourishment, the effects of missile-like debris, breaches in the sandy barrier islands, and the timing and duration of such investigations.

ATC-R-1: The report, *Cyclic Testing of Narrow Plywood Shear Walls*, was developed with funding from the Henry J. Degenkolb Memorial Endowment Fund of the Applied Technology Council. Available through the ATC office (Published 1995, 64 pages)

ABSTRACT: This report documents ATC's first self-directed research program: a series of static and dynamic tests of narrow plywood wall panels having the standard 3.5-to-1 height-to-width ratio and anchored to the sill plate using typical bolted, 9-inch, 5000-lb. capacity hold-down devices. The report provides a description of the testing program and a summary of results, including comparisons of drift ratios found during testing with those specified in the seismic provisions of the 1991 *Uniform Building Code*.

ATC BOARD OF DIRECTORS (1973-Present)

| | | | |
|-------------------------|----------------------|-----------------------|--------------------|
| Milton A. Abel | (1979-85) | John F. Meehan* | (1973-78) |
| James C. Anderson | (1978-81) | Andrew T. Merovich | (1996-99) |
| Thomas G. Atkinson* | (1988-94) | David L. Messinger | (1980-83) |
| Albert J. Blaylock | (1976-77) | Stephen McReavy | (1973) |
| Robert K. Burkett | (1984-88) | Bijan Mohraz | (1991-97) |
| James R. Cagley | (1998-2001) | William W. Moore* | (1973-76) |
| H. Patrick Campbell | (1989-90) | Gary Morrison | (1973) |
| Arthur N. L. Chiu | (1996-99) | Robert Morrison | (1981-84) |
| Anil Chopra | (1973-74) | Ronald F. Nelson | (1994-95) |
| Richard Christopherson* | (1976-80) | Joseph P. Nicoletti* | (1975-79) |
| Lee H. Cliff | (1973) | Bruce C. Olsen* | (1978-82) |
| John M. Coil* | (1986-87, 1991-97) | Gerard Pardoen | (1987-91) |
| Eugene E. Cole | (1985-86) | Stephen H. Pelham | (1998-2001) |
| Edwin T. Dean | (1996-99) | Norman D. Perkins | (1973-76) |
| Robert G. Dean | (1996-2001) | Richard J. Phillips | (1997-2000) |
| Edward F. Diekmann | (1978-81) | Maryann T. Phipps | (1995-96) |
| Burke A. Draheim | (1973-74) | Sherrill Pitkin | (1984-87) |
| John E. Droeger | (1973) | Edward V. Podlack | (1973) |
| Nicholas F. Forell* | (1989-96) | Chris D. Poland | (1984-87) |
| Douglas A. Foutch | (1993-97) | Egor P. Popov | (1976-79) |
| Paul Fratessa | (1991-92) | Robert F. Preece* | (1987-93) |
| Sigmund A. Freeman | (1986-89) | Lawrence D. Reaveley* | (1985-91) |
| Barry J. Goodno | (1986-89) | Philip J. Richter* | (1986-89) |
| Mark R. Gorman | (1984-87) | John M. Roberts | (1973) |
| Gerald H. Haines | (1981-82, 1984-85) | Charles W. Roeder | (1997-2000) |
| William J. Hall | (1985-86) | Arthur E. Ross* | (1985-91, 1993-94) |
| Gary C. Hart | (1975-78) | C. Mark Saunders* | (1993-2000) |
| Lyman Henry | (1973) | Walter D. Saunders* | (1975-79) |
| James A. Hill | (1992-95) | Lawrence G. Selna | (1981-84) |
| Ernest C. Hillman, Jr. | (1973-74) | Wilbur C. Schoeller | (1990-91) |
| Ephraim G. Hirsch | (1983-84) | Samuel Schultz* | (1980-84) |
| William T. Holmes* | (1983-87) | Daniel Shapiro* | (1977-81) |
| Warner Howe | (1977-80) | Jonathan G. Shipp | (1996-99) |
| Edwin T. Huston* | (1990-97) | Howard Simpson* | (1980-84) |
| Paul C. Jennings | (1973-75) | Mete Sozen | (1990-93) |
| Carl B. Johnson | (1974-76) | Donald R. Strand | (1982-83) |
| Edwin H. Johnson | (1988-89, 1998-2001) | James L. Stratta | (1975-79) |
| Stephen E. Johnston* | (1973-75, 1979-80) | Scott Stedman | (1996-97) |
| Joseph Kallaby* | (1973-75) | Edward J. Teal | (1976-79) |
| Donald R. Kay | (1989-92) | W. Martin Tellegen | (1973) |
| T. Robert Kealey* | (1984-88) | John C. Theiss* | (1991-98) |
| H. S. (Pete) Kellam | (1975-76) | Charles H. Thornton* | (1992-99) |
| Helmut Krawinkler | (1979-82) | James L. Tipton | (1973) |
| James S. Lai | (1982-85) | Ivan Viest | (1975-77) |
| Gerald D. Lehmer | (1973-74) | Ajit S. Virdee* | (1977-80, 1981-85) |
| James R. Libby | (1992-98) | J. John Walsh | (1987-90) |
| Charles Lindbergh | (1989-92) | Robert S. White | (1990-91) |
| R. Bruce Lindermann | (1983-86) | James A. Willis* | (1980-81, 1982-86) |
| L. W. Lu | (1987-90) | Thomas D. Wosser | (1974-77) |
| Walter B. Lum | (1975-78) | Loring A. Wyllie | (1987-88) |
| Kenneth A. Luttrell | (1991-98) | Edwin G. Zacher | (1981-84) |
| Newland J. Malmquist | (1997-2000) | Theodore C. Zsutty | (1982-85) |
| Melvyn H. Mark | (1979-82) | | |
| John A. Martin | (1978-82) | | |

* President

ATC EXECUTIVE DIRECTORS (1973-Present)

| | | | |
|--------------------|----------------|------------------|-----------|
| Ronald Mayes | (1979-81) | Roland L. Sharpe | (1973-79) |
| Christopher Rojahn | (1981-present) | | |

Applied Technology Council

Sponsors, Supporters, and Contributors

Sponsors

Structural Engineers Association of California
James R. & Sharon K. Cagley
John M. Coil
Burkett & Wong

Supporters

Charles H. Thornton
Degenkolb Engineers
Japan Structural Consultants Association

Contributors

Lawrence D. Reaveley
Omar Dario Cardona Arboleda
Edwin T. Huston
John C. Theiss
Reaveley Engineers
Rutherford & Chekene
E. W. Blanch Co.

